USGS
science for a changing world

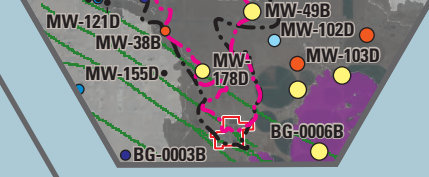

Prepared in cooperation with the Lahontan Regional Water Quality Control Board

Predevelopment Water Levels, Groundwater Recharge, and Selected Hydrologic Properties of Aquifer Materials, Hinkley and Water Valleys, California

Chapter H of

Natural and Anthropogenic (Human-Made) Hexavalent Chromium, Cr(VI), in Groundwater near a Mapped Plume, Hinkley, California

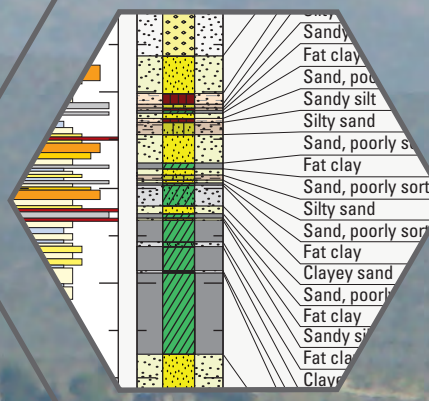

Professional Paper 1885-H

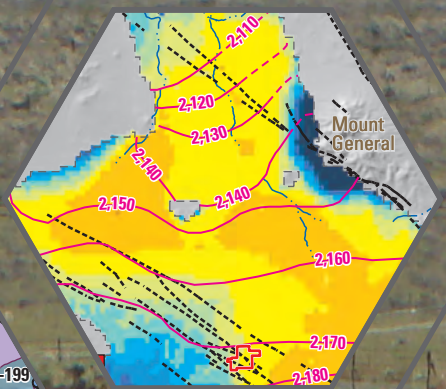

U.S. Department of the Interior
U.S. Geological Survey

Front cover

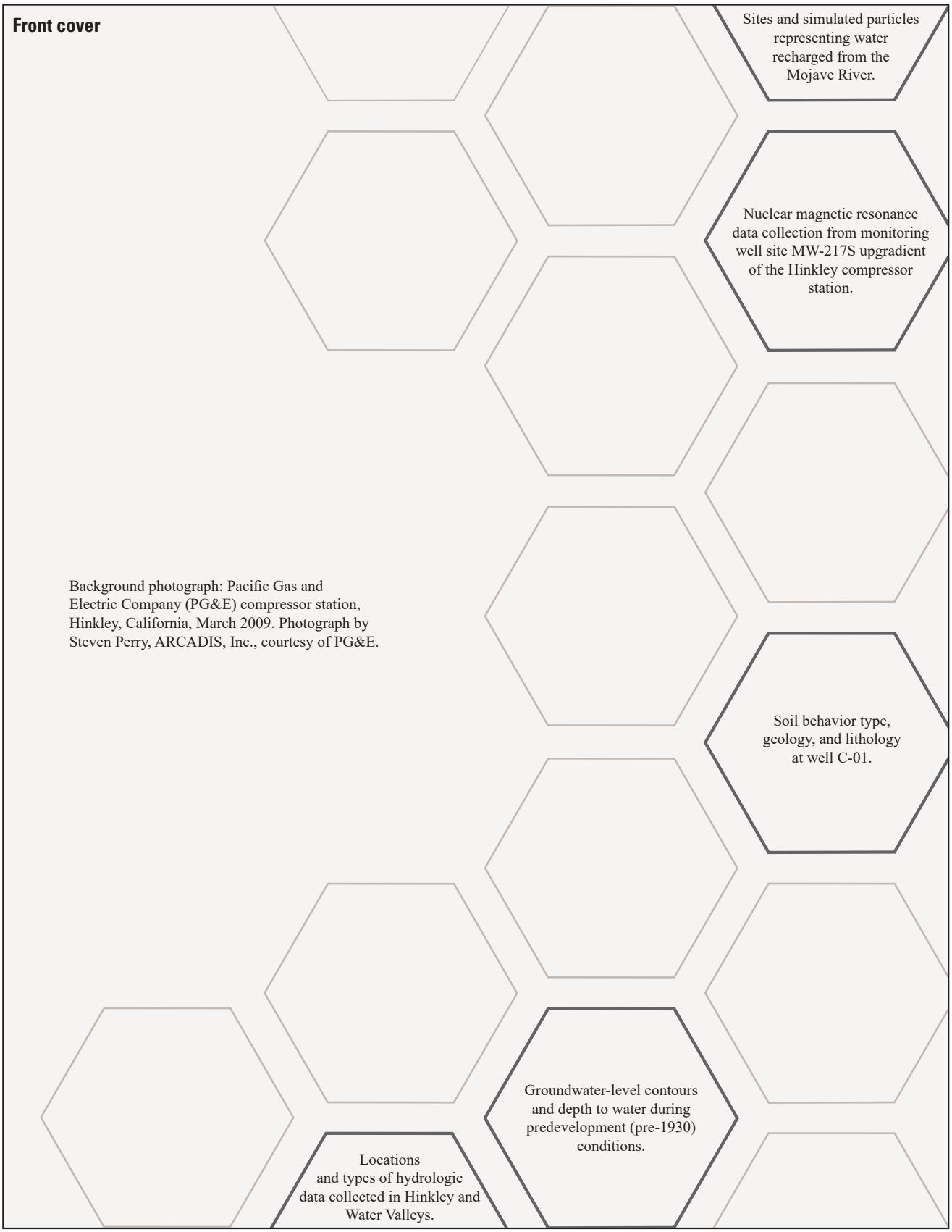

Background photograph: Pacific Gas and Electric Company (PG&E) compressor station, Hinkley, California, March 2009. Photograph by Steven Perry, ARCADIS, Inc., courtesy of PG&E.

Predevelopment Water Levels, Groundwater Recharge, and Selected Hydrologic Properties of Aquifer Materials, Hinkley and Water Valleys, California

Chapter H of
Natural and Anthropogenic (Human-Made) Hexavalent Chromium, Cr(VI), in Groundwater near a Mapped Plume, Hinkley, California

By Krishangi D. Groover, John A. Izbicki, Whitney A. Seymour, Anthony N. Brown, Randall E. Bayless, Carole D. Johnson, Katherine L. Pappas, Gregory A. Smith, Dennis A. Clark, Joshua Larsen, Meghan C. Dick, Lorraine E. Flint, Christina L. Stamos, and John G. Warden

Prepared in cooperation with the Lahontan Regional Water Quality Control Board

Professional Paper 1885-H

U.S. Department of the Interior
U.S. Geological Survey

U.S. Geological Survey, Reston, Virginia: 2023

Suggested citation:
Groover, K.D., Izbicki, J.A., Seymour, W.A., Brown, A.N., Bayless, R.E., Johnson, C.D., Pappas, K.L., Smith, G.A., Clark, D.A., Larsen, J., Dick, M.C., Flint, L.E., Stamos, C.L., and Warden, J.G., 2023, Predevelopment water levels, groundwater recharge, and selected hydrologic properties of aquifer materials, Hinkley and Water Valleys, California, Chapter H of Natural and anthropogenic (human-made) hexavalent chromium, Cr(VI), in groundwater near a mapped plume, Hinkley, California: U.S. Geological Survey Professional Paper 1885-H, 64 p., https://doi.org/10.3133/pp1885H.

Associated data for this publication:
Groover, K.D., Izbicki, J.A., Larsen, J.D., Dick, M.C., Nawikas, J., and Kohel, C.A., 2021, Hydrologic data in Hinkley and Water Valleys, San Bernardino County, California, 2015–2018: U.S. Geological Survey data release, https://doi.org/10.5066/P9BUXAX1.

ISSN 2330-7102 (online)

Acknowledgments

This study was developed by the U.S. Geological Survey (USGS) with input from a technical working group (TWG) composed of community members, the Lahontan Regional Water Quality Control Board (RWQCB), the Independent Review Panel Manager (Project Navigator, Ltd.), Pacific Gas and Electric Company (PG&E), and consultants for PG&E. The study was funded cooperatively under an agreement between the Lahontan RWQCB and the USGS. Funding for the study was provided by PG&E to the Lahontan RWQCB. Logistical support for field work, including access to wells, was provided by PG&E. The TWG met approximately quarterly during the study to provide input to the study, and the Hinkley community was updated annually on study progress.

The authors thank the many people involved in the design and implementation of this study including the staff of the Lahontan RWQCB, the staff of PG&E and their consultants, and the staff of Project Navigator, Ltd. The authors also acknowledge and thank the many involved community members who allowed access to their properties for sample collection, and who collectively donated thousands of hours on behalf of the local community in support of this project and for resolution of other issues related to anthropogenic hexavalent chromium, Cr(VI), within the Hinkley area.

Contents

Figures

Tables

Conversion Factors

U.S. customary units to International System of Units

Multiply	By	To obtain
	Length	
inch (in.)	2.54	centimeter (cm)
inch (in.)	25.4	millimeter (mm)
foot (ft)	0.3048	meter (m)
mile (mi)	1.609	kilometer (km)
	Area	
square foot (ft^2)	929.0	square centimeter (cm^2)
square foot (ft^2)	0.09290	square meter (m^2)
square mile (mi^2)	259.0	hectare (ha)
square mile (mi^2)	2.590	square kilometer (km^2)
	Volume	
acre-foot (acre-ft)	1,233	cubic meter (m^3)
acre-foot (acre-ft)	0.001233	cubic hectometer (hm^3)
	Flow rate	
acre-foot per year (acre-ft/yr)	1,233	cubic meter per year (m^3/yr)
acre-foot per year (acre-ft/yr)	0.001233	cubic hectometer per year (hm^3/yr)
foot per minute (ft/min)	0.3048	meter per minute (m/min)
foot per day (ft/d)	0.3048	meter per day (m/d)
gallon per minute (gal/min)	0.06309	liter per second (L/s)
inch per year (in/yr)	25.4	millimeter per year (mm/yr)

Multiply	By	To obtain
	Hydraulic conductivity	
foot per day (ft/d)	0.3048	meter per day (m/d)
	Transmissivity	
square foot per day (ft^2/d)	0.09290	meter squared per day (m^2/d)
	Well drawdown	
gallons per minute per foot of drawdown	0.1922	liters per second per meter of drawdown

International System of Units to U.S. customary units

Multiply	By	To obtain
	Length	
centimeter (cm)	0.3937	inch (in.)
millimeter (mm)	0.03937	inch (in.)
meter (m)	3.281	foot (ft)
kilometer (km)	0.6214	mile (mi)
	Area	
square centimeter (cm^2)	0.001076	square foot (ft^2)
square meter (m^2)	10.76	square foot (ft^2)
hectare (ha)	0.003861	square mile (mi^2)
square kilometer (km^2)	0.3861	square mile (mi^2)
	Volume	
cubic meter (m^3)	0.0008107	acre-foot (acre-ft)
cubic hectometer (hm^3)	810.7	acre-foot (acre-ft)
	Mass	
milligram (mg)	0.00003527	ounce, avoirdupois (oz)
kilogram (kg)	2.205	pound avoirdupois (lb)
	Flow rate	
cubic meter per year (m^3/yr)	0.000811	acre-foot per year (acre-ft/yr)
cubic hectometer per year (hm^3/yr)	811.03	acre-foot per year (acre-ft/yr)
meter per minute (m/min)	3.281	foot per minute (ft/min)
meter per day (m/d)	3.281	foot per day (ft/d)
liter per second (L/s)	15.85	gallon per minute (gal/min)
millimeter per year (mm/yr)	0.03937	inch per year (in/yr)
	Hydraulic conductivity	
meter per day (m/d)	3.281	foot per day (ft/d)
	Transmissivity	
meter squared per day (m^2/d)	10.76	foot squared per day (ft^2/d)
	Well drawdown	
liter per second per meter of drawdown	5.203	gallon per minute per foot of drawdown

Temperature in degrees Fahrenheit (°F) may be converted to degrees Celsius (°C) as follows:

$$°C = (°F - 32) / 1.8.$$

Datum

Vertical coordinate information is referenced to the North American Vertical Datum of 1988 (NAVD 88).

Horizontal coordinate information is referenced to the North American Datum of 1983 (NAD 83).

Below land surface (bls) is the datum used to describe depth.

Altitude, as used in this professional paper, refers to distance above the vertical datum.

Supplemental Information

Specific conductance is given in microsiemens per centimeter at 25 degrees Celsius (µS/cm at 25 °C).

Carbon-14 activities expressed as percent modern carbon (pmc), 100 pmc is 12.88 disintegrations per minute per gram of carbon. Years before present (ybp) is the timescale used for carbon-14 age dates in archeology, geology, and other disciplines.

Concentrations of chemical constituents in water are given in either milligrams per liter (mg/L) or micrograms per liter (µg/L).

Concentrations of chemical constituents in solid materials are given in milligrams per kilogram (mg/kg).

Kilohertz is a measurement of frequency equal to 1,000 hertz or 1,000 cycles per second.

Ohm-meters is a measure of electrical resistivity used to describe the resistance of geologic materials to an electric current.

Abbreviations

σ	standard deviation
BCM	Basin Characterization Model
CPT	cone penetration test
Cr(III)	trivalent chromium
Cr(VI)	hexavalent chromium having an oxidation state of +6
EM	electromagnetic
EPA	U.S. Environmental Protection Agency
LTU	land treatment unit
MRI	magnetic resonance imaging
NMR	nuclear magnetic resonance
PG&E	Pacific Gas and Electric Company
PVC	polyvinyl chloride
PVP	point-velocity probe
Q4 2015	October–December 2015
R^2	coefficient of determination
RWQCB	Regional Water Quality Control Board
SDR	Schlumberger-Doll Research
SSURGO	Soil Survey Geographic Database
T_2	water molecule magnetic field relaxation time
U_2	penetration pore pressure
USGS	U.S. Geological Survey
UTL_{95}	95-percent upper tolerance limit

Predevelopment Water Levels, Groundwater Recharge, and Selected Hydrologic Properties of Aquifer Materials, Hinkley and Water Valleys, California

By Krishangi D. Groover, John A. Izbicki, Whitney A. Seymour, Anthony N. Brown, Randall E. Bayless, Carole D. Johnson, Katherine L. Pappas, Gregory A. Smith, Dennis A. Clark, Joshua Larsen, Meghan C. Dick, Lorraine E. Flint, Christina L. Stamos, and John G. Warden

Abstract

Hydrologic and geophysical data were collected to support updates to an existing groundwater-flow model of Hinkley Valley, California, in the Mojave Desert about 80 miles northeast of Los Angeles, California. These data provide information on predevelopment (pre-1930) water levels, groundwater recharge, and selected hydrologic properties of aquifer materials.

A predevelopment groundwater-level map, drawn using water-level measurements from 48 wells collected as early as 1918, showed groundwater movement from recharge areas along the Mojave River to evaporative discharge areas near the margin of Harper (dry) Lake in Water Valley. During predevelopment conditions, depth to water ranged from near land surface along the Mojave River to above land surface near Harper (dry) Lake, consistent with flowing wells in Water Valley at that time. Depths to water in much of Hinkley Valley downgradient from the Lockhart fault were less than 20 feet below land surface. By 2017, water-level declines as a result of agricultural pumping, were as much as 60 feet near the Hinkley compressor station.

Areal recharge from infiltration of precipitation on the valley floor is negligible. Average annual recharge as infiltration of runoff from upland drainages to Hinkley and Water Valleys averages 64.7 acre-feet per year. In most years recharge does not occur; in years when it occurs, recharge to Hinkley Valley is typically about 296 acre-feet. In contrast, average recharge as infiltration of streamflow from the Mojave River from 1931 to 2015 was between 13,400 and 17,100 acre-feet per year; in some years recharge from the Mojave River exceeded 100,000 acre-ft. Estimates of predevelopment groundwater movement through Hinkley Gap and groundwater discharge to Harper (dry) Lake ranged from 570 to 1,900 and 820 to 2,460 acre-feet per year, respectively; at the time of this study in 2017, groundwater movement through Hinkley Gap was estimated to be about 83 acre-feet per year.

Hydraulic-conductivity values estimated from slug-test data for 95 monitoring wells ranged from less than 0.1 to 680 feet per day (ft/d); values generally decreased with depth. Median hydraulic-conductivity values calculated from nuclear magnetic resonance (NMR) data for Mojave River alluvium and near-shore lake deposits were 73 and 11 ft/d, respectively; median hydraulic-conductivity values for locally derived alluvium and weathered bedrock were 6 and 2 ft/d, respectively. Hydraulic-conductivity values, estimated from NMR data for formerly saturated deposits overlying the 2017 water table, were as high as 300 ft/d near the Hinkley compressor station. Downgradient from the Hinkley compressor station, formerly saturated deposits had hydraulic-conductivity values of about 150 ft/d, which were higher than values in saturated material. Coarse-textured, permeable material in formerly saturated deposits above the 2017 water table may have allowed groundwater, released from the Hinkley compressor station that may have contained Cr(VI), to move rapidly downgradient.

The Lockhart fault is an impediment to groundwater flow within Hinkley Valley. Groundwater-flow directions from horizontal point-velocity probe data were deflected to the west on the upgradient side of the fault compared to the nominal direction of groundwater flow estimated from water-level data. Younger groundwater was present on the upgradient and downgradient sides of the fault, and older groundwater with unadjusted carbon-14 ages as old as 5,650 years before present was in water from wells within splays of the Lockhart fault, consistent with limited groundwater movement across the fault. As a result, groundwater and Cr(VI) released from the Hinkley compressor station moved to the northwest along the downgradient side of the fault.

Coupled well-bore flow and depth-dependent water-quality data show water from wells C-01 and IW-03 within the Q4 2015 (October–December 2015) regulatory Cr(VI) plume was yielded from thin layers within the aquifer that are composed of well-sorted lake-margin (beach) deposits that likely have high lateral and longitudinal connectivity. Collectively, data show highly permeable deposits above the regional water table and thin permeable deposits within saturated portions of the upper aquifer that may have conducted groundwater and Cr(VI) downgradient when releases from the Hinkley compressor station first occurred.

H.1. Introduction

The Pacific Gas and Electric Company (PG&E) Hinkley compressor station, in the Mojave Desert about 80 miles (mi) northeast of Los Angeles, California, is used to compress natural gas as it is transported through a pipeline from Texas to California. Between 1952 and 1964, cooling water used at the compressor station was treated with a compound containing hexavalent chromium, Cr(VI), to prevent corrosion. The cooling wastewater was discharged to unlined ponds, resulting in contamination of soil and groundwater in the underlying unconsolidated aquifer (Lahontan Regional Water Quality Control Board, 2013). Since 1964, cooling-water management practices have been used that do not contribute Cr(VI) to groundwater.

In 2007, a PG&E study of the background concentrations of Cr(VI) in groundwater estimated an average concentration in the Hinkley area of 1.2 micrograms per liter (µg/L), with a 95-percent upper tolerance limit (UTL_{95}) of 3.1 µg/L (CH2M Hill, 2007). The 3.1 µg/L UTL_{95} was adopted by the Lahontan Regional Water Quality Control Board (RWQCB) as the maximum background Cr(VI) concentration used to map the plume extent. In response to limitations associated with the study's methodology and to an increase in the mapped extent of the regulatory Cr(VI) plume between 2008 and 2012, the Lahontan RWQCB (Lahontan Regional Water Quality Control Board, 2012) agreed that the 2007 PG&E Cr(VI) background-concentration study be updated; the U.S. Geological Survey was requested to do the updated Cr(VI) background study.

The Pacific Gas and Electric Company has a model (ARCADIS and CH2M Hill, 2011) that simulates groundwater flow in part of Hinkley Valley near and downgradient from the Hinkley compressor station from 1990 to 2010. The model is used to evaluate various plume-management alternatives. In support of the U.S. Geological Survey (USGS) Cr(VI) background study, consultants for PG&E updated the groundwater flow model (Jacobs Engineering Group, Inc., 2019). The updates included expanding the model extent to hydrologic boundaries that define Hinkley and Water Valleys. Important hydrologic features within the updated model extent in Hinkley and Water Valleys included (1) the Lockhart fault, (2) Hinkley Gap, and (3) the mapped extent of Cr(VI) greater than 3.1 µg/L extending downgradient from the Hinkley compressor station into Water Valley (Jacobs Engineering Group, Inc., 2019). In addition, the temporal extent of the updated model was expanded to include predevelopment (pre-1930) to 2015. Water levels were higher during predevelopment (Thompson, 1929; Conkling, 1934), and portions of the aquifer overlying the water table at the time of this study were saturated in the past.

H.1.1. Site Description

Hinkley Valley is about 62 square miles (mi^2) and contains about 36 mi^2 of unconsolidated deposits that were saturated under predevelopment conditions. Aquifers of interest in Hinkley Valley are composed primarily of unconsolidated "Mojave-type" deposits consisting of alluvium and lake-margin deposits sourced from the Mojave River (chapter A, table A.1; Miller and others, 2018a, 2020). Locally derived alluvium and weathered bedrock also are important aquifers for domestic supply in some areas.

Hinkley Valley was divided into eastern, western, and northern subareas on the basis of differences in geology and hydrology (fig. H.1). The eastern subarea is closest to recharge areas along the Mojave River. Mojave-type deposits in this area are commonly less than 160 feet (ft) thick and overlie fine-textured lacustrine (lake) deposits described as "blue clay" in drillers' and geologists' logs (chapter A, fig. A.6; ARCADIS and CH2M Hill, 2011). Fine-textured deposits described as "brown clay" are interspersed throughout the upper aquifer. In some places, these fine-textured deposits are confining units that separate the upper aquifer into shallow and deep zones (chapter A, fig. A.6; ARCADIS and CH2M Hill, 2011). Mudflat/playa deposits sourced from the Mojave River that are present at land surface near Mount General and at depth within the eastern subarea also are described as brown clay in drillers' and geologists' logs. The western subarea consists of Mojave-type deposits, overlying groundwater-discharge deposits, fine-textured lacustrine deposits, and weathered bedrock (CH2M Hill, 2013; Miller and others, 2018a, 2020). The northern subarea consists of Mojave-type deposits, overlying fine-textured lacustrine and mudflat/playa deposits sourced from the Mojave River and from local materials (Stantec, 2013; Miller and others, 2018a, 2020). Aquifers within Water Valley are composed of lake-margin deposits sourced from the ancestral Mojave River along the margins of Harper (dry) Lake (chapter A, fig. A.5) that overlie and interfinger with locally derived alluvium (Miller and others, 2018a, 2020).

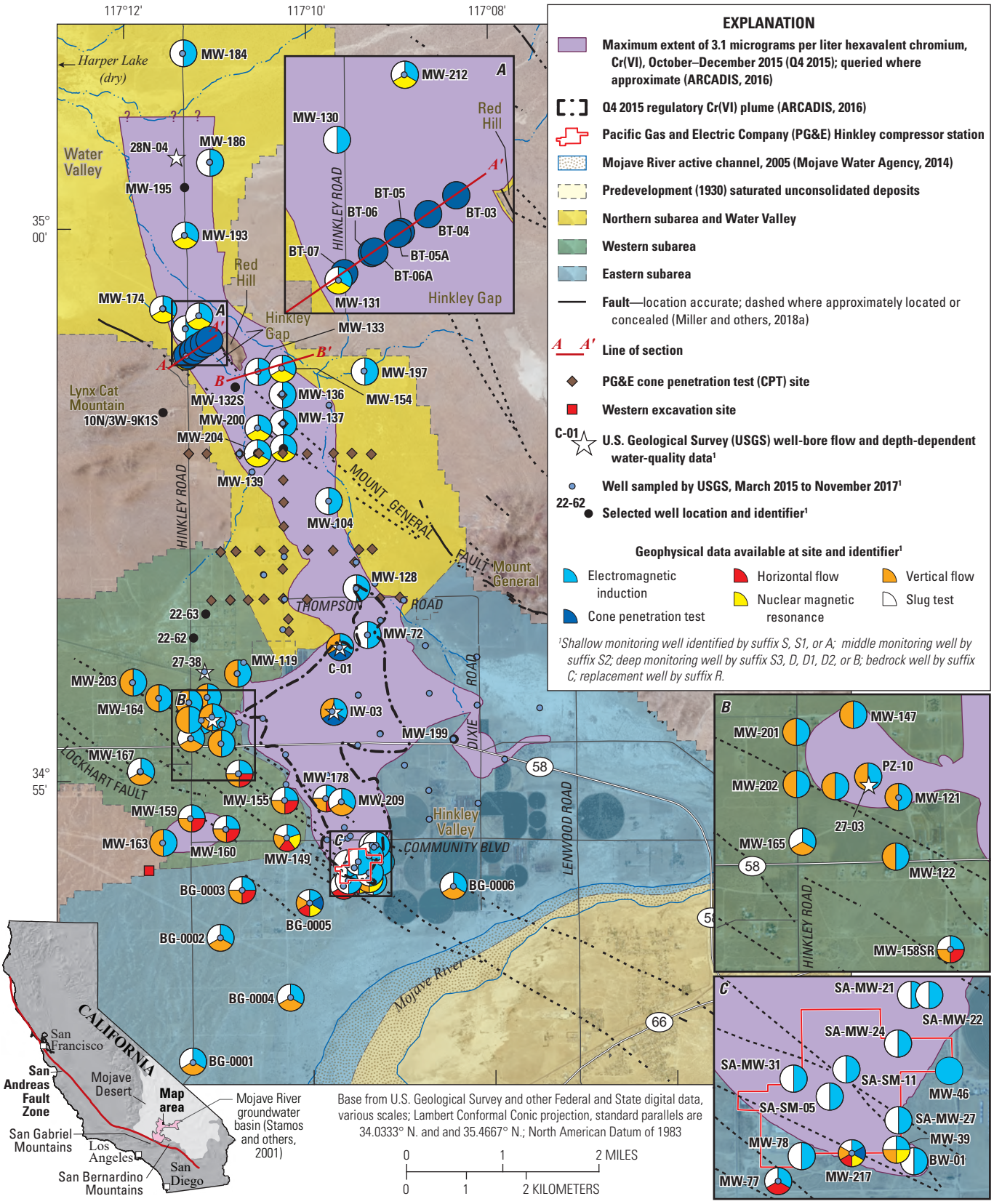

Figure H.1. Locations and types of hydrologic data collected in Hinkley and Water Valleys, western Mojave Desert, California. Well location data are available in U.S. Geological Survey (2021), and types of hydrologic data are available in appendix H.1 (table H.1.1).

Groundwater recharge originates primarily from intermittent flows in the Mojave River that occur on average once every 5 to 7 years (Lines, 1996; Stamos and others, 2001; Seymour, 2016). Prior to development, groundwater flowed from the Mojave River northward toward Hinkley Gap into Water Valley, where groundwater discharged by evaporation along the margins of Harper (dry) Lake (Thompson, 1929). The Lockhart fault impedes groundwater flow in Hinkley Valley. Less is known about the effect of the Mount General fault on groundwater flow. The Lockhart and Mount General faults consist of numerous mapped strands (Miller and others, 2018a, 2020).

Beginning in the early 1950s and continuing until the time of this study, water levels measured in wells declined by as much as 60 ft near the Hinkley compressor station as a result of agricultural pumping (Stone, 1957; California Department of Water Resources, 1967; Seymour and Izbicki, 2018). As a consequence of water-level declines, saturated Mojave-type deposits in much of the western subarea are a thin veneer (commonly less than 10 ft) overlying fine-textured lacustrine and groundwater-discharge deposits and weathered bedrock (CH2M Hill, 2013; Miller and others, 2020). Similarly, saturated Mojave-type deposits in much of the northern subarea are a thin veneer overlying fine-textured lacustrine and mudflat/playa deposits (Stantec, 2013; Miller and others, 2020). Many monitoring wells in the western subarea are completed partly or entirely in weathered bedrock aquifers, and many monitoring wells in the northern subarea are completed partly or entirely in fine-textured lacustrine and mudflat/playa deposits. Younger Mojave-type deposits in much of Hinkley Valley and lake-margin deposits in much of Water Valley were formerly extensively pumped for agricultural supply and were largely above the water table at the time of this study (Stamos and others, 2001; Miller and others, 2018a, 2020). As a result of groundwater development, deep percolation of irrigation return water, and to a lesser extent septic discharges, were important components of recharge at the time of this study (Stamos and others, 2001; Jacobs Engineering Group, Inc., 2019).

The Hinkley compressor station and most of the regulatory Cr(VI) plume are within the eastern subarea. In October–December 2015 (Q4 2015), the regulatory Cr(VI) plume extended 3 mi downgradient from the historical discharge location within the Hinkley compressor station (fig. H.1; ARCADIS, 2016). However, Cr(VI) concentrations in water from wells greater than the interim regulatory background of 3.1 µg/L were present as far downgradient as Water Valley, more than 8 mi north of the Hinkley compressor station (fig. H.1; ARCADIS, 2016), and the actual extent of Cr(VI) associated with the release was uncertain. Remediation of Cr(VI) in Hinkley Valley began in 1992; and in 2010, clean-up was projected to require from 10 to 95 years (Haley and Aldrich, Inc., 2010; Pacific Gas and Electric Company, 2011).

Monitoring wells installed for regulatory purposes by PG&E were most commonly identified by the prefix MW, with sites numbered sequentially in the order they were drilled. Shallow wells at a site, commonly screened across or just below the water table, were identified with the suffixes S or S1. Deeper wells were identified with the suffixes D, D1, or D2; deeper wells were identified with suffixes S2 or S3 if a hydrologically important intervening clay layer was not present. Older monitoring wells were identified with the suffixes A or B for shallower or deeper wells, respectively. Wells installed by PG&E as part of the USGS Cr(VI) background study were identified with the prefix BG; the sites were numbered sequentially in the order they were permitted, and wells at each site were identified from shallowest to deepest with the suffixes A, B, or C. Although drilling methods changed over time and in response to site conditions, most monitoring wells were drilled with auger rigs. Core material was available for most wells drilled after 2011 from near the water table to the bottom of the borehole, often to below the depth of the deepest well at a site.

H.1.2. Purpose and Scope

The purpose of this chapter is to describe predevelopment conditions, groundwater recharge, and the hydrologic properties of aquifer materials within Hinkley and Water Valleys that were measured as part of the USGS Cr(VI) background study. Scope of the work included collection and interpretation of hydrologic and geophysical data to estimate predevelopment water-level conditions, aquifer recharge, aquifer hydraulic properties, the movement of groundwater near faults, and layering of aquifer hydraulic properties. Data were used to support updates to an existing groundwater-flow model within Hinkley and Water Valleys done by consultants for PG&E (Jacobs Engineering Group, Inc., 2019).

H.2. Methods

Hydrologic data collected in Hinkley and Water Valleys between June 2015 and February 2018 included (1) review of predevelopment water-level data to determine changes in water-table elevations since groundwater development; (2) estimation of areal recharge and runoff; (3) cone penetration tests (CPT) to assess aquifer lithology; (4) slug tests to estimate the hydraulic conductivity of aquifer material; (5) borehole geophysical logs, including electromagnetic (EM) induction logs, nuclear magnetic resonance (NMR) data, and point-velocity probe (PVP) data; and (6) depth-dependent well-bore flow data and depth-dependent water-sample collection to assess layering of aquifer properties. Geophysical log data (including EM, NMR, and PVP logs) are available in the online USGS GeoLog Locator (U.S. Geological Survey, 2019; https://webapps.usgs.gov/GeoLogLocator/#1/). Water-quality data from these sites are available in the National Water Information System (NWIS; U.S. Geological Survey, 2021; https://waterdata.usgs.gov/nwis) and may be retrieved using USGS site identification numbers in appendix H.1 (table H.1.1). Cone penetration test and slug-test data are available in Groover and others (2021).

H.2.1. Predevelopment Water-Level Data

Regional groundwater-flow models within the Mojave River groundwater basin, including Hinkley and Water Valleys, were developed in 1971 (Hardt, 1971) and 2001 (Stamos and others, 2001) to evaluate groundwater conditions at those times. Predevelopment (pre-1930) water-level maps were prepared to support calibration of those models. However, these maps were regional in scope and did not include all data available from early reports (Thompson, 1929; Conkling, 1934, California Department of Water Resources, 1967). The USGS NWIS (U.S. Geological Survey, 2021; https://waterdata.usgs.gov/nwis) was updated to include water-level measurements from 121 wells in Hinkley Valley, Water Valley, and surrounding areas. Data from 48 of those wells, collected as early as 1918, were used to update predevelopment water-level maps in Hinkley and Water Valleys (Seymour and Izbicki, 2018). Well information and predevelopment water-level data for these 48 wells are available in appendix H.1 (table H.1.2).

Predevelopment and 2017 water-level maps were compared with bedrock altitude data to produce maps of predevelopment and the 2017 saturated thickness. Bedrock altitude was estimated from gravity data collected as part of this study (Langenheim and others, 2019; Miller and others, 2020).

H.2.2. Estimation of Areal Recharge and Local Runoff

Areal recharge and local runoff from selected upland drainages tributary to Hinkley and Water Valleys were calculated using the Basin Characterization Model (BCM; Flint and others, 2013, 2021). The BCM is a grid-based model that calculates the water balance at selected time steps and spatial scales. The model was developed at a 270-meter (m) spatial resolution using monthly data and has been supported by numerous Federal, State, and local agencies and international organizations. Data are available in appendix H.1 (table H.1.3).

Input data for BCM include gridded monthly climate data from PRISM (Daly and others, 2008); geology (Jennings, 1977); water content at field capacity and wilting point, porosity; and soil thickness data from the Soil Survey Geographic Database (SSURGO; Natural Resources Conservation Service, 2006). Also included in the input datasets are annual values for precipitation, minimum and maximum air temperature, potential evapotranspiration, actual evapotranspiration, and climatic water deficit (Flint and Flint, 2014). Potential evapotranspiration is calculated from solar radiation and accounts for topographic shading and cloudiness; changes in soil water storage are calculated as excess water moves through the soil profile. Changes in soil water are used to calculate actual evapotranspiration. Climatic water deficit is calculated by subtracting actual evapotranspiration from potential evapotranspiration. Depending on soil properties and the permeability of underlying bedrock, water may become recharge or runoff. Input data for BCM are available in Flint and Flint (2014) and input files are available online in Blodgett and others (2011; https://doi.org/10.3133/ofr20111157).

Areal recharge from direct infiltration of precipitation on the valley floor was evaluated on the basis of chloride accumulation within the unsaturated zone (Allison and Hughes, 1978; Allison and others, 1994; Prudic, 1994). Chloride and other selected anions were analyzed on water extracts from unsaturated zone core material collected by PG&E consultants at four undisturbed sites in Hinkley and Water Valleys. Extractions were done at 5-ft intervals on core material collected, using auger drilling techniques, by PG&E consultants and methods described by Izbicki and others (2000a). Extracts were prepared on a 1 to 1 sample-to-water ratio by mass and shaken for 24-hours prior to centrifugation, filtration, and analyses. Extracts for chloride and other soluble anions were analyzed using ion chromatography (American Public Health Association, 1992) at the USGS San Diego office laboratory. Chromium concentrations were measured on filtered extract samples from well MW-195 by Zeeman-corrected Graphite Furnace Atomic Absorption Spectroscopy using U.S. Environmental Protection Agency (EPA) Method 7010 (U.S. Environmental Protection Agency, 2007) at the USGS Trace Element Laboratory in Boulder, Colorado. Data are available in appendix H.1 (table H.1.4).

H.2.3. Cone Penetration Testing

The lithology of unconsolidated materials above the water table at the time of this study was inferred at selected locations in Hinkley Valley using CPT data. Cone penetration test data were collected using a 30-ton, truck-mounted rig by a contract driller according to ASTM International (2012) standard D5778-12. At each site, data were collected at approximately 2-inch (in.) intervals by pushing a small-diameter, approximately 1.5-in. sensor into the ground. The sensor measures tip resistance (q_c) and sleeve resistance (f_s) to sensor penetration, from which the lithology of unconsolidated materials was inferred using empirically derived relations (Robertson, 1990; Lunne and others, 1997; Noce and others, 2003). Penetration pore pressure data (U_2) also were collected as the sensor was pressed into the ground.

Core penetration test data were collected in May 2017 (1) at five sites across the western side of Hinkley Gap; (2) adjacent to monitoring wells MW-217, immediately south of the Hinkley compressor station and BG-0005, upgradient of the Lockhart fault; and (3) adjacent to production wells C-01 and IW-03 where coupled well-bore flow depth-dependent water-quality data were collected (fig. H.1; appendix H.1, table H.1.1). Inferred lithology from CPT data was compared to aquifer lithology from core material and aquifer-property data estimated from borehole geophysical-log data at sites adjacent to CPT data collection. Although core material was available from monitoring wells within the saturated portion of the aquifer at the time of this study, core material and detailed lithology were not available for formerly saturated deposits above the water table at the time of this study. Inferred lithology from CPT data was used to estimate aquifer hydraulic properties in formerly saturated alluvium overlying the water table that could not be measured by conventional means to inform model updates by PG&E consultants.

Cone penetration test data also were collected in April 2017 (using the same equipment and contract driller) by PG&E consultants at 34 sites in the northern subarea in support of the USGS Cr(VI) background study (fig. H.1); 15 of those sites were adjacent to monitoring wells installed by PG&E for regulatory purposes and had core material and borehole geophysical data. Core penetration test data also were collected (using the same equipment and contract driller) by PG&E consultants between 2006 and 2010 at almost 300 sites throughout and near the mapped Q4 2015 regulatory Cr(VI) plume in Hinkley Valley.

The CPT data collected in May 2017 are available in the online USGS GeoLog Locator archive (U.S. Geological Survey, 2019; https://webapps.usgs.gov/GeoLogLocator/#1/). The CPT data collected by PG&E consultants in April 2017 are available in Groover and others (2021). The CPT data collected prior to this study were not archived by the USGS but may be available from PG&E upon request.

H.2.4. Slug Tests

Pacific Gas and Electric Company has data on the hydraulic properties of saturated deposits estimated from (1) multiple-well aquifer tests, (2) single-well specific capacity tests, and (3) lithologic data and other sources within the extent of the groundwater-flow model developed by ARCADIS and CH2M Hill (2011). To support model development outside of the existing model area, hydraulic-property data were estimated for 95 PG&E monitoring wells from slug-test data collected between 2015–18 (appendix H.1, table H.1.1).

Depending on site conditions, physical slug-test data were collected using procedures described by Cunningham and Schalk (2011), or pneumatic slug-test data were collected using procedures described by Greene and Shapiro (1995). If the water table was within the screened interval of the well, physical slug-test data were collected; if the water table was above the screened interval of the well, pneumatic slug-test data were collected.

Physical slug tests were done on 47 wells (Groover and others, 2021). Physical slugs, with diameters appropriate for the well diameter, were instantaneously lowered into (displacement or rising head test) or pulled above (recovery or falling head test) the water table to cause a water-level response. Details of physical slug sizes and slugs used in each well are available in Groover and others (2021).

Pneumatic tests were done on 48 wells (Groover and others, 2021). The pneumatic tests used inert nitrogen gas to depress the water levels within the sealed wells, and a pressure release valve was used to instantly release the pressure following procedures discussed in Greene and Shapiro (1995) and Groover and others (2021). The pneumatic test was used whenever possible but could not be used in wells that had water levels within the screened interval.

For physical and pneumatic slug tests, water levels were recorded continuously using a vented In-Situ Level TROLL 500 (In-Situ, Inc., Fort Collins, Colorado). Water levels were recorded starting approximately 15 minutes before the start of the test to ensure that the water level in the well had stabilized, and water-level data were collected at 1-second intervals. Interferences associated with nearby pumping were observed in some tests based on decreases in water levels between pre-test and post-test conditions. Most interferences were minor, and resulting changes in depth to water were less than 0.5 ft. Water-level responses for tests ranged from 20 seconds to more than 90 minutes after a test was initiated. Most physical and pneumatic slug tests were repeated at least three times within each well. However, tests at six sites were only done once due to lack of water-level response or very slow response (Groover and others, 2021). Hydraulic-conductivity values for wells lacking or having slow water-level responses to tests were either not calculated or were assigned a value less than 0.01 foot per day (ft/d).

Slug-test computations were done using an Excel macro-enabled spreadsheet (Halford and Kuniansky, 2002) using approaches outlined in Butler and Garnett (2000), Butler and others (2003), and Greene and Shapiro (1995). The spreadsheet allows for concurrent analysis of multiple tests at the same well. A curve can be automatically or manually fit to observed data by adjusting the damping coefficient (Butler and others, 2003) or the ratio of storage in the formation to the storage in the borehole (Greene and Shapiro 1995). For physical slug tests, data from displacement (slug-in) and recovery (slug-out) tests were analyzed separately. For pneumatic tests, only the recovery curves were analyzed.

Additional information on slug-test data, interpretation of those data, and calculated hydraulic-conductivity values are available in Groover and others (2021). Calculated hydraulic-conductivity values from slug-test data are listed in appendix H.1 (table H.1.1).

H.2.5. Borehole Geophysical Logs

Electromagnetic induction, NMR, and PVP logs were collected from selected wells in Hinkley and Water Valleys. These logs were interpreted to supplement available geologic and hydrologic data.

H.2.5.1. Electromagnetic Induction Logs

Electromagnetic (EM) induction logs were collected in 93 wells (fig. H.1; appendix H.1, table H.1.1) between June 2015 and February 2018. Logs were collected according to manufacturer's calibration and operation specifications using a Century model 9511 tool (Century Geophysical Corporation, Tulsa, Oklahoma). The tool uses an electromagnetic field to induce an electrical current in the surrounding formation (Johnson and Williams, 2003). The induced current sets up a secondary magnetic field that is measured, amplified, and then transmitted to the surface as a direct current. The magnitude of the direct current is proportional to the electrical conductivity of the formation, which is a function of lithology and pore-fluid conductivity (Keys, 1990; Paillet and others, 1999). The volume of the material measured by a typical EM logging tool is a donut-shaped torus (Geonics Limited, 2005; Century Geophysical Corporation, 2008). The size of the torus is dependent upon the coil spacing within the tool. The inner and outer diameters of the torus measured by the Century 9511 tool are approximately 18–50 in., respectively (Century Geophysical Corporation, 2008), and the EM resistivity measured by the tool is not sensitive to backfill material within the borehole near the well. The Century 9511 tool also includes sensors for natural gamma, fluid resistivity, and fluid temperature. Electromagnetic induction log and other data were used to guide collection of horizontal PVP data, well-bore flow data, and depth-dependent water-quality data.

H.2.5.2. Nuclear Magnetic Resonance Logs

Nuclear magnetic resonance (NMR) logs were collected in April 2017 at 12 auger- or sonic-drilled wells and 2 mud-rotary drilled wells (appendix H.1, table H.1.1) to measure the distribution of porosity and water content in shallow aquifers and overlying unconsolidated materials. Nuclear magnetic resonance well-bore logging was initially developed for the oil and gas industry, but NMR logging techniques have become available for environmental applications (Dlubac and others, 2013; Behroozmand and others, 2015; Knight and others, 2015). Nuclear magnetic resonance uses a strong electromagnet and a pulsed radio frequency field to induce movement of water molecules in the aquifer, similar to the technique used in medical magnetic resonance imaging (MRI). The electromagnet aligns water molecules within the radius of investigation, and the radio frequency field then "tips" molecules into a different alignment (Behroozmand and others, 2015). The NMR logging tool then measures the time it takes for the water molecules to realign within the magnetic field (magnetic field relaxation time). Water molecules affected by the NMR logging tool realign at different rates depending on the porosity of the aquifer and the ratios of clay, silt, and sand within aquifer deposits (Legchenko and Valla, 2002). The water molecule magnetic field relaxation time is shorter for immobile water in fine-textured material and is longer for mobile water in coarse-textured material (Legchenko and Valla, 2002). The water molecule magnetic field relaxation time can be related to the hydraulic conductivity of the formation (Legchenko and others, 2002). The hydraulic conductivities of saturated aquifer materials were estimated from NMR data using the Schlumberger-Doll Research (SDR) equation and empirically derived constants (Dlubac and others, 2013; Knight and others, 2015).

$$\text{SDR equation: } K = C^{*}\ \Phi^{N}{*}(MLT_2)^2 \qquad \text{(H.1)}$$

where

K is hydraulic conductivity of saturated aquifer materials;
C is 8,900;
N is 1 for aquifer materials considered in Hinkley and Water Valleys;
Φ is porosity; and
MLT_2 is the logarithmic mean of measured magnetic field relaxation time, T_2.

Nuclear magnetic resonance data were collected using a Javelin JP238 wireline tool and data collection system according to the manufacturer's calibration and operation specifications (Vista Clara, Inc., Mukilteo, Washington). The tool is designed for shallow environmental logging in cased boreholes. The Javelin JP238 tool is 7.1 ft long and has a diameter of 2.38 in. The tool was used in 4 in. polyvinyl chloride (PVC) cased water-table monitoring wells (fig. H.2) and could not be used in deeper 2-in. diameter wells. Data were collected approximately every 1.6 ft from land surface to the total depth of the well. Measurements were taken using frequencies at 249 kilohertz (kHz) and 300 kHz for 4 seconds with 10 data stacks (repetitions) for the main data collection mode at each measurement depth and burst mode measurements were done for 1 second with 120 data stacks at each depth of investigation. Additional measurements in the unsaturated zone below the predevelopment water table were collected at 1.6-ft (0.5-m) depth increments for 150 milliseconds (ms) with 200 data stacks, although as many as 1,000 data stacks were collected at some sites. Data were processed with a clay-bound water cutoff of 3 ms and a capillary-bound water cutoff of 33 ms.

Hydraulic-conductivity values calculated for the saturated zone using the SDR equation (eq. 1) were compared to NMR-measured immobile water content to develop an equation that could be used to estimate hydraulic conductivity in the unsaturated zone (Groover and others, 2017). Clay-bound water content in the unsaturated zone below the predevelopment water table was used in the equation to generate a hydraulic-conductivity estimate.

Photograph by K. Groover, U.S. Geological Survey, April 2018

Figure H.2. Nuclear magnetic resonance (NMR) data collection from monitoring well site MW-217S upgradient of the Hinkley compressor station, Hinkley Valley, western Mojave Desert, California, April 2017. Location and construction data for well MW-217S are available in appendix H.1 (table H.1.1).

Some NMR data collected at MW-200S1 in the northern subarea (U.S. Geological Survey, 2019) were affected by electrical noise from a nearby well and were unusable. Nuclear magnetic resonance data from monitoring well sites MW-39 and MW-46 near the Hinkley compressor station also were unusable because the wells were drilled using mud rotary rather than auger or sonic drilling techniques.

H.2.5.3. Point-Velocity Probe Data Collection

Point-velocity probe data included vertical flow data collected using an EM flowmeter, and horizontal flow data were collected using a colloidal borescope or a heat-pulse flowmeter. Vertical PVP data were used along with examination of core material and EM induction logs to select depth intervals for horizontal PVP data collection within and near the Lockhart fault.

H.2.5.3.1. Vertical Point-Velocity Probe

Vertical PVP data were collected in 44 wells using a Century Geophysical EM flowmeter according to manufacturer calibration and operation specifications (appendix H.1, table H.1.1). The EM flowmeter relies on an electrical conductor (water) passing through a magnetic field inside of a hollow, cylindrical section (within the flowmeter) that is surrounded by electromagnets. Movement of water in the magnetic field generates an electric field in accordance with Faraday's Law (Young and Pearson, 1995; Paillet, 2000), which is measured by the EM flowmeter. The EM flowmeter has no moving parts and a large, dynamic range capable of measuring velocities ranging from less than 0.3 to more than 250 feet per minute (ft/min; Newhouse and others, 2005). The EM flowmeter also measures fluid temperature and fluid resistivity.

Vertical flow in monitoring wells was measured at 1-foot intervals for 2 minutes within the screened interval of the well. Heat produced by the tool affected monitoring well-bore temperature and flow data during longer measurement periods. Additional measurements were taken in unscreened sections above and below the screened interval of the well when possible. Data collected in the screened interval of the well were compared to data collected in the unscreened intervals, where flow was not present, to evaluate flow of water within the well screen:

$$V_a = \overline{X}_a \quad \text{(H.2)}$$

Minimum error:

$$V_{a-n} = \overline{X}_a - \sigma_a \quad \text{(H.3)}$$

Maximum error:

$$V_{a+n} = \overline{X}_a + \sigma_a \quad \text{(H.4)}$$

where

V_a is the average vertical flow counts at a given depth *a* within the screened interval;

$\overline{X}_a$ is the average of flow values at a given measurement depth *a*;

σ_a is the standard deviation of flow values at a given measurement depth *a*; and

V_{a-n} and V_{a+n} are the lower and upper ranges of error for each flow measurement at a given depth, respectively.

Flow in the well screens that plot to the left of the minimum flow in the unscreened section of the well indicate downward flow, whereas flow in the screened interval that plot to the right of the maximum flow in the unscreened section indicate upward flow (fig. H.3*A*). Vertical flow in the screened intervals within the range of flow measured in the unscreened sections (fig. H.3*B*) indicate vertical flow at those depths that cannot be resolved using the EM flowmeter; these zones were interpreted as not having vertical flow. Vertical flow data were collected in counts per second; data were not converted to units of flow (length per unit time). Count-based flow data were used to guide collection of horizontal PVP data.

H.2.5.3.2. Horizontal Point-Velocity Probe

Horizontal PVP data were collected using a colloidal borescope or a heat-pulse flowmeter in wells within and near the Lockhart fault in May 2017. Additional data were collected in August 2017 to examine the effects of pumping from supply wells on groundwater flow near monitoring wells MW-217S and MW-217D upgradient from the Hinkley compressor station.

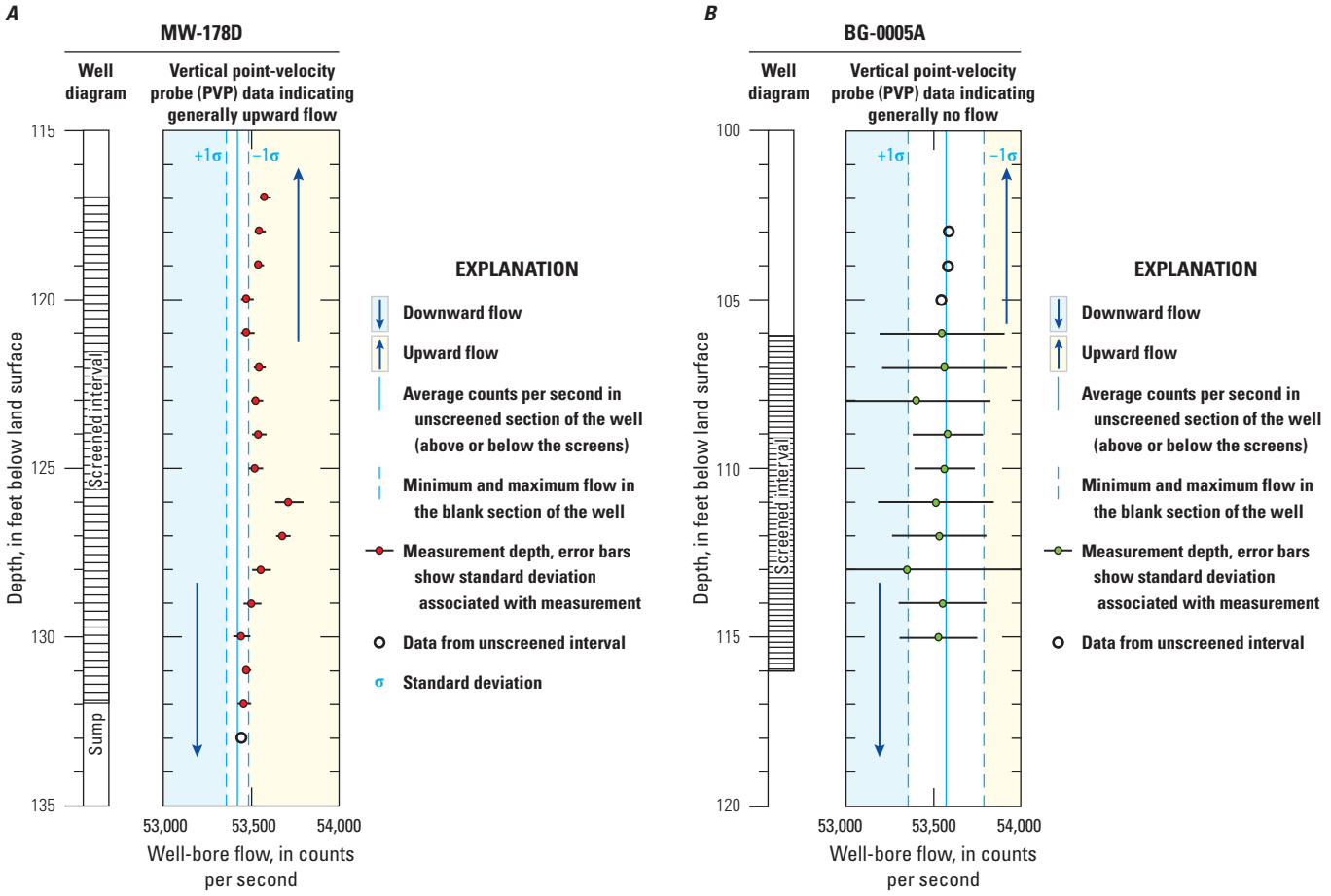

Figure H.3. Electromagnetic (EM) flowmeter data from two monitoring wells showing *A*, upward groundwater flow in monitoring well site MW-178D and *B*, no vertical groundwater flow in monitoring well site BG-0005A, Hinkley Valley, western Mojave Desert, California, January 2017. Data are available in U.S. Geological Survey (2019).

The colloidal borescope consists of a small camera and light source with a built-in compass that is lowered into the well screen on a cable. Once the water level in the well has equilibrated to the insertion of the colloidal borescope, the camera records a video of particulates travelling in the well, and motion tracking software measures the direction and velocity the particulates are travelling (James and others, 2006). The borescope was held at the measurement depth for a minimum of 1 hour to allow particles in the well to equilibrate after insertion of the tool. Measurement times with the colloidal borescope ranged from 3 to 8 hours.

The colloidal borescope could not be used in some wells, and the heat-pulse flowmeter was used in wells that had too few particles for the colloidal borescope to track. The heat-pulse flowmeter is within a porous packer, filled with silica or glass beads. The instrument is lowered into the well using interlocking aluminum rods (Kerfoot, 1988, 1995). Once the flowmeter has been lowered to the measurement location and allowed to equilibrate, a heat source within the probe is triggered to release a pulse of heat. Natural groundwater flow will then move the heat pulse through the packer in the direction of groundwater flow. The outer part of the probe consists of thermistors that measure the arrival of the heat that can be used to estimate the direction and speed of groundwater flow (Kerfoot, 1988).

Water levels were measured every 15 minutes prior to data collection for the colloidal borescope and the heat-pulse flowmeter to ensure the wells recovered from insertion of the tools. Water levels were measured at approximately 30-minute intervals during data collection to ensure conditions within the well were stable during the measurement period. Measurements taken using the colloidal borescope and the heat-pulse flowmeters are sensitive to disturbance and cannot be used near major highways or in intervals with large vertical groundwater flow. Both tools measure the direction of groundwater flow and can measure groundwater velocities as low as 0.1 ft/d (Bayless and others, 2011).

Groundwater-velocity data measured using these tools require corrections to compensate for a number of factors including the gravel pack surrounding a screen and the presence of an open void (the well itself) which may artificially accelerate groundwater in the vicinity of the well (Drost and others, 1968; Kearl and Roemer, 1998; James and others, 2006; Bayless and others, 2011; Bayer-Raich and others, 2019). Groundwater velocities measured using horizontal PVP data were adjusted for the presence of the borehole and well using the following equation:

$$V_F = \frac{V_B}{\alpha} \quad \text{(H.5)}$$

where

V_F is the estimated groundwater velocity in the formation;

V_B is the velocity measured in the borehole; and

α is the borehole acceleration factor calculated using methods discussed by Drost and others (1968) and Bayless and others (2011).

The colloidal borescope measures horizontal flow within a 6.1×10^{-5} cubic inch volume (1-cubic-millimeter) within the well. Measurement depths for colloidal borescope data collection were selected after physical examination of archived core material and analyses of vertical EM-induction and EM-flow-log data. Nuclear magnetic resonance and CPT data also were used to select measurement depths where available. In general, two measurements were taken within each well: (1) near coarse-textured material where water was entering the well and (2) near coarse-textured material where water was exiting the well. Hydraulic-conductivity values estimated from slug-test data for the well screened interval were used to calculate the borehole acceleration factor (Drost and others, 1968; Bayless and others, 2011). Use of slug test data ensured consistent data were used at tested wells because the hydraulic-conductivity values estimated from NMR data have a greater vertical resolution within the well screened interval and were not available for all sites.

H.2.6. Well-Bore Flow and Depth-Dependent Data Collection

Between June 2015 and March 2016, coupled well-bore flow and depth-dependent water-quality data were collected from five production wells within Hinkley and Water Valleys to assess vertical layering of aquifer hydraulic properties and vertical differences in the chemical and isotopic composition of groundwater within the aquifer. Coupled well-bore flow and depth-dependent data are direct measurements of aquifer yields to wells that are more representative of aquifer properties than indirect data inferred from lithologic or geophysical data or data collected from slug tests. Each dataset consists of (1) a set of geophysical logs collected according to manufacturer calibration and operation specifications under unpumped and pumped conditions, (2) water-quality samples collected from the surface discharge of pumps within the well, and (3) water-quality samples collected during pumped conditions from selected depths within the well.

Collection of various geophysical logs (including unpumped and pumped well-bore flow logs) and collection of water-quality samples at a single well commonly required four people working 5 days. Data were collected by USGS field crews with site access and logistical support from local landowners, including PG&E. Data from two sampled wells were supplemented with CPT data collected as part of this study, and one well had step-drawdown data collected by PG&E consultants when the well was first installed (Christopher Maxwell, Stantec, written commun., 2017).

Production pumps were removed from the wells prior to logging to allow entry for geophysical logging tools (fig. H.4). Natural-gamma and caliper logs were collected from wells under unpumped conditions to provide geologic information and to confirm well-construction data. Fluid resistivity, fluid temperature, and well-bore flow logs also were collected during unpumped conditions. After collection of unpumped logs, a temporary submersible pump was installed; and fluid resistivity, fluid temperature, and well-bore flow logs were collected under pumped conditions. Depth-dependent water samples were collected, while the well was pumped using the temporary pump, from a 2-in-diameter PVC pipe installed at selected depths within the well. Sample collection depths were selected on the basis of well-construction data and unpumped and pumped log data. Coupled well-bore flow and depth-dependent water-quality data provide information on well yield and water quality with depth in the well (Izbicki and others, 1999).

Photograph by Greg Smith, U.S. Geological Survey, June 2015

Figure H.4. Borehole geophysical logging in well 27-03 after the production pump was removed, Hinkley Valley, western Mojave Desert, California, June 2016. Well location and construction data for well 27-03 are available in appendix H.1 (table H.1.1).

Wells were pumped using temporary submersible pumps at rates ranging from 4 to 45 gallons per minute (gal/min). The lowest pump rate was in well 27-38 (the former Hinkley School well), which was completed in bedrock. Although pumping stresses are smaller, data collected using the temporary pumps were considered analogous to conditions within wells imposed at higher pumping rates by production pumps. Water levels were monitored during pumping, and instantaneous and cumulative discharge from temporary pumps were measured at the surface using a sonic flowmeter. Pumped water was either contained in tanks for later treatment or discharged to agricultural or vacant land depending on site conditions.

Unpumped and pumped well-bore flow data were collected in the downward direction at three trolling speeds (5, 10, and 15 ft/min). Centralizers were used to ensure the EM flowmeter stayed near the center of the well, but diverters were not used to allow passage of the tool around the temporary pumps.

Unpumped flow-log data collected at each of the three (nominal) trolling speeds were plotted with depth to ensure the EM flowmeter response increased proportionately with trolling speed throughout the well (fig. H.5*A*). The average flowmeter response (in counts per second) from an unscreened interval within the well where no flow was present (fig. H.5*A*) was related to the trolling speed (the average measured line speed) using linear regression by the method of least-squares (Neter and Wasserman, 1974; Helsel and others, 2020). The regression equation developed from these data (fig. H.5*B*) was used to estimate unpumped flow throughout the well in ft/min. If an unscreened section was not available, a section where flow within the well was not increasing or decreasing was used to relate flowmeter response to trolling speed and estimate unpumped flow. Well diameter, obtained from caliper log data, was used to calculate the cross-sectional area of the well and convert well-bore flow measured in length per time (L/t) to volume per time (L^3/t). The precision of unpumped flow logs collected as part of this study was estimated as plus or minus 1 standard deviation (σ) of the EM flowmeter response measured in the unscreened section of the well.

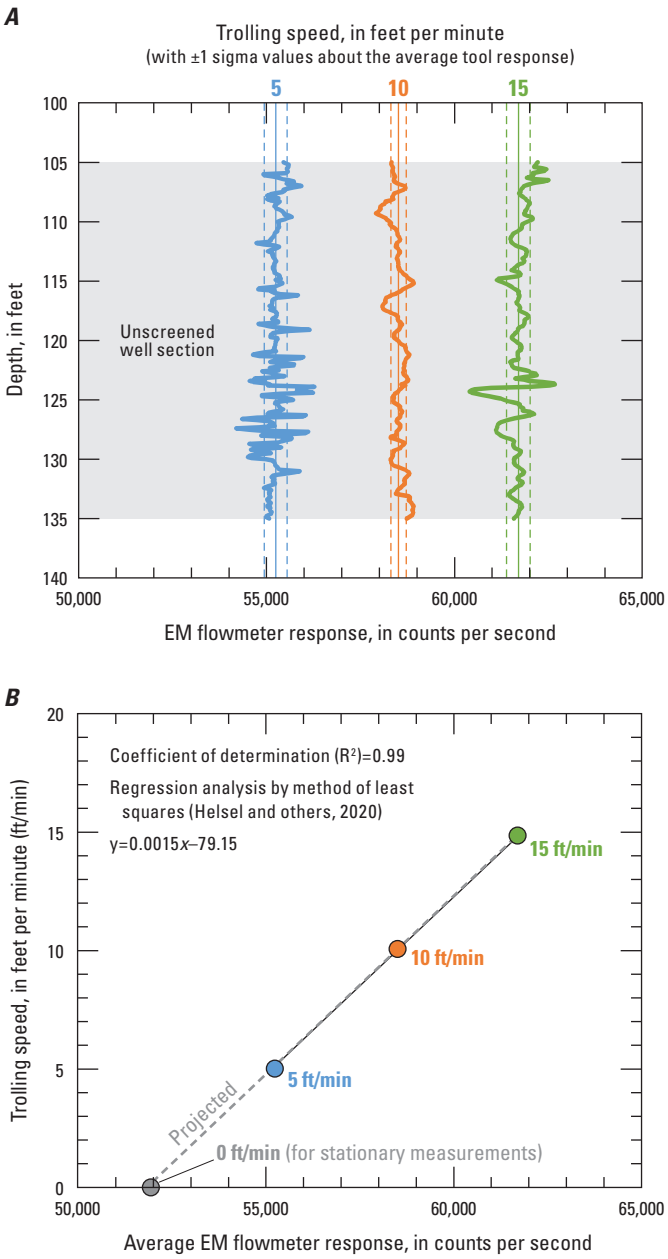

Figure H.5. Unpumped electromagnetic (EM) well-bore flowmeter data showing *A*, EM flowmeter response at selected downward trolling speeds and *B*, EM flowmeter response as a function of trolling speed, for Pacific Gas and Electric Company (PG&E) well C-01 (10N/3W-26B1S), Hinkley Valley, western Mojave Desert, California, March 21, 2016. R^2 is coefficient of determination. Data are available in U.S. Geological Survey (2019).

Pumped flow-log data collected at each of the three trolling speeds were plotted with depth to ensure the EM flow response increased proportionately with trolling speed throughout the well (fig. H.6*A*). Two least-squares regression equations (Neter and Wasserman, 1974; Helsel and others, 2020) were developed to describe the relations between flowmeter responses (in counts per second) measured throughout the entire well at different trolling speeds (fig. H.6*B*). The first regression equation related flowmeter responses to trolling speeds of 5 and 10 ft/min, and the second regression equation related flowmeter responses to trolling speeds of 5 and 15 ft/min. For a linear flowmeter response, both regression lines would have a slope of 1 and the difference in counts per second over the range of flowmeter responses between the two regression equations would be constant. The EM flowmeter response was generally non-linear over the range of flows encountered in pumped wells, and the flowmeter response in counts per second generally increased with increased flow. To correct for non-linearity, the difference between the two regression lines (counts per second at a trolling speed of 5 ft/min) was used to develop a regression equation to estimate pumped flow throughout the well in ft/min (fig. H.6*C*). Flow was then calculated according to the following equation:

$$Flow = CPS - \frac{PZF}{(CPS^{*}Y) - X} + Tr \qquad \text{(H.6)}$$

where

Flow is well-bore flow in ft/min;

CPS is measured tool response (pumped) in counts per second;

PZF is the point of zero flow (measured tool response in counts per second at selected trolling speed where well-bore flow is equal to zero); *PZF* can be estimated from field data (in order of preference) as

(1) data collected within an unscreened interval of the well having no flow (commonly an interval above the pump),

(2) data collected in an interval of the well below the pump having no flow (commonly near the bottom of the well), or

(3) from unpumped log data.

Y is the slope of the regression line (fig. H.6*C*);

X is the intercept of the regression line (fig. H.6*C*); and

Tr is the trolling rate in ft/min, for logs collected in the down direction *Tr* is negative.

Well-bore velocity was calculated from the 5 ft/min trolling log (or from the 10 ft/min trolling log if the 5 ft/min log was of poor quality). In some wells, well-bore flow was calculated from the running average of the flow response over a short interval (commonly 2 ft) to smooth data from noisy intervals within the well. Previous studies have shown that without correcting for non-linearity, there may be as much as a plus or minus 20 percent error in measured flow within a well (Izbicki and others, 2015). In contrast, corrected flow commonly agrees with flow measured at the surface discharge of the well within plus or minus 6 percent (Izbicki and others, 2015). Well-bore velocity was converted to well-bore flow using well diameter from the caliper log data in the same manner as unpumped flow logs.

Stationary log data (stop counts) were collected during pumped and unpumped conditions in the large diameter wells by suspending the EM flowmeter within the well at a selected depth for 5 to 10 minutes. Measurements in counts per second were converted to well-bore flow velocities using unpumped or pumped regression equations described previously (fig. H.6*C*). Unlike trolling logs, stationary logs are not continuous measures of well-bore flow. However, stationary-log data are used for quality assurance and to confirm unusual features identified using trolling logs.

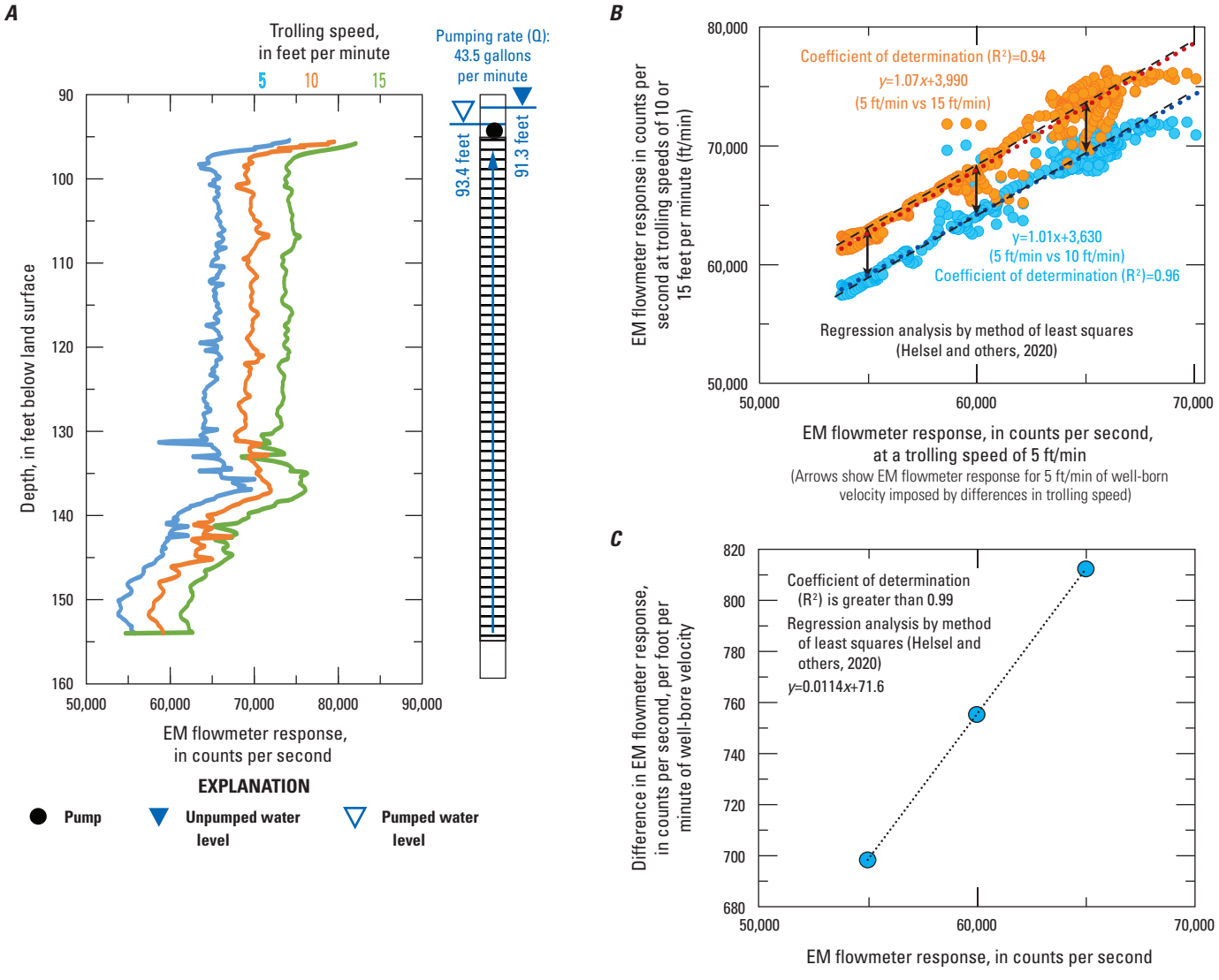

Figure H.6. Pumped electromagnetic (EM) well-bore flowmeter data showing *A*, EM flowmeter response at selected downward trolling speeds, *B*, EM flowmeter response at 10 feet per minute (ft/min) as a function of 5 ft/min and EM flowmeter response at 15 ft/min as a function of 5 ft/min, and *C*, counts per second at 1 ft/min for selected EM flowmeter responses, for Pacific Gas and Electric Company (PG&E) well IW-03 (10N/3W-26L34S), Hinkley Valley, western Mojave Desert, California, March 1, 2015. Data are available in U.S. Geological Survey (2019).

Depth-dependent water-quality samples were collected from wells during pumping conditions from new 2-in. diameter PVC pipes emplaced in the well with the open end of the pipe at the sample depth. Sample water was pumped from the pipes using sample pumps in the same manner as an observation well. The chemistry of water sampled from the deepest depth within a well is representative of the chemistry of water in the aquifer at that depth. The chemistry of water entering the well at each subsequently shallower sample depth is a mixture of water from the deeper depth and water that entered the well between the two sample depths. The chemistry of water that entered the well between the two sample depths was calculated for each constituent of interest on the basis of measured changes in well-bore flow between the two intervals and changes in concentration between the two intervals according to the following equation (Izbicki, and others, 1999; Izbicki, 2004):

$$(C_3 * V_3) = (C_1 * V_1) + (C_2 * V_2) \quad \text{(H.7)}$$

Rearranged to

$$C_2 = \frac{(C_3 * V_3) - (C_1 * V_1)}{V_2} \quad \text{(H.8)}$$

where

V is flow, in volume (unit length cubed per unit time, L^3/t); and

C is concentration, in unit mass per unit length cubed, M/L^3.

Subscripts in the equations refer to sample depth; V_2 was calculated from measured flow data as the equation below:

$$V_2 = V_3 - V_1. \quad \text{(H.9)}$$

where

1 is the measurement point at the bottom of the sample interval;

2 is the interval between the sample points; and

3 is the measurement point at the top of the sample interval.

Depth-dependent water-quality data for the five sampled production wells are available in appendix H.1 (table H.1.5). The data also are available in U.S. Geological Survey (2021).

H.3. Results and Discussion

Results describing (1) predevelopment water-level data, (2) estimation of areal recharge and local runoff, (3) lithology and hydraulic conductivity of aquifer materials, (4) groundwater movement near the Lockhart fault, and (5) coupled well-bore flow and depth-dependent water-quality data are presented. Results are discussed with respect to understanding of the groundwater-flow system in Hinkley and Water Valleys.

H.3.1. Predevelopment Water Levels, Water-Level Change, and Saturated Thickness

During predevelopment conditions, water-levels ranged from about 2,220 ft above sea level (referenced to the North American Vertical Datum of 1988, NAVD 88) along the Mojave River south of Iron Mountain to about 2,020 ft near Harper (dry) Lake (fig. H.7; appendix H.1, table H.1.2). Groundwater flowed north through Hinkley Valley from recharge areas along the Mojave River and through Hinkley Gap to discharge areas near the margin of Harper (dry) Lake. Impediments to groundwater flow along the Lockhart and Mount General faults were not observed in water-level data collected under predevelopment conditions. Water levels were above or near land surface along parts of the Mojave River and near the margin of Harper (dry) Lake where flowing wells were present during predevelopment conditions (Thompson, 1929). Water levels less than 20 ft below land surface (bls) throughout much of the area (fig. H.8*A*) allowed early development of agriculture and railroad infrastructure within Hinkley and Water Valleys. Predevelopment depths to water near the Hinkley compressor station were about 27 ft bls (fig. H.8*A*).

Thompson (1929) described areas of extensive salt grass and rabbit brush extending more than 1 mi upgradient from the margin of Harper (dry) Lake; this vegetation would have been supported by water levels near or above land surface where groundwater would have discharged by evaporation during predevelopment conditions (fig. H.8*A*). Average annual evapotranspiration rates for other areas in the Mojave River groundwater basin with similar vegetation types and densities were estimated to range from 1 to 3 acre-feet per year (acre-ft/yr) with an average value of about 2 acre-ft/yr (Lines, 1996), indicating groundwater discharge along the margins of Harper (dry) Lake would have been about 1,640 acre-ft/yr and may have ranged from 820 to 2,460 acre-ft/yr. Most of this water was recharged from the Mojave River (Thompson, 1929; Stamos and others, 2001; Izbicki, 2004) and flowed through Hinkley Gap. Groundwater movement through Hinkley Gap during predevelopment conditions has been estimated in previous studies to range from about 820 to 2,460 acre-ft/yr (California Department of Water Resources, 1967; Stamos and others, 2001; Aquifer Science and Technology, 2007; Laton and others, 2007). Miller and others (2018b) suggested, on the basis of the extent of groundwater discharge deposits and Native American artifacts found throughout the area, that the volume of groundwater moving from the Mojave River through Hinkley Gap to discharge areas along Harper (dry) Lake was greater in prehistoric times.

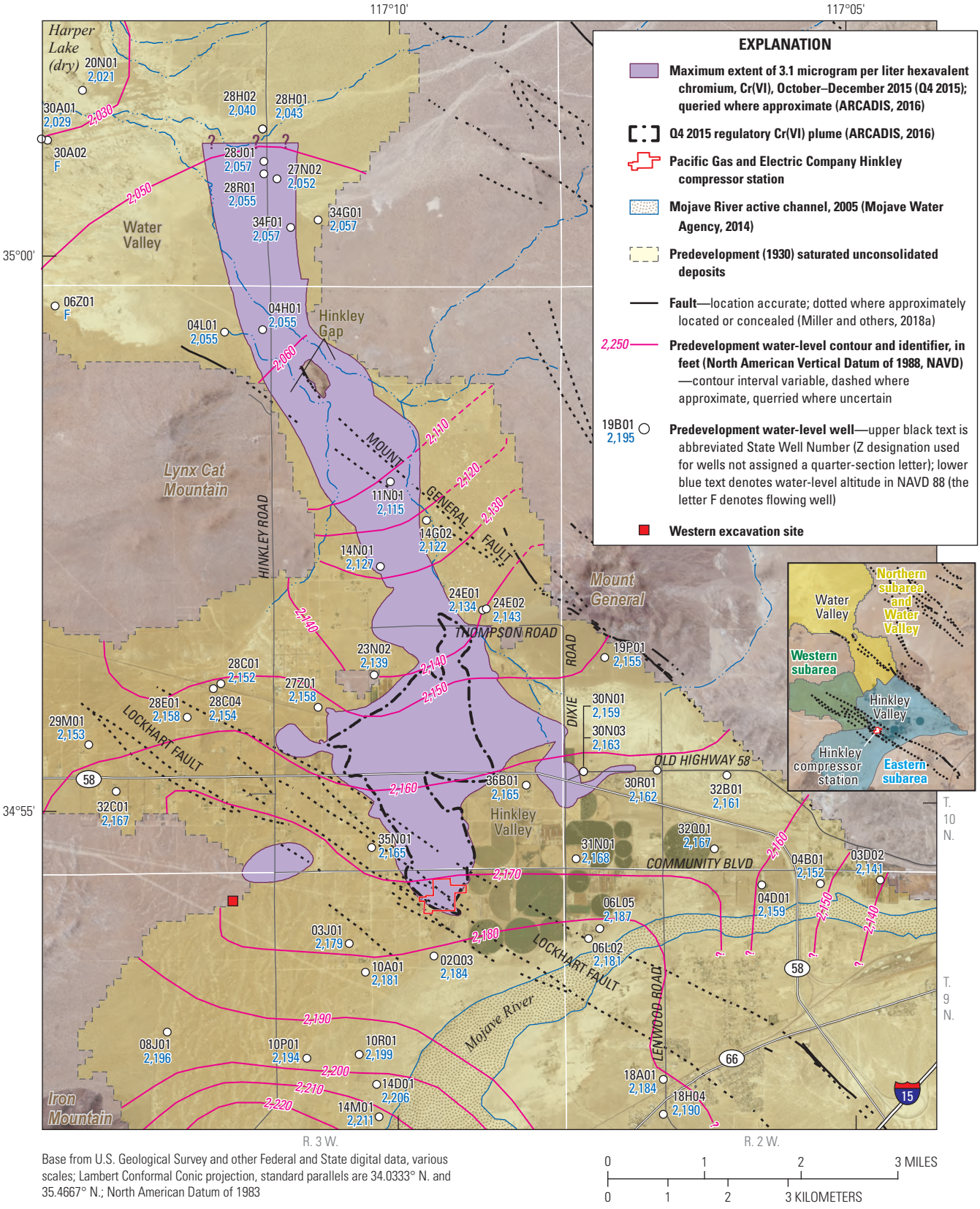

Figure H.7. Predevelopment (pre-1930) groundwater-level contours and wells with data, Hinkley and Water Valleys, western Mojave Desert, California. Data are available in U.S. Geological Survey (2021) and appendix H.1 (table H.1.2).

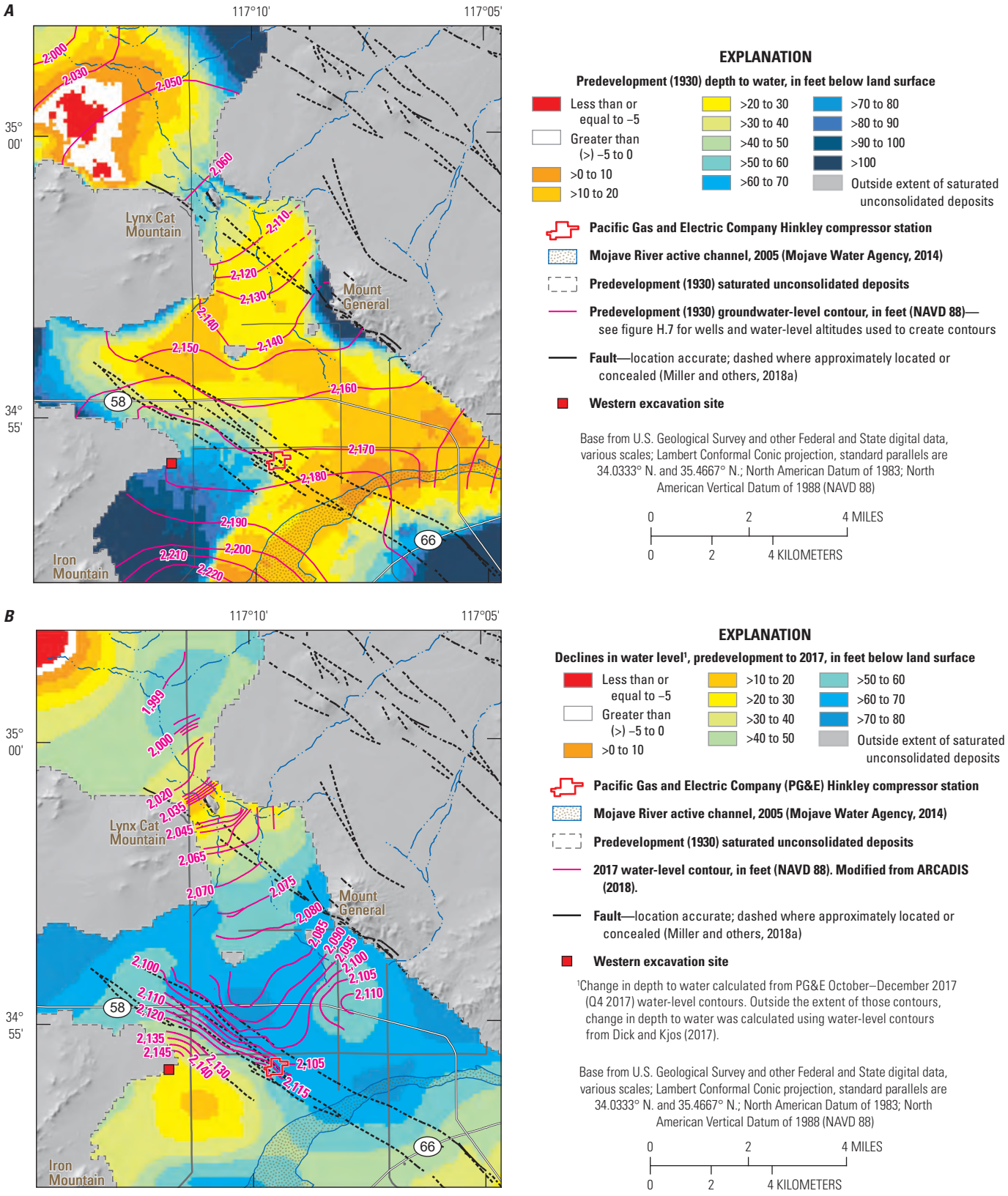

Figure H.8. Groundwater-level contours and depth to water during *A*, predevelopment (pre-1930) conditions, *B*, the change in water levels between predevelopment and 2017 conditions, *C*, the predevelopment thickness of saturated alluvium, and *D*, the saturated thickness of saturated alluvium at the time of this study, Hinkley and Water Valleys, western Mojave Desert, California. Data are available in ARCADIS (2018), U.S. Geological Survey (2021), and appendix H.1 (table H.1.2).

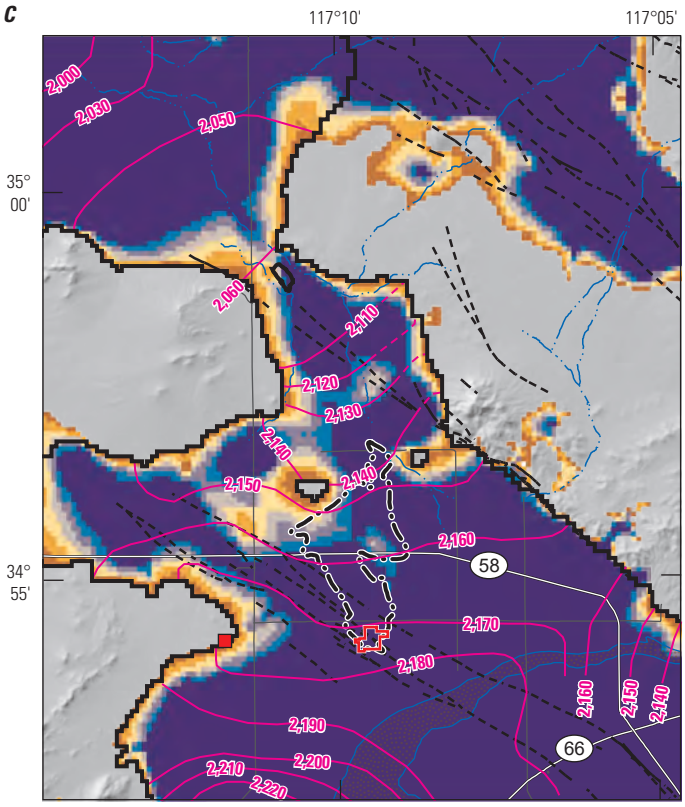

EXPLANATION

Predevelopment (1930) saturated alluvial thickness, in feet below land surface

- Less than or equal to 0
- Greater than (>) 0 to 25
- >25 to 50
- >50 to 75
- >75 to 100
- >100 to 125
- >125 to 150
- >150

- **October–December 2015 (Q4 2015) regulatory hexavalent chromium, Cr(VI), plume (ARCADIS, 2016)**
- **Pacific Gas and Electric Company Hinkley compressor station**
- **Mojave River active channel, 2005 (Mojave Water Agency, 2014)**
- **Predevelopment (1930) saturated unconsolidated deposits**
- **Predevelopment (1930) water-level contour, in feet (NAVD 88)**—see figure H.7 for wells and water-level altitudes used to create contours
- **Fault**—location accurate; dashed where approximately located or concealed (Miller and others, 2018a)
- **Western excavation site**

Base from U.S. Geological Survey and other Federal and State digital data, various scales; Lambert Conformal Conic projection, standard parallels are 34.0333° N. and 35.4667° N.; North American Datum of 1983; North American Vertical Datum of 1988 (NAVD 88)

0 2 4 MILES
0 2 4 KILOMETERS

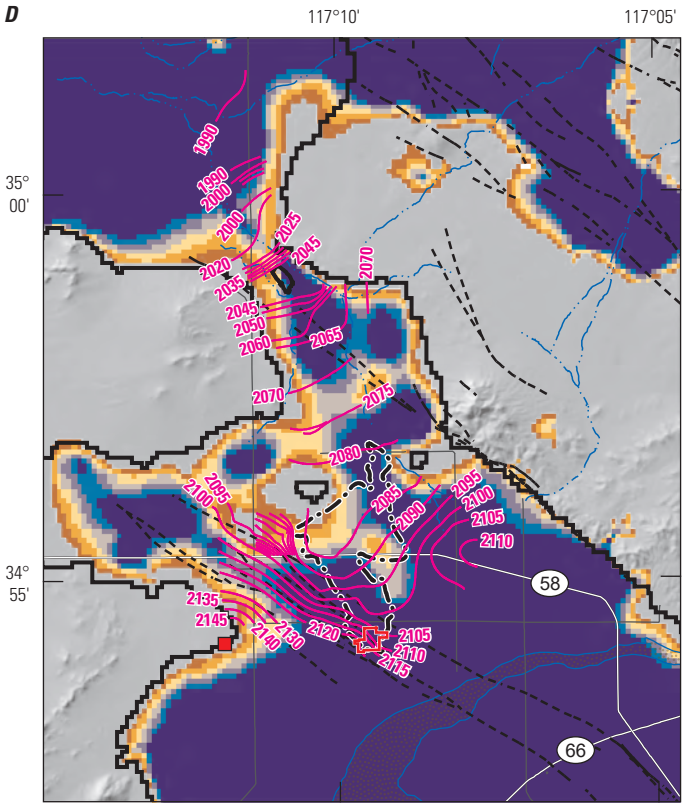

EXPLANATION

2017 saturated alluvial thickness[1], in feet below land surface

- Less than or equal to 0
- Greater than (>) 0 to 25
- >25 to 50
- >50 to 75
- >75 to 100
- >100 to 125
- >125 to 150
- >150

- **October–December 2015 (Q4 2015) regulatory hexavalent chromium, Cr(VI), plume (ARCADIS, 2016)**
- **Pacific Gas and Electric Company (PG&E) Hinkley compressor station**
- **Mojave River active channel, 2005 (Mojave Water Agency, 2014)**
- **Predevelopment (1930) saturated unconsolidated deposits**
- **2017 water-level altitude, in feet (NAVD 88). Modified from ARCADIS (2018; see figure H.8*B*)**
- **Fault**—location accurate; dashed where approximately located or concealed (Miller and others, 2018a)
- **Western excavation site**

[1]Saturated thickness calculated from PG&E October–December 2017 (Q4 2017) water-level contours. Outside the extent of those contours, saturated thickness was calculated using water-level contours from Dick and Kjos (2017).

Base from U.S. Geological Survey and other Federal and State digital data, various scales; Lambert Conformal Conic projection, standard parallels are 34.0333° N. and 35.4667° N.; North American Datum of 1983; North American Vertical Datum of 1988 (NAVD 88)

0 2 4 MILES
0 2 4 KILOMETERS

Figure H.8.—Continued

Groundwater levels in Hinkley Valley declined rapidly with the onset of large-scale agriculture beginning in about 1950, and by 1953 a large pumping depression was present in Hinkley Valley about 2 mi north of the Hinkley compressor station (Stone, 1957; Kunkel, 1962). Water levels beneath the Hinkley compressor station during predevelopment were about 27 ft bls; water levels at the time of the Cr(VI) releases are not precisely known. At the time of this study, between 2015 and 2018, water levels beneath the Hinkley compressor station were about 87 ft bls, and water levels throughout most of Hinkley and Water Valleys had declined by more than 60 ft from predevelopment levels (fig. H.8*B*). The total amount of groundwater removed from storage within aquifers underlying Hinkley and Water Valleys since predevelopment was estimated to be more than 660,000 acre-feet (acre-ft; Stamos and others, 2001).

Unconsolidated deposits underlying residential areas along Hinkley Road south of Lynx Cat Mountain sustained domestic pumping prior to water-level declines. In 2017, the aquifers in this area consisted of a thin layer of saturated alluvium overlying fractured bedrock that separated the western and northern subareas (fig. H.8*D*). At the time of this study, remaining residential wells in this area were screened in bedrock and were commonly pumped dry during heavy usage.

In many areas, formerly saturated deposits underlying Hinkley and Water Valleys are composed of coarse-textured Mojave River alluvium and are highly permeable. These formerly saturated deposits that may have contained Cr(VI) released from the Hinkley compressor station may have been intermittently saturated between 1952, the beginning of the Cr(VI) releases, and 2017, as a result of water-level rises caused by intermittent recharge from the Mojave River; such water-level rises have exceeded 50 ft in a single year in wells near the river (Lines, 1996).

H.3.2. Areal Recharge and Local Runoff

During predevelopment conditions, most groundwater recharge to Hinkley and Water Valleys occurred as infiltration of streamflow from the Mojave River. As a consequence of development, in 2015 some recharge also occurred as infiltration of irrigation return water and septic discharges. Local recharge for Hinkley and Water Valleys was extracted from regional estimates of runoff and streamflow computed using the Basin Characteristic Model (BCM; Flint and others, 2013, 2021; Flint and Flint, 2014).

On the basis of BCM data, the climate in Hinkley and Water Valleys is hyper-arid with annual precipitation, falling mostly as rain, of slightly more than 4 inches per year (in/yr; 110 millimeters per year, mm/yr) on the valley floor, and less than 6 in/yr (150 mm/yr) at the higher altitudes in the local mountains. High temperatures in the summer months commonly exceed 100 degrees Fahrenheit (°F) and potential evaporation approaches 60 in/yr (1,500 mm/yr) throughout the area. Potential evaporation exceeds monthly precipitation in every month of the year. Areal recharge on the valley floor and infiltration of precipitation to depths below the root zone within the local mountains are negligible and less than 0.04 in/yr (1 mm/yr).

Large accumulations of chloride were measured in water extractions from core material collected from the unsaturated zone at four undisturbed sites (MW-193, MW-195, MW-199, and MW-202) in Hinkley and Water Valleys; maximum chloride concentrations at these sites ranged from 363 to 1,280 milligrams per kilogram (mg/kg; appendix H.1, table H.1.4). Chloride is highly soluble and moves readily with infiltrating water. Accumulation of chloride from infiltrating precipitation at depths below the root zone is common in desert areas and concentrations as high as 170 mg/kg in the Mojave Desert west of Hinkley Valley (Izbicki and others, 2000b) and as high as 420 mg/kg in the Mojave Desert east of Hinkley Valley (Prudic, 1994) have been measured in the unsaturated zone. These high concentrations indicate that infiltration of precipitation below the root zone and areal groundwater recharge does not occur during the climatic conditions at the time of this study and that chloride has been accumulating in the subsurface beneath the Mojave Desert for thousands of years (Prudic, 1994; Izbicki and others, 2000b, 2002).

Chromium concentrations measured in water extractions from core material collected from the unsaturated zone overlying the water table (above 84 ft bls) at site MW-195, ranged from less than the reporting level of 0.2 to 2.3 µg/L, with a median concentration of 1.2 µg/L (appendix H.1, table H.1.4). Chromium concentrations in the unsaturated zone overlying the predevelopment water table at site MW-195 (estimated to be about 40 ft bls; fig. H.8*A*) were less than 0.4 µg/L. On the basis of these data, mobilization of chromium from the unsaturated zone during initial application of irrigation water or initial infiltration of septic discharges was not considered to be an important source of Cr(VI) to the water table.

Small amounts of recharge may occur as infiltration of streamflow in small streams draining local mountains after storms. Runoff from local precipitation in upland areas was calculated using BCM for 22 locations near the margins of the valley floor in Hinkley and Water Valleys, for 2 locations south of the Mojave River, and for 1 location west of Iron Mountain outside of Hinkley Valley (fig. H.9). Drainage areas for these sites ranged from 0.1 to 140 mi^2 (appendix H.1, table H.1.3). The largest drainage area directly contributing runoff to Hinkley Valley was 6.1 mi^2; two large drainages with areas of 67.5 and 57.7 mi^2 were present in Water Valley; and two large drainages with areas of 140 and 39.3 mi^2 were present south of the Mojave River (table H.1). The 19.9 mi^2 area draining from Iron Mountain west of Hinkley Valley was used as a surrogate for smaller drainages draining to Hinkley Valley east of Iron Mountain (table H.1).

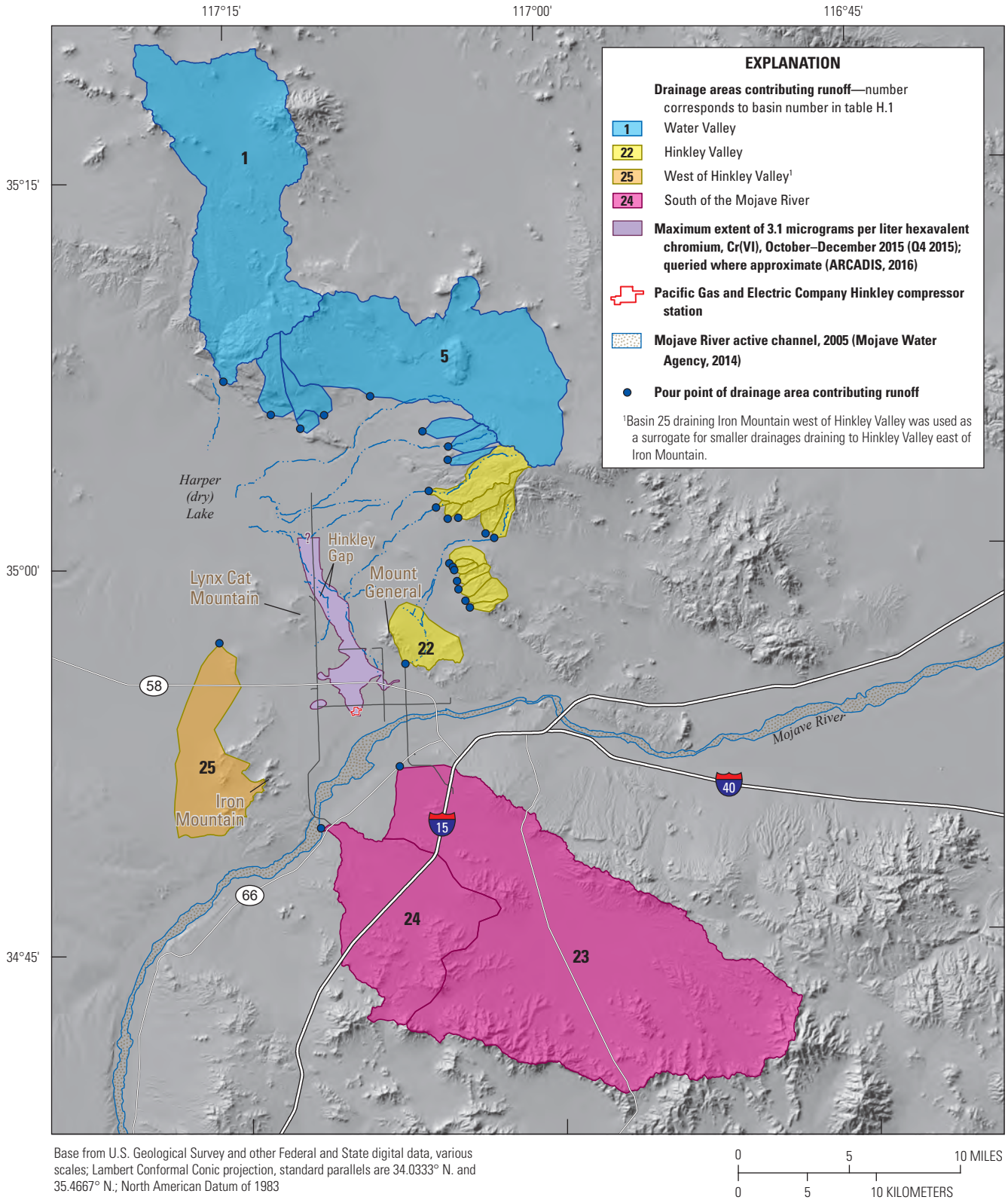

Figure H.9. Pour point locations for drainage areas contributing runoff to Hinkley and Water Valleys, western Mojave Desert, California. Location data are available in appendix H.1 (table H.1.3).

The BCM calculations for 1930 to 2015 show that runoff from upland drainages in the local mountains surrounding Hinkley and Water Valleys (excluding drainages south of the Mojave River) averages 64.7 acre-ft/yr (calculated as the sum of average annual runoff from upland drainages flowing to Hinkley and Water Valleys; table H.1), with 14.0 acre-ft/yr contributed directly to Hinkley Valley (calculated as the sum of average annual runoff from upland drainages flowing to Hinkley Valley; table H.1). Average conditions and runoff do not occur in most years (appendix H.1, table H.1.3); in years when it occurs, runoff is typically about 1,200 acre-ft (calculated as the sum of "average in month when runoff occurs" from all upland drainages, value rounded; table H.1). Most of this runoff is from larger drainages to the south of the Mojave River and in Water Valley, with only about 296 acre-ft contributed directly to Hinkley Valley (sum of "average in month when runoff occurs" values from drainages flowing to Hinkley Valley; table H.1). In February 1944, when the highest monthly runoff occurred, local runoff from small streams draining to Hinkley and Water Valleys was about 6,170 acre-ft (calculated as the sum of "maximum runoff [February 1944]" from all upland drainages, value rounded; table H.1), with about 652 acre-ft contributed directly to Hinkley Valley (appendix H.1, table H.1.3). Groundwater recharge occurs as infiltration of local runoff from upland areas in stream channels as it flows across the valley floor. Because runoff from precipitation occurs only briefly, much of the runoff from upland areas flows through stream channels to Harper (dry) Lake or to small playas within Hinkley and Water Valleys, where it evaporates and does not become groundwater recharge. Consequently, groundwater recharge is less than local runoff estimated from BCM.

Local runoff data calculated by BCM were used by PG&E consultants in support of model updates (Jacobs Engineering Group, Inc., 2019). The updated PG&E groundwater-flow model of Hinkley and Water Valleys had an average value of 85 acre-ft/yr for groundwater recharge from infiltration of local runoff (Jacobs Engineering Group, Inc., 2019). This value is similar to the BCM estimated value of 64.7 acre-ft/yr for local runoff (table H.1). For comparison, average recharge from infiltration of streamflow in the Mojave River between 1931 and 1990 was estimated to be about 17,100 acre-ft/yr from the USGS regional groundwater-flow model (Stamos and others, 2001) and between 1931 and 2015 was estimated to be about 13,400 acre-ft/yr from the updated PG&E model (Jacobs Engineering Group, Inc., 2019). In some years, recharge as infiltration of streamflow from the Mojave River can exceed 100,000 acre-ft (chapter F, fig. F.2; Stamos and others, 2001).

Table H.1. Summary of runoff data from upland drainages estimated from Basin Characteristic Model (BCM), Hinkley and Water Valleys, western Mojave Desert, California, 1930–2015.

[Data were extracted from Flint and others (2013, 2021) and are available in appendix H.1 (table H.1.3).The maximum runoff occurred in February 1944. Abbreviations: mi², square mile; acre-ft/yr, acre-foot per year; acre-ft, acre-foot]

Basin number[1]	Drainage area, in mi²	Average annual runoff, in acre-ft/yr	Number of months runoff occurred	Average in month when runoff occurs, in acre-ft	Maximum runoff (February 1944), in acre-ft
Water Valley					
1	67.5	40	16	217	270
5	57.7	3.0	14	218	639
Other Water Valley sites	11.0	7.7	5–13	92	157
Hinkley Valley					
22	6.1	2.8	9	27	105
[2]25	19.9	6.5	3	188	445
Other Hinkley Valley sites	13.7	4.7	0–5	81	102
South of Mojave River					
23	140	341	116	253	3,650
24	39.3	42	30	123	803

[1]Basin numbers shown on figure H.9 and in appendix H.1, table H.1.3.

[2]Site 25 is along the west side of Iron Mountain outside of Hinkley Valley. Runoff at this site provides an estimate of aggregated upland runoff to Hinkley Valley from the east side of Iron Mountain.

Local recharge from infiltration of runoff from upland areas is less than 1 percent of the recharge to Hinkley Valley from infiltration of Mojave River streamflow. These values are consistent with delta oxygen-18 and delta deuterium data that show almost all water in Hinkley and Water Valleys was recharged from the Mojave River (chapter F, fig. F.3). Water from wells having delta oxygen-18 and delta deuterium compositions consistent with local recharge. present in a few deep wells near the margins of the aquifer, was likely recharged at a time when the climate in the area was cooler and wetter (chapter F).

Groundwater recharge temperature data, excess-air data (chapter F), and physical measurements of streamflow losses at gaging stations along the Mojave River (Lines 1996; Stamos and others, 2001) show changes in the timing and amount of recharge from the Mojave River have occurred as a result of groundwater development. Average recharge values calculated between 1931 and 2015 are not representative of predevelopment groundwater recharge to Hinkley Valley because recharge from infiltration of streamflow from the Mojave River has changed as a result of groundwater development.

H.3.3. Lithology and Hydraulic Conductivity of Aquifer Materials

The hydraulic conductivity of saturated aquifer materials was evaluated on the basis of slug-test data collected from 95 monitoring wells in Hinkley and Water Valleys between October 2015 and August 2017 (fig. H.1). On the basis of slug-test data, hydraulic conductivities measured in selected wells ranged from 0.01 to 680 ft/day (appendix H.1, table H.1.1). Hydraulic conductivities were higher in Mojave River alluvium, with the highest value in well BG-0005A screened in older Mojave River alluvium upgradient of the Lockhart fault. Values were lowest in wells completed in mudflat/playa deposits. Where shallower and deeper wells were tested at the same site, hydraulic conductivities decreased with depth at 70 percent of sites.

Slug-test data commonly underestimate aquifer hydraulic conductivity (Butler and Healey, 1998) but provide a basis for comparison of wells having higher and lower values. Hydraulic-conductivity values from slug-test data were used to estimate initial hydraulic properties in the updated groundwater-flow model in areas where other data were not available (Jacobs Engineering Group, Inc., 2019).

H.3.3.1. Lithology and Groundwater Movement through Hinkley Gap and the Northern Subarea of Hinkley Valley

Under predevelopment conditions, groundwater in Hinkley Valley flowed to the north from recharge areas along the Mojave River through Hinkley Gap to evaporative discharge areas near the margin of Harper (dry) Lake (Thompson, 1929). Hinkley Gap separates Hinkley and Water Valleys and is partly backfilled by unconsolidated deposits separated on the west and east by Red Hill (fig. H.1). Groundwater movement through Hinkley Gap is an important component of the water budget in Hinkley Valley.

On the basis of CPT data, depth to bedrock in the western part of Hinkley Gap is about 90 ft, and aquifer deposits in this area are composed primarily of coarse-textured Mojave River alluvium (fig. H.10*A*). Access was not available to collect CPT data on the eastern side of Hinkley Gap. However, saturated thickness calculated from gravity data (figs. H.8*C*, *D*) indicates that unconsolidated deposits are thicker on the eastern side of Hinkley Gap. Thickness and lithology of unconsolidated deposits in the eastern side of Hinkley Gap were evaluated on the basis of drill cuttings and core material at monitoring well sites MW-132, MW-133, and MW-154, including geophysical logs collected at MW-154 (appendix H.1, table H.1.1). Although unconsolidated deposits on the east side of the gap are composed of fine-textured lacustrine deposits at depth, coarse-textured Mojave River and lake-margin deposits described by Miller and others (2018a) were present above the water table at the time of this study (fig. H.10*B*). These coarse-textured deposits would have been partially saturated during predevelopment.

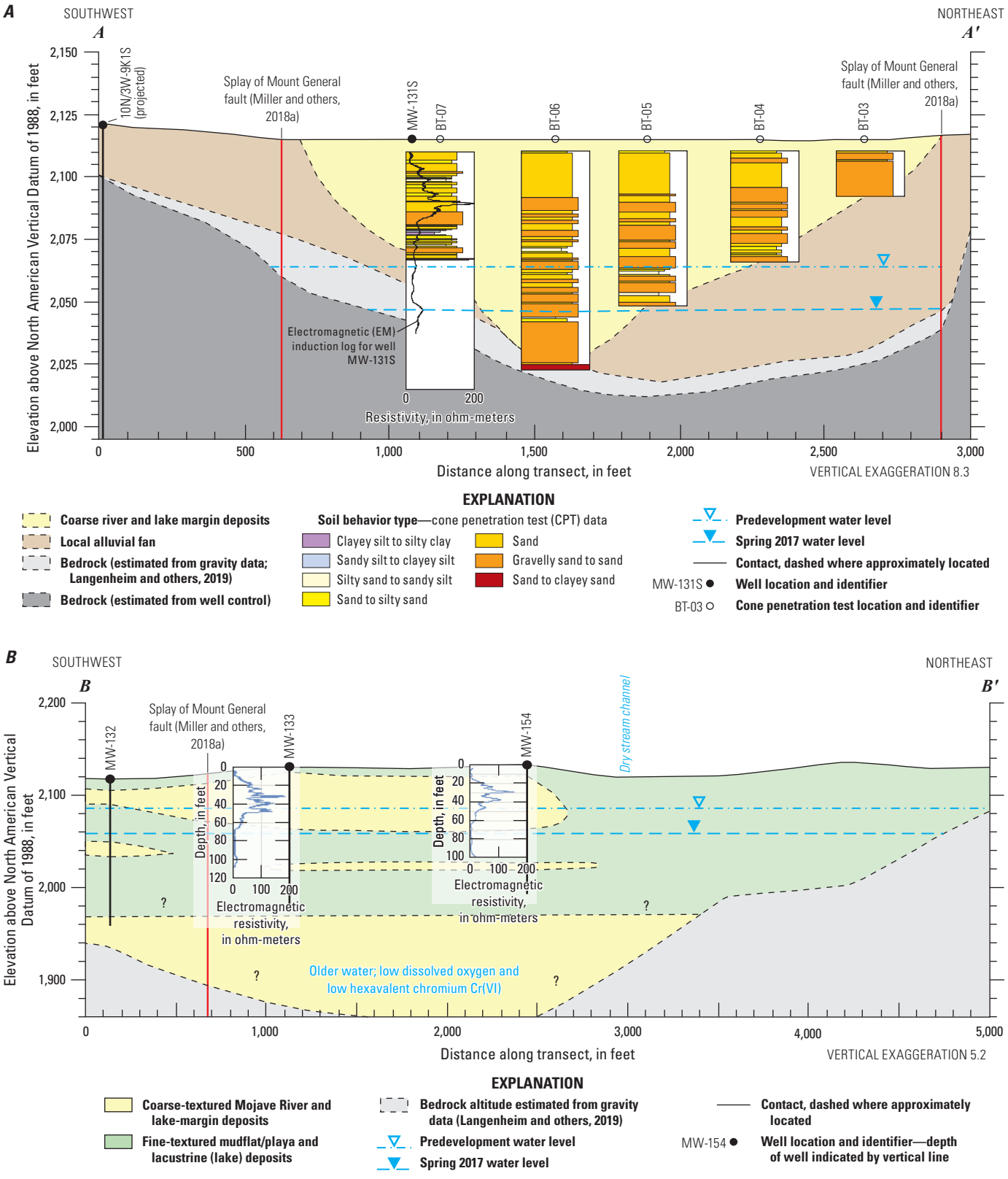

Figure H.10. Cross sections across Hinkley Gap *A*, section A–A′, western Hinkley Gap; and *B*, section B–B′, eastern Hinkley Gap, Hinkley and Water Valleys, western Mojave Desert, California. Cross-section locations are shown on figure H.1. Cone penetration test and electromagnetic resistivity log data are available in U.S. Geological Survey (2019), and geologic provenance data are available in Miller and others (2020).

Darcy calculations (Freeze and Cherry, 1979) were used to estimate groundwater movement from Hinkley Valley through Hinkley Gap during predevelopment. Estimated hydraulic conductivities of 200 and 6 ft/d were used for coarse-textured Mojave-type deposits and fine-textured materials, respectively (fig. H.10*A*). A groundwater gradient of 0.008 estimated from predevelopment water-level data (fig. H.8*A*) was used in the calculations. Predevelopment groundwater movement through the western part of the gap was estimated to be about 320 acre-ft/yr, and groundwater movement through shallow deposits underlying the eastern part of Hinkley Gap was about 250 acre-ft/yr, resulting in a total predevelopment groundwater movement of about 570 acre-ft/yr through Hinkley Gap. Groundwater movement through deeper, coarse-textured deposits in the eastern part of Hinkley Gap (fig. H.10*B*) was not calculated. Previous estimates of groundwater movement through Hinkley Gap during predevelopment range from 820 to 2,460 acre-ft/yr (California Department of Water Resources, 1967; Stamos and others, 2001; Aquifer Science and Technology, 2007; Laton and others, 2007). Mojave River deposits through Hinkley Gap likely were deposited in a fast-flowing stream environment; if the hydraulic conductivity of formerly saturated Mojave-type deposits in Hinkley Gap is closer to the maximum measured hydraulic conductivity of 680 ft/d for Mojave River deposits, then the calculated groundwater movement through the gap during predevelopment would have been close to 1,900 acre-ft/yr. With declining water levels and a smaller groundwater gradient of 0.0018 (fig. H.8*D*), groundwater movement through the western part of Hinkley Gap at the time of this study in 2017 was about 26 and 57 acre-ft/yr through the western and eastern part of Hinkley Gap, respectively, for a total of about 83 acre-ft/yr.

Cone penetration test data collected at 34 sites in the northern subarea of Hinkley Valley by PG&E consultants (appendix H.1.1; fig. H.1; Groover and others, 2021) show coarse-textured Mojave River deposits in formerly saturated alluvium above the water table at the time of this study. These coarse-textured deposits have high permeability, are longitudinally continuous throughout the northern subarea, and likely extend upgradient into the eastern subarea near the Q4 2015 regulatory Cr(VI) plume. Cone penetration test data at these sites were used to estimate initial hydraulic properties in updated model layers representing formerly saturated alluvium (Jacobs Engineering Group, Inc., 2019).

H.3.3.2. Lithology and Hydraulic Conductivity of Formerly Saturated Material

By 2017, water levels in Hinkley and Water Valleys declined more than 60 ft from predevelopment levels as a result of agricultural pumping beginning in the early 1950s. Water-level declines caused saturated coarse-textured deposits to drain freely with the lowering water table, whereas formerly saturated fine-textured clays and silts have a greater attraction to water molecules, drain less freely, and retain predevelopment water (Hillel, 1982; Jury and others, 1991; Izbicki and others, 2007).

Nuclear magnetic resonance data collected in the formerly saturated zone (the interval between the predevelopment water table and the water table in 2017 at the time of this study) were used to assess residual moisture within fine-textured deposits. Dry intervals within the formerly saturated zone were interpreted as coarse-textured deposits that had freely drained with the lowering water table between predevelopment and aquifer conditions at the time of data collection (April 2017). Nuclear magnetic resonance-derived hydraulic-conductivity values calculated for the saturated zone using the SDR equation (eq. 1) were compared to measured immobile (clay-bound) water content (fig. H.11) to develop an equation that could be used to estimate hydraulic conductivity of aquifer materials that compose the formerly saturated zone (Groover and others, 2017).

$$K = 300.56 * e^{(-18.03 * X)} \quad \text{(H.10)}$$

where

K is the hydraulic conductivity;
e is the natural logarithm; and
X is the measured immobile (clay-bound) water content at a given depth.

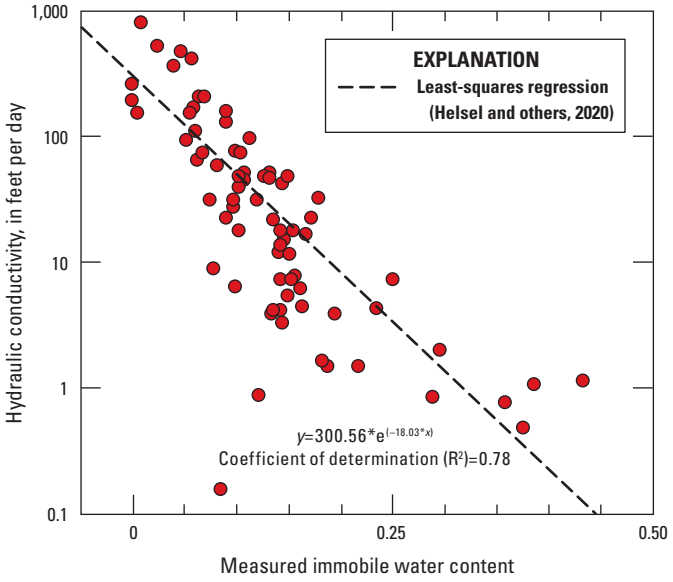

Figure H.11. Comparison between nuclear magnetic resonance (NMR) calculated hydraulic conductivity and NMR measured immobile water content for the saturated intervals of monitoring wells, Hinkley and Water Valleys, western Mojave Desert, California. Data are available in U.S. Geological Survey (2019).

Predevelopment water levels were less than 20 ft bls throughout much of Hinkley Valley and about 27 ft beneath the Hinkley compressor station. At the time of this study, water levels in well MW-217S upgradient from the Hinkley compressor station were about 87 ft bls (fig. H.12). Cone penetration test data collected adjacent to MW-217S show formerly saturated deposits composed a 30-ft-thick sequence of coarse-textured Mojave River alluvium overlain by finer-textured deposits. Increases in CPT U_2 (not shown on fig. H.12) with depth corresponded to the water table at the time of this study, and changes in pore pressure at the predevelopment water table also were measured.

The hydraulic conductivity of saturated alluvium estimated from NMR data collected within MW-217S decreases with depth below the water table from more than 100 to 7 ft/d as aquifer lithology changed with depth (fig. H.12). The geometric mean hydraulic-conductivity value for these materials of 50 ft/d compares favorably to model-derived estimates of saturated hydraulic conductivity in this area ranging from 50 to 60 ft/d (ARCADIS and CH2M Hill, 2011; Jacobs Engineering Group, Inc., 2019). Nuclear magnetic resonance estimated hydraulic conductivity for formerly saturated deposits above the 2017 water table at MW-217 were as high as 300 ft/d (fig. H.12). The distribution of these values with depth compares favorably with CPT and EM resistivity data collected at the site, indicating that more easily collected CPT and EM resistivity data can be used to estimate relative differences in the hydraulic conductivity of formerly saturated alluvium within Hinkley and Water Valleys.

Nuclear magnetic resonance-derived hydraulic-conductivity values for saturated alluvium at sites throughout Hinkley and Water Valleys were highly correlated (coefficient of determination, R^2=0.93) with hydraulic-conductivity values estimated from slug-test data (fig. H.13*A*). However, NMR hydraulic-conductivity values were typically greater than slug-test hydraulic-conductivity values for the same wells. Lower slug-test hydraulic-conductivity values compared to NMR values may reflect a greater degree of averaging within the well screen that can occur during slug tests within heterogeneous deposits.

Nuclear magnetic resonance-derived hydraulic-conductivity data show Mojave River alluvium and lake-margin deposits have median values in the saturated deposits of 73 and 11 ft/d and values as high as 784 and 93 ft/d, respectively (fig. H.13*B*). Locally derived alluvium and bedrock have median NMR-derived hydraulic-conductivity values between 6 and 2 ft/d and values as high as 47 and 16 ft/d, respectively. Mudflat/playa deposits had the lowest hydraulic-conductivity values, with a median of 0.2 ft/d, consistent with the fine-textured nature of these deposits. On the basis of NMR and slug-test data, the hydraulic conductivity of Mojave-type deposits appears to be slightly higher in the southern portion of Hinkley Valley closer to the Mojave River and lower in the northern part of Hinkley Valley (not shown on fig. H.13).

Formerly saturated deposits throughout much of Hinkley and Water Valleys are composed of Mojave River alluvium and lake-margin deposits. Nuclear magnetic resonance data indicate that prior to water-level declines from pumping, much of the formerly saturated deposits underlying Hinkley and Water Valleys had a high hydraulic conductivity, typically about 150 ft/d (fig. H.13*C*). High hydraulic conductivity values in formerly saturated mudflat/playa deposits compared to saturated mudflat/playa (figs. H.13*B*, *C*) result from geologic differences in the material. Mudflat/playa deposits within the saturated zone represent playa lake sequences (often tens of feet thick) deposited over long time intervals. In contrast, shallower mudflat/playa deposits in formerly saturated materials represent thinner, fine-textured materials (1 to 2 ft tick) deposited as overbank deposits or as sloughs within the active channel of the Mojave River (Miller and others, 2018a); despite their fine texture these materials may have been more correctly classified as Mojave River stream deposits (chapter A, table A.1).

Nuclear magnetic resonance data were used to estimate initial hydraulic properties in updated model layers representing formerly saturated alluvium (Jacobs Engineering Group, Inc., 2019). The NMR data show generally higher hydraulic conductivities in formerly saturated alluvium overlying the 2017 water table than in saturated deposits below the water table. The NMR data show hydraulic-conductivity values in formerly saturated alluvium near the Hinkley compressor station as high as 300 ft/d.

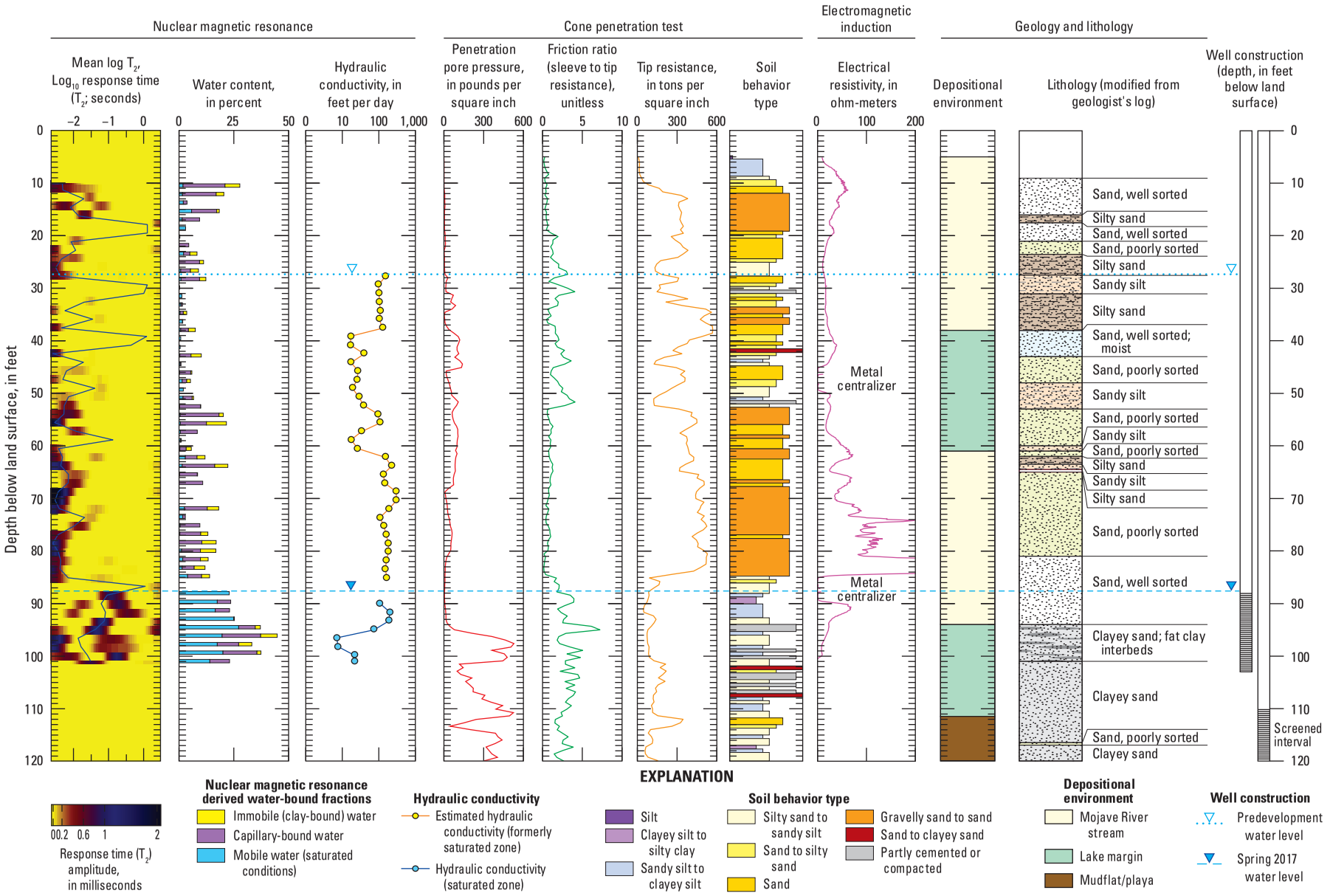

Figure H.12. Geophysical data collected at monitoring well site MW-217, Hinkley Valley, western Mojave Desert, California, March through May 2017. Geophysical log data are available in U.S. Geological Survey (2019); geologic provenance data are available in Miller and others (2020); geologists log from (Christopher Maxwell, Stantec, written commun., 2017); and hydraulic conductivity values for formerly saturated deposits were estimated using nuclear magnetic resonance geophysical log data from Groover and others (2021).

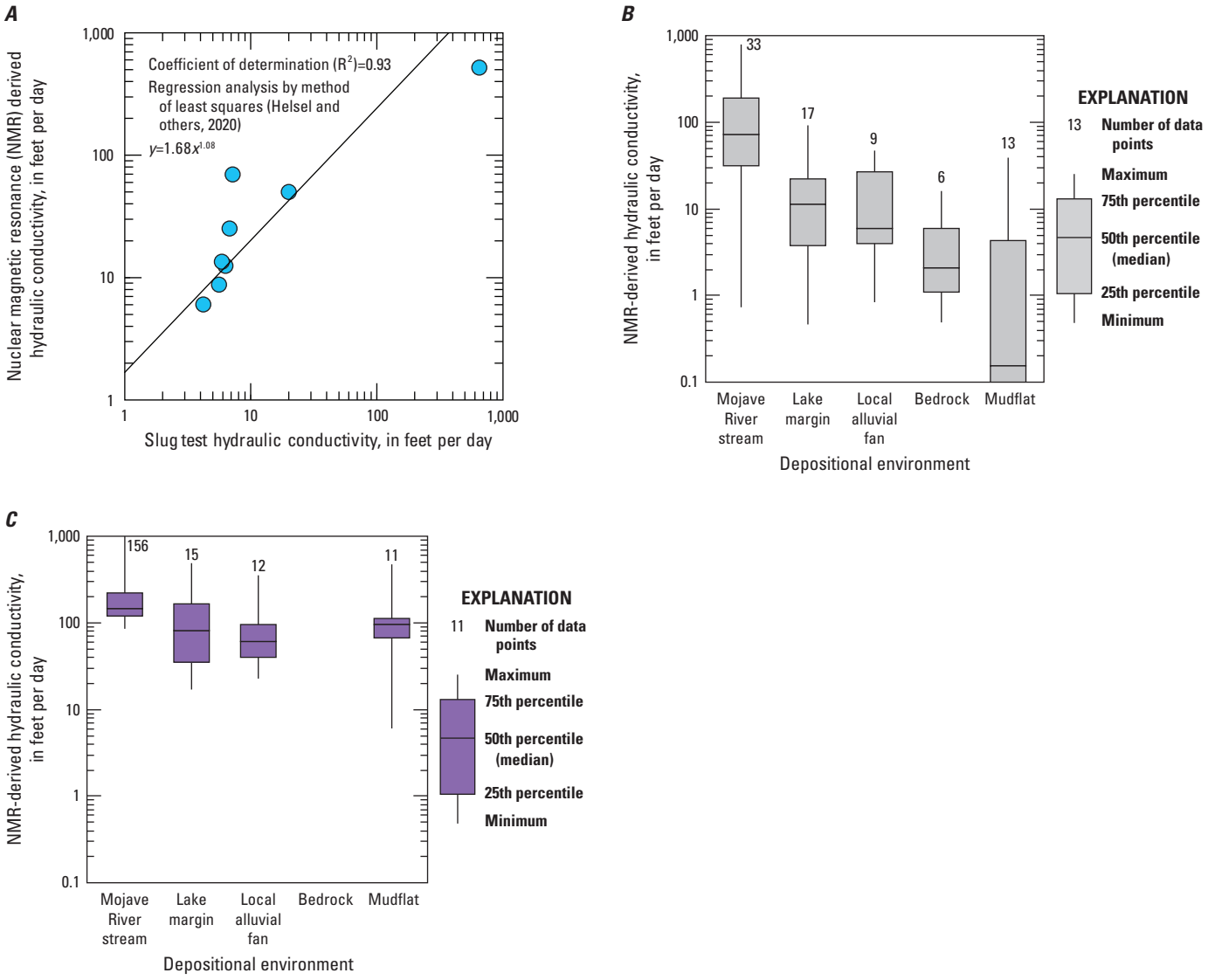

Figure H.13. Nuclear magnetic resonance (NMR) data showing *A*, relation between NMR-derived hydraulic-conductivity data and slug-test hydraulic-conductivity data, *B*, NMR-derived hydraulic-conductivity data for saturated deposits by depositional environment and *C*, NMR-derived hydraulic-conductivity data for formerly saturated deposits by depositional environment, Hinkley and Water Valleys, western Mojave Desert, California, April 2017. Nuclear magnetic resonance data are available in U.S. Geological Survey (2019), and geologic provenance data are available in Miller and others (2020).

H.3.4. Groundwater Movement Near the Lockhart Fault

The Lockhart fault is composed of multiple fault strands in the southern part of Hinkley Valley (Haddon and others, 2018; Miller and others, 2018a). The complex nature of the fault was not recognized during previous studies (Thompson, 1929; Dibblee, 1967; Jennings, 2010). Splays of the Lockhart fault follow a northwest trending gravity low mapped by Miller and others (2020). Subsurface geology across the Lockhart fault, mapped as part of this study by Miller and others (2018a), shows disruption of aquifer materials, with tilted beds and changes in the depth of key lithologic units penetrated by boreholes, such as the blue clay, across a 1 mi wide fault zone near the Hinkley compressor station (fig. H.14). Changes in the water-table elevation across the fault indicate that the Lockhart fault impedes groundwater flow within unconsolidated deposits (Stone, 1957; California Department of Water Resources, 1967; Stamos and others, 2001). Ground ruptures associated with the fault extend to land surface, consistent with movement of the fault after deposition of aquifer deposits. The surficial ground ruptures indicate that effects of the fault on groundwater flow extend throughout the deposits (Miller and others, 2020). The Mojave River has incised the alluvial deposits and that incision has been partly backfilled by younger deposits. The Lockhart fault is not an impediment to groundwater flow within those younger deposits (Stamos and others, 2001).

Vertical water-level gradients in multiple-well sites and vertical PVP-flow data collected as part of this study did not consistently show upward movement of water on the upgradient side of the fault or downward movement of water on the downgradient side of the fault, similar to other faults within the region (Lines, 1996; Miller and others, 2018b). However, some wells near mapped fault strands show upward movement of groundwater on the upgradient side of those strands.

Horizontal groundwater-flow directions were measured in selected wells between May 2 and 19, 2017 (table H.2), using either the colloidal borescope or the heat-pulse flowmeter PVP. Data were compared to water-level data and water-level contour maps prepared by PG&E consultants for Q2 2017 (April–June 2017; ARCADIS, 2017). Most wells near the Lockhart fault were measured using the colloidal borescope. Horizontal groundwater flow within deep wells MW-160D or MW-158CR could not be measured using the colloidal borescope due to a lack of particles within the well water. Horizontal flow in wells MW-77D and BG-0003B were measured using the heat-pulse flowmeter (table H.2).

Groundwater-flow directions across the Lockhart fault near the Hinkley compressor station measured using PVPs ranged from northeasterly along the eastern part of the fault to northwesterly along the western part of the fault (fig. H.14). In shallow wells, measured groundwater-flow directions were generally similar to the nominal direction of groundwater flow estimated from water-level data (fig. H.14). However, measured groundwater-flow directions in wells MW-159S, BG-0003A, and BG-0005A on the upgradient side of the fault were deflected to the west compared to the nominal direction of groundwater flow. Measured groundwater-flow directions in wells MW-155S and MW-158SR within fault strands to the northwest also were deflected to the west. Measured groundwater-flow directions, in wells MW-149S, MW-77S, and MW-217S within fault strands to the southeast near the Hinkley compressor station and in well MW-178S on the downgradient side of the fault, align with the nominal direction of groundwater flow estimated from water-level data (fig. H.14). In deeper wells, measured groundwater-flow directions did not consistently align with the direction of groundwater flow in shallow wells or the nominal direction of groundwater flow estimated from water-level data. The direction of groundwater flow in some wells was affected by pumping in nearby domestic wells (table H.2). Pumping may have altered the vertical gradients commonly observed near other faults in the region. Point-velocity probe data show the effect of the Lockhart fault on groundwater flow on the upgradient side of the fault and to the northwest along the fault may be greater than indicated by water-level data. These data indicate that fault properties may differ along the fault or that proximity to the incised channel of the Mojave River and variable recharge fluxes from the river may influence groundwater movement across the fault.

Groundwater-flow velocities, corrected using the borehole acceleration factor (eq. 5; Drost and others, 1968; Bayless and others, 2011), ranged from 0.29 to 21 ft/d (table H.2). Corrected velocities were highest near the water table and decreased with depth, similar to the vertical distribution of hydraulic-conductivity values calculated from slug-test and NMR data. Corrected velocities were highest at monitoring well site BG-0005A that is upgradient of the Lockhart fault; BG-0005A had a hydraulic conductivity of 680 ft/d, which is the highest value measured from slug-test data (appendix H.1, table H.1.1). Groundwater-flow velocities in monitoring wells within splays of the Lockhart fault ranged from 0.54 to 6.8 ft/d and were generally lower than measured velocities in wells upgradient and downgradient of the Lockhart fault (fig. H.14).

Table H.2. Groundwater-flow directions and velocity data estimated from horizontal point-velocity probe data and calculated borehole acceleration factors, Hinkley Valley, western Mojave Desert, California. Data calculated from point velocity probe data are available in U.S. Geological Survey (2019).

[Measurement date in month/day/year. Uncorrected and corrected flow velocities are estimates of flow velocities at the measurement depths and are not representative of the bulk movement of groundwater. Borehole acceleration factor, α, Drost and others (1968) and Bayless and others (2011). Shallow monitoring wells are identified by suffix S or A; middle monitoring wells identified by suffix B; and deep monitoring wells identified by suffix D or C. The suffix SR is used for a replacement shallow well; the suffix CR is used for a replacement well in bedrock. Measurement type CB is colloidal borescope; HP is heat-pulse. **Abbreviations**: mm/dd/yyyy, month/day/year; ft bls, feet below land surface; ft/d, foot per day; BG, background study; MW, monitoring well; —, no data or not measured]

Site name	Measurement date (mm/dd/yyyy)	Water level depth, in ft bls	Measurement depth, in ft bls	Flow direction, in azimuth degrees	Uncorrected flow velocity, in ft/d	Borehole acceleration factor, unitless	Corrected flow velocity, in ft/d	Measurement type
BG-0003A	05/02/2017	102.60	115	348	39	3.43	11	CB
BG-0003A	05/02/2017	102.60	119.5	331	53	3.43	15	CB
BG-0003B	05/02/2017	107.67	163	77	1.1	3.84	0.29	HP
BG-0003C	05/02/2017	108.02	185	10	36	3.68	9.8	CB
BG-0005A	05/04/2017	100.95	107.8	21	47	2.54	18	CB
BG-0005B	05/04/2017	109.73	172	33	33	3.86	8.6	CB
MW-77S	05/03/2017	89.70	91	66	12	4.02	3.0	CB
MW-77S	05/03/2017	89.70	91	94	13	4.02	3	CB
MW-77D	05/03/2017	85.96	115	188	1.8	3.95	0.46	HP
MW-149S	05/05/2017	109.37	110	57	36	3.47	10	CB
MW-155S	05/05/2017	111.56	116	15	11	3.51	3	CB
MW-155S	05/05/2017	111.56	124	13	24	3.51	6.8	CB
MW-155D	05/01/2017	104.10	147	39	17	3.86	4.4	CB
MW-158SR	05/16/2017	102.61	111	—	—	3.56	—	CB
MW-158SR	05/16/2017	102.61	114.5	20	1.6	3.56	0.44	CB
MW-158CR	05/16/2017	96.59	142	—	—	3.47	—	CB
MW-158CR	05/16/2017	96.59	147	—	—	3.47	—	CB
MW-159S	05/15/2017	91.86	101	294	21	3.60	5.9	CB
MW-159D	05/18/2017	91.67	[1]110	95	30	3.86	8	CB
MW-159D	05/18/2017	91.67	[1]113	163	72	3.86	19	CB
MW-159D	05/18/2017	91.67	[1]116	23	49	3.86	13	CB
MW-159C	05/18/2017	94.98	[1]136	307	72	3.47	21	CB
MW-159C	05/18/2017	94.98	[1]156	304	39	3.47	11	CB
MW-160D	05/19/2017	100.24	124	—	—	3.95	—	CB
MW-160D	05/19/2017	100.24	126	—	—	3.95	—	CB
MW-160C	05/19/2017	98.24	[1]175	256	53	3.51	15	CB
MW-178S	05/17/2017	100.76	106	346	27	3.52	7.6	CB
MW-178D	05/17/2017	98.90	[1]123	51	21	3.87	5.4	CB
MW-178D	05/17/2017	98.90	[1]127	293	19	3.87	4.9	CB
MW-217S	05/03/2017	—	[1]89	160	11	3.44	3.2	CB
MW-217S	05/03/2017	—	[1]89	300	11	3.44	3.2	CB
MW-217D	05/04/2017	—	[1]109.6	15	2.2	3.95	0.54	CB
MW-217D	05/04/2017	—	[1]109.6	95	2.2	3.95	0.54	CB

[1]Measurement affected by nearby pumping.

Carbon-14 data were collected from selected wells through the Lockhart fault, including well MW-149S on the upgradient side of the fault, wells MW-155S and MW-155D (colocated with MW-155S) within strands of the fault, and wells MW-178S and MW-178D (colocated with MW-178S) on the downgradient side of the fault (fig. H.14). The wells are generally aligned with the nominal direction of groundwater flow estimated from water-level data. Carbon-14 activities (denormalized from laboratory-reported percent modern values) were 95 percent modern carbon (pmc) in water from the upgradient well MW-149S; 65 and 51 pmc in water from wells MW-155S and MW-155D, respectively, within strands of the fault; and 112 and 119 pmc in water from wells MW-178S and MW-178D, respectively (chapter E, appendix E.1, table E.1.1), on the downgradient side of the Lockhart fault. Water from wells MW-178S and MW-178D contained measurable tritium consistent with carbon-14 activities greater than 100 pmc and post-1952 groundwater. Although tritium was not detected in water from well MW-149S, carbon-14 activities were consistent with near modern (post-1952) water. In contrast, unadjusted groundwater ages (not adjusted for reactions with aquifer materials) in water from wells MW-155S and MW-155D within strands of the Lockhart fault were 3,520 and 5,650 years before present (ybp), respectively. Groundwater-age data indicate limited movement of water through the Lockhart fault during 2017 conditions at the time of this study.

Hexavalent chromium concentrations in water from wells MW-178S and MW-178D were 150 and 190 milligrams per liter (mg/L), respectively. These concentrations of Cr(VI) were consistent with Cr(VI) released from the Hinkley compressor station and with measured horizontal PVP groundwater-flow directions to the northwest (fig. H.14). Hexavalent chromium concentrations in water from wells MW-149S, MW-155S, and MW-155D did not exceed 1.5 µg/L. On the basis of these data, groundwater does not move through the Lockhart fault in a simple manor from the upgradient side to the downgradient side of the fault, and most groundwater appears to move through unfaulted aquifer deposits along the downgradient side of the Lockhart fault from groundwater recharge areas along the Mojave River—passing near the Hinkley compressor station.

Groundwater in wells MW-217S and MW-217D, south of the Hinkley compressor station, was affected by pumping from supply wells for the Hinkley compressor station, FW-1 and FW-2, approximately 1,650 ft to the south near the Mojave River. In August 2017, pumping times and rates were controlled over 2 days at wells FW-1 and FW-2, and horizontal PVP data were collected in wells MW-217S and MW-217D using the colloidal borescope. Data collected from the shallow well, MW-217S, were not used due to noise within the data. Data collected each day from the deep monitoring well, MW-217D, showed a change in the direction of particle movement and measured groundwater flow within the well from northward (azimuth direction approximately 20 degrees east of north) to the northeast (azimuth approximately 60 degrees east of north), 35 minutes after pumping began in wells FW-1 and FW-2. Northward groundwater flow resumed at MW-217D approximately 35 minutes after pumps were stopped for the day. No change in groundwater-flow direction was measured on the day prior to the test. Point-velocity probe data from well MW-217D showed a hydraulic connection to pumping stresses across strands of the Lockhart fault near the Hinkley compressor station. A carbon-14 activity of 90 pmc and measurable tritium in water from well MW-77S (chapter E, appendix E.1, table E.1.1) near the Hinkley compressor station also are consistent with a hydraulic connection to recharge sources along the Mojave River in this area. Point-velocity probe and pumping data are not available along the Lockhart fault to the northwest, near wells MW-155S and MW-155D, where unadjusted carbon-14 ages within strands of the Lockhart fault are 3,550 and 5,500 ybp.

Water-level data from previous studies show the Lockhart fault is an impediment to groundwater flow. Groundwater-age data collected upgradient, within fault strands, and downgradient from the fault indicate limited movement of water through much of the fault under conditions at the time of this study. However, groundwater-age data show movement of post-1952 water through splays of the fault near the Hinkley compressor station and the Mojave River.

Groundwater-flow directions and velocities measured using PVPs are not representative of bulk groundwater movement assessed on the basis of water-level or groundwater-age data but rather represent movement of water within thin permeable units measured within selected wells. These units may be responsible for much of the movement of groundwater across the Lockhart fault. Point-velocity probe data show movement of groundwater within these units differs from the nominal direction of groundwater flow evaluated on the basis of water-level data along some sections of the Lockhart fault. Differences between measured groundwater flow and nominal groundwater-flow directions along the Lockhart fault may be related to changes in fault properties or may be associated with the incision and subsequent backfilling of alluvial deposits by the Mojave River and the proximity to intermittent recharge fluxes along the Mojave River.

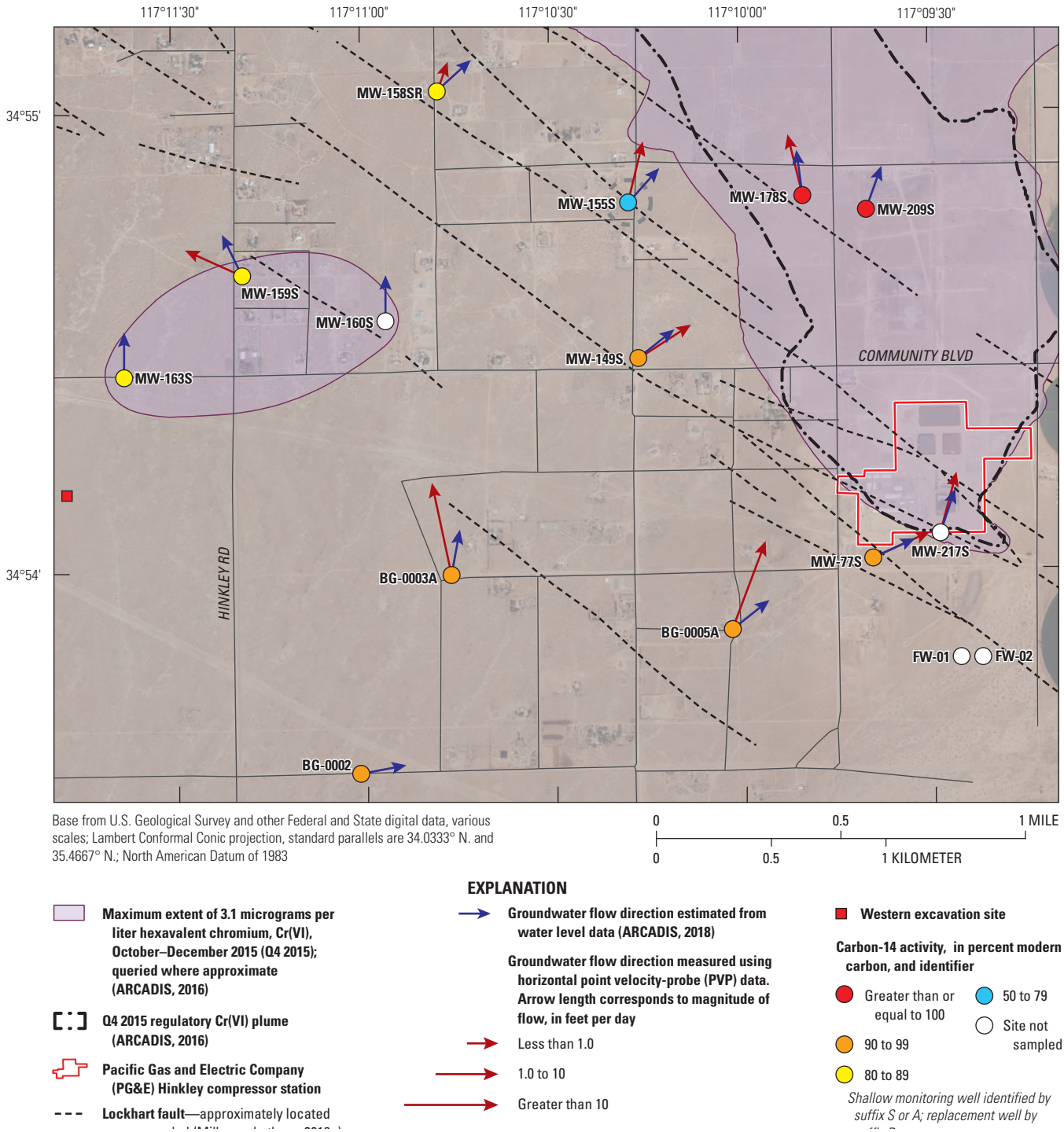

Figure H.14. Horizontal groundwater-flow directions and carbon-14 activities measured in water from shallow wells near the Lockhart fault zone, Hinkley Valley, western Mojave Desert, California, March through May 2017. Groundwater directions from point velocity probe data are available in U.S. Geological Survey (2019).

H.3.5. Coupled Well-Bore Flow and Depth-Dependent Water-Quality Data

Coupled well-bore flow and depth-dependent water-quality data were collected from five production wells within Hinkley and Water Valleys between June 2015 and March 2016. Coupled well-bore flow and depth-dependent data are direct measurements of aquifer yields to wells that are more representative of aquifer properties than indirect data inferred from lithologic or geophysical data. The sites were selected to represent a range of hydrologic conditions in Hinkley and Water Valleys. Wells IW-03 and C-01 are in the eastern subarea within the mapped Q4 2015 regulatory Cr(VI) plume downgradient from the Hinkley compressor station. Well 27-03 is in the western subarea near the margin of the Q4 2015 regulatory Cr(VI) plume, about 1 mi east of residential areas within the community of Hinkley. Well 27-38 (the former Hinkley Elementary School well) is in the western subarea, 0.2 mi south of residential areas within the community of Hinkley. Well 28N-04 is in Water Valley in formerly agricultural land.

H.3.5.1. Wells IW-03 and C-01

The Pacific Gas and Electric Company production well IW-03 (State well number 10N/3W-26L34S), within the Q4 2015 regulatory Cr(VI) plume, is about 1.6 mi downgradient from the Hinkley compressor station. The well is fully screened throughout the shallow and deep zones within the upper aquifer to a depth of 160 ft bls (fig. H.15). Water from well IW-03 is used to irrigate agricultural fields within land treatment units (LTUs) operated by PG&E where Cr(VI) is reduced to trivalent chromium, Cr(III), within the crop root zone (chapter A). Caliper and other geophysical-log data show evidence of corrosion within the well, and low well yield at depths below 145 ft indicate that the well screens may be partly clogged below that depth and no longer yield water freely from the aquifer (fig. H.15).

Unpumped well-bore flow data from IW-03 show upward flow through the well at rates less than 1 gal/min that are within the measurement uncertainty. However, unpumped temperature and fluid resistivity logs are consistent with water movement through the well under unpumped conditions (fig. H.15).

When pumped at a rate of 43.5 gal/min, IW-03 had a specific capacity of 29 gallons per minute per foot (gal/min/ft) of drawdown. Aquifer transmissivity, estimated by multiplying specific capacity by 200 (Driscoll, 1986), was 5,800 square feet per day (ft^2/d). Pumped well-bore flow data show layered aquifer properties with higher yields from permeable deposits near the water table and from permeable deposits at depth within the well (fig. H.15). Approximately half of the yield to well IW-03 was from the upper 8 ft of the well screen; hydraulic conductivity of this material would likely exceed 250 ft/d.

Examination of core material from the upper 8 ft of the well screen shows fine, well-sorted beach sand (Miller and others, 2018a); this interval was characterized on the CPT log as sand to silty sand. High permeability beach sands are widespread in Hinkley Valley. These materials would have a high degree of hydraulic connectivity, laterally and longitudinally, because they were deposited by shallow areally extensive lakes that transgressed and regressed across the valley in the geologic past (chapter A, fig. A.5). There was generally poor agreement between coarser-textured sand material (as indicated on the CPT log) and intervals within the well that yield water (fig. H.15), this may occur because of a low degree of hydraulic connectivity within coarser-textured alluvial deposits. The CPT did not penetrate depths below 135 ft.

Groundwater chemistry and isotopic composition were relatively uniform throughout well IW-03 (appendix H.1, table H.1.5). Calculated Cr(VI) concentrations in water entering the well ranged from 5.5 µg/L in the deeper part of the well to 6.2 µg/L in the upper part of the screened interval (not shown on fig. H.15). Water from the well contained measurable tritium and had a modern (post-1952) component. The fraction of modern water entering well IW-03 from the aquifer ranged from 0.4 at depth to 0.6 within the upper part of the well screen. The data are consistent with a higher fraction of younger (post-1952) water in the shallow zone of the upper aquifer and a higher fraction of older (pre-1952) water at depth within the deep zone of the upper aquifer.

Pacific Gas and Electric Company production well C-01 (State well number 10N/3W-26B1), within the Q4 2015 mapped Cr(VI) regulatory plume, is about 2.2 mi downgradient from the Hinkley compressor station and 0.7 mi downgradient from well IW-03. The well is screened in two sections separated by a blank casing: (1) the upper section within the shallow zone of the upper aquifer and (2) the lower section within the deep zone of the upper aquifer (fig. H.16). The well depth is 180 ft bls. Similar to well IW-03, water from C-01 is used to irrigate agricultural fields within LTUs operated by PG&E where Cr(VI) is reduced to Cr(III) within the crop root zone (chapter A). Caliper-log and other geophysical log data indicate the lower 10 ft of the upper well screen and deeper parts of the lower well screen may be partly clogged and no longer yield water freely from the aquifer (fig. H.16).

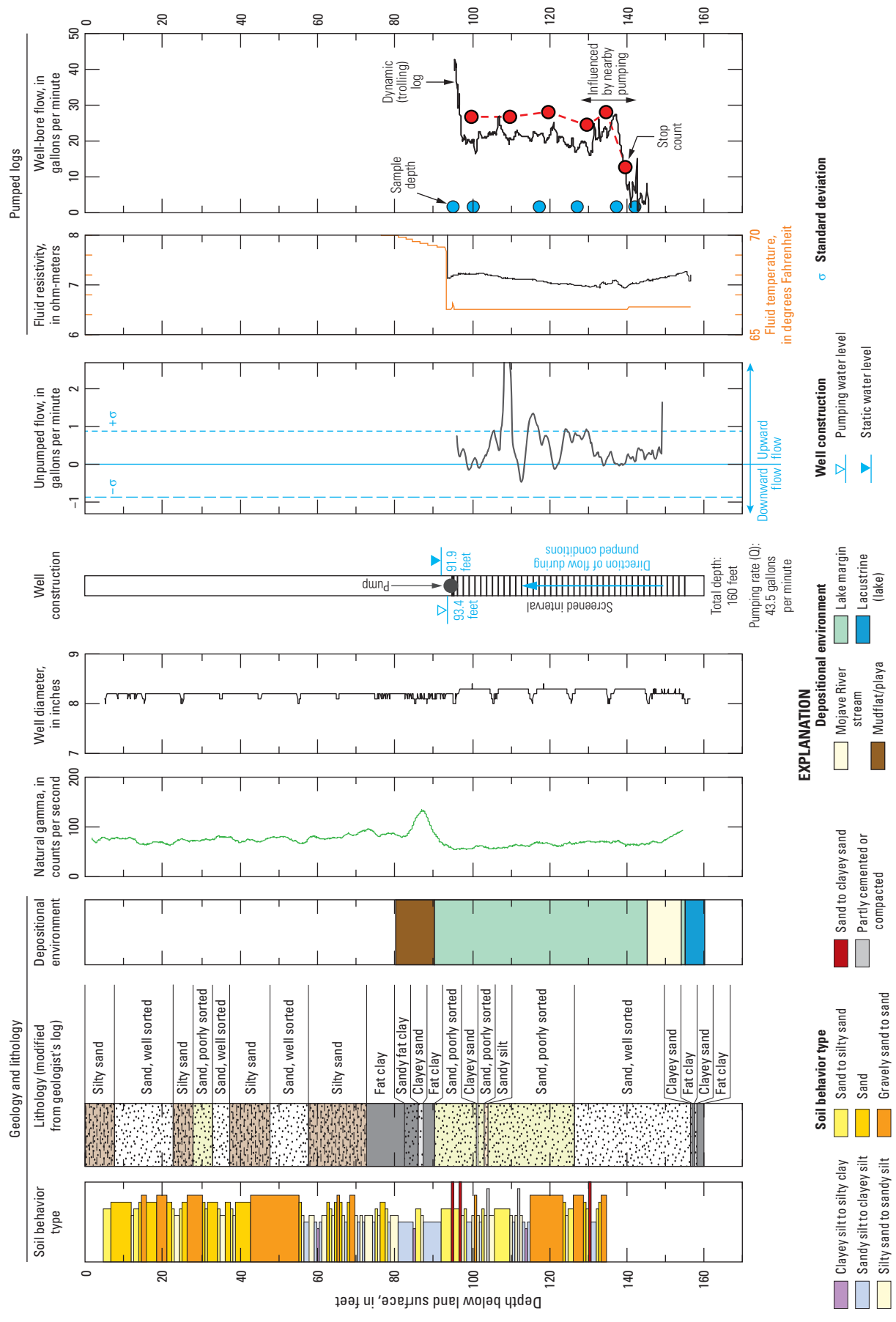

Figure H.15. Selected well-bore flow and other geophysical data collected under unpumped and pumped conditions from the Pacific Gas and Electric Company (PG&E) well IW-03, State well number 10N/3W-26L34S, Hinkley Valley, western Mojave Desert, California, November 30 through December 4, 2015. Geophysical log data and well construction information from video log data are available in U.S. Geological Survey (2019); geologic provenance data are available in Miller and others (2020); geologists log from (Christopher Maxwell, Stantec, written commun., 2017); and water chemistry data are available in U.S. Geological Survey (2019, 2021).

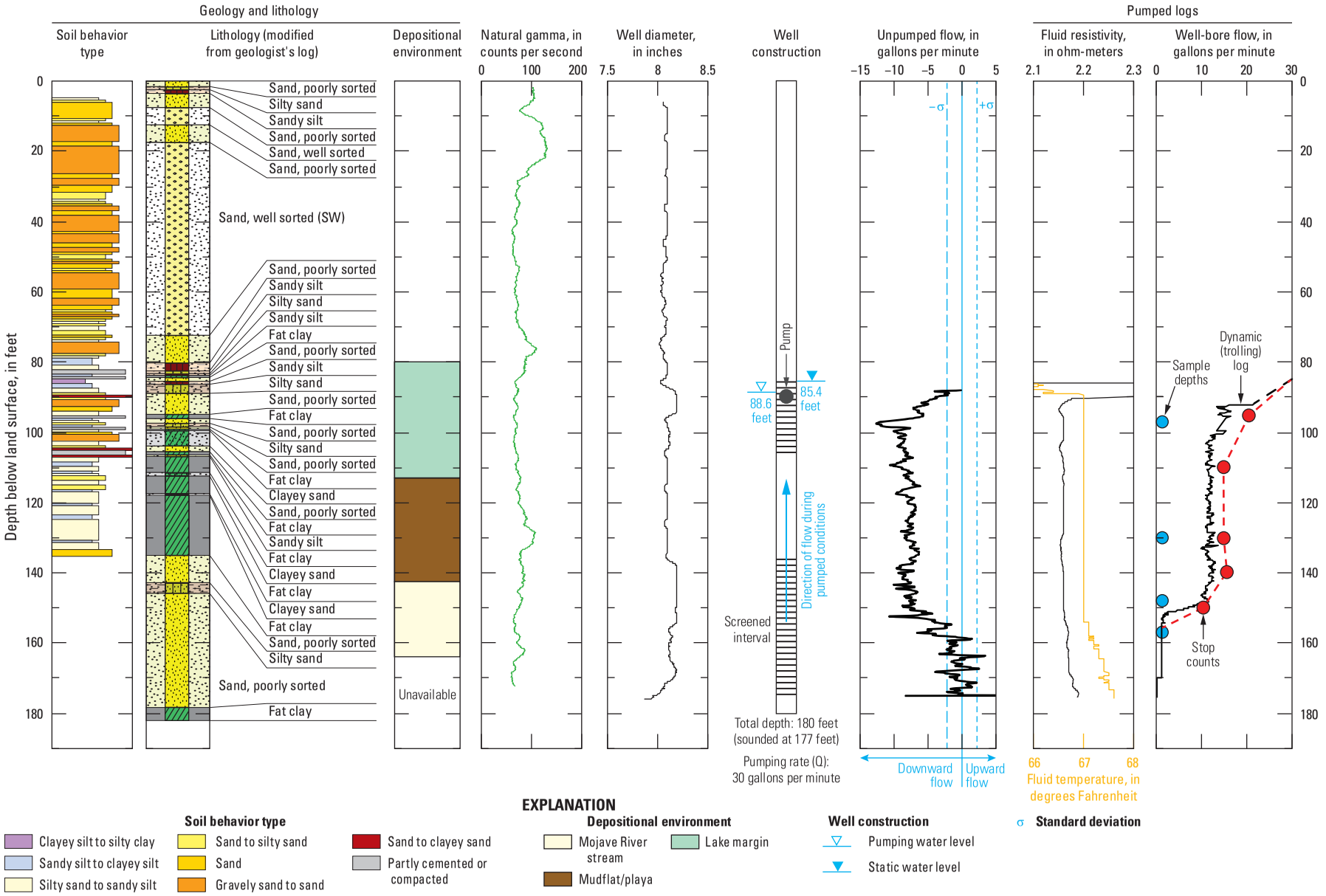

Figure H.16. Well-bore flow and other geophysical data collected during unpumped and pumped conditions from Pacific Gas and Electric Company (PG&E) well C-01, State well number 10N/3W-26B1S, Hinkley Valley, western Mojave Desert, California, March 21–26, 2016. Geophysical log data and well construction information from video log data are available in U.S. Geological Survey (2019); geologic provenance data are available in Miller and others (2020); geologists log from (Christopher Maxwell, Stantec, written commun., 2017); and water chemistry data are available in U.S. Geological Survey (2021).

Unpumped well-bore flow data from C-01 show downward flow through the well at rates as high as 7 gal/min (fig. H.16), indicating a strong downward hydraulic gradient in this area. When pumped at a rate of 30 gal/min, C-01 had a specific capacity of 9.4 gal/min/ft with an approximate transmissivity of 1,900 ft^2/d (Driscoll, 1986). Similar to IW-03, pumped well-bore flow data from C-01 also show layered aquifer properties with higher yield in permeable layers near the water table and at depth within the well (fig. H.16). Approximately half of the yield to the well was from the upper 10 ft of the well screen within the shallow zone of the upper aquifer. Although core material was not available, cone penetration test logs show sand-textured material present within the upper part of the well screen. These data are consistent with the presence of permeable well-sorted beach sands, having a high degree of hydraulic connectivity, that were encountered near the water table in well IW-03. The CPT did not penetrate depths below 135 ft.

Groundwater chemistry and isotopic composition were relatively uniform throughout well C-01 (appendix H.1, table H.1.5). Calculated Cr(VI) concentrations in water entering the well ranged from 2.5 µg/L in the deeper part of the well (not shown on fig. H.16) to 3.0 µg/L in the upper part of the screened interval (fig. H.16). Although water from the well had a modern-recharge (post-1952) component (chapter F), the fraction of modern water ranged from 0.3 in water entering the upper part of the well screen to less than 0.2 in water entering the well at depth. Similar to IW-03, the distribution of groundwater age data in well C-01 are consistent with a higher fraction of younger (post-1952) water in the shallow zone of the upper aquifer and older (pre-1952) water within the deep zone of the upper aquifer.

Although subsurface geologic conditions likely differ elsewhere in Hinkley Valley, the upper aquifer layers near the water table penetrated by wells IW-03 and C-01 within the Q4 2015 regulatory Cr(VI) plume are more permeable than similar layers at depth. Pumping at production rates from wells IW-03 and C-01 may locally drawdown water levels to below the upper permeable layers penetrated by these wells, as indicated by step-drawdown data from IW-03 collected in April 2011 at the time the well was drilled (Christopher Maxwell, Stantec, written commun., 2019; fig. H.17). Available water-level data (Stone, 1957; California Department of Water Resources, 1967) indicate that these upper layers may have been dewatered throughout large areas underlying Hinkley Valley beginning in the mid-1950s as a result of agricultural pumping—limiting the downgradient movement of Cr(VI)-containing groundwater from the Hinkley compressor station at that time. These dewatered layers would have resaturated beginning in the mid to late 1980s as agricultural pumping declined and water levels increased (Stamos and Predmore, 1995; Stamos and others, 2001)—allowing the downgradient movement of Cr(VI)-containing ground water after that time. Deeper permeable layers penetrated by these wells remained saturated during these periods.

H.3.5.2. Well 27-03

Well 27-03 (State well number 10N/3W-27M3), near the western margin of the Q4 2015 mapped Cr(VI) regulatory plume, is fully screened in saturated portions of the upper aquifer (fig. H.18). Although owned by PG&E, well 27-03 is an older well that was not drilled by PG&E. Well-drillers reports are not available, and CPT data were not collected at this site. Water from well 27-03 was unused at the time of data collection (June 2015). Caliper-log data and physical observation indicate the well screen is corroded and the well is likely less efficient, with greater drawdown during pumping, than when first constructed.

Unpumped flow data from well 27-03 show upward flow through the well at rates as high as 1.5 gal/min. Flow enters the well through the bottom 20 ft of the screened interval and reenters the aquifer near 110 ft bls, with smaller vertical flow in the upper 10 ft of the well screen. Differences in unpumped flow direction with depth in the well may result from nearby injection at the Northwest Injection Barrier (chapter A, fig. A.6), which was installed to limit expansion of the mapped plume toward residential development in the western part of Hinkley Valley (CH2M Hill, 2009).

When pumped at a rate of 30 gal/min, the well had a specific capacity of 12.5 gal/min/ft with an approximate transmissivity of 2,500 ft^2/d (Driscoll, 1986). Unlike wells IW-03 and C-01, pumped well-bore flow data show relatively uniform yield with depth through the aquifer deposits that are penetrated by well 27-03 (fig. H.18). Aquifer property data estimated from well 27-03 are consistent with data measured during a 3-day aquifer test done at this site (ARCADIS, 2014).

Groundwater chemistry and isotopic composition also were relatively uniform throughout well 27-03, although specific conductance increased slightly with depth from 1,090 to 1,140 microsiemens per centimeter (µS/cm; appendix H.1, table H.1.5). Hexavalent chromium concentrations within the well showed almost no variation and ranged from 1.4 µg/L in the upper part of the screened interval to 1.5 µg/L in the deeper part of the well (not shown on fig. H.18). Water from the well had concentrations of tritium less than or equal to the study reporting level of 0.05 tritium units (TU) and carbon-14 activities of 82–84 pmc (appendix H.1, table H.1.5) that likely represent groundwater recharged from the Mojave River just prior to the modern (post-1952) era (chapter F).

H.3.5.3. Well 27-38

Well 27-38 (State well number 10N/3W-27D7S) near the western margin of the Q4 2015 mapped Cr(VI) regulatory plume is screened to a depth of 252 ft bls within saturated alluvium overlying weathered bedrock and bedrock (fig. H.19). Well 27-38 was one of four wells at the site that provided water to the Hinkley Elementary School before the school closed in 2013 due to declining enrollment. At the time of data collection, water from the well was used for irrigation and maintenance of school grounds.

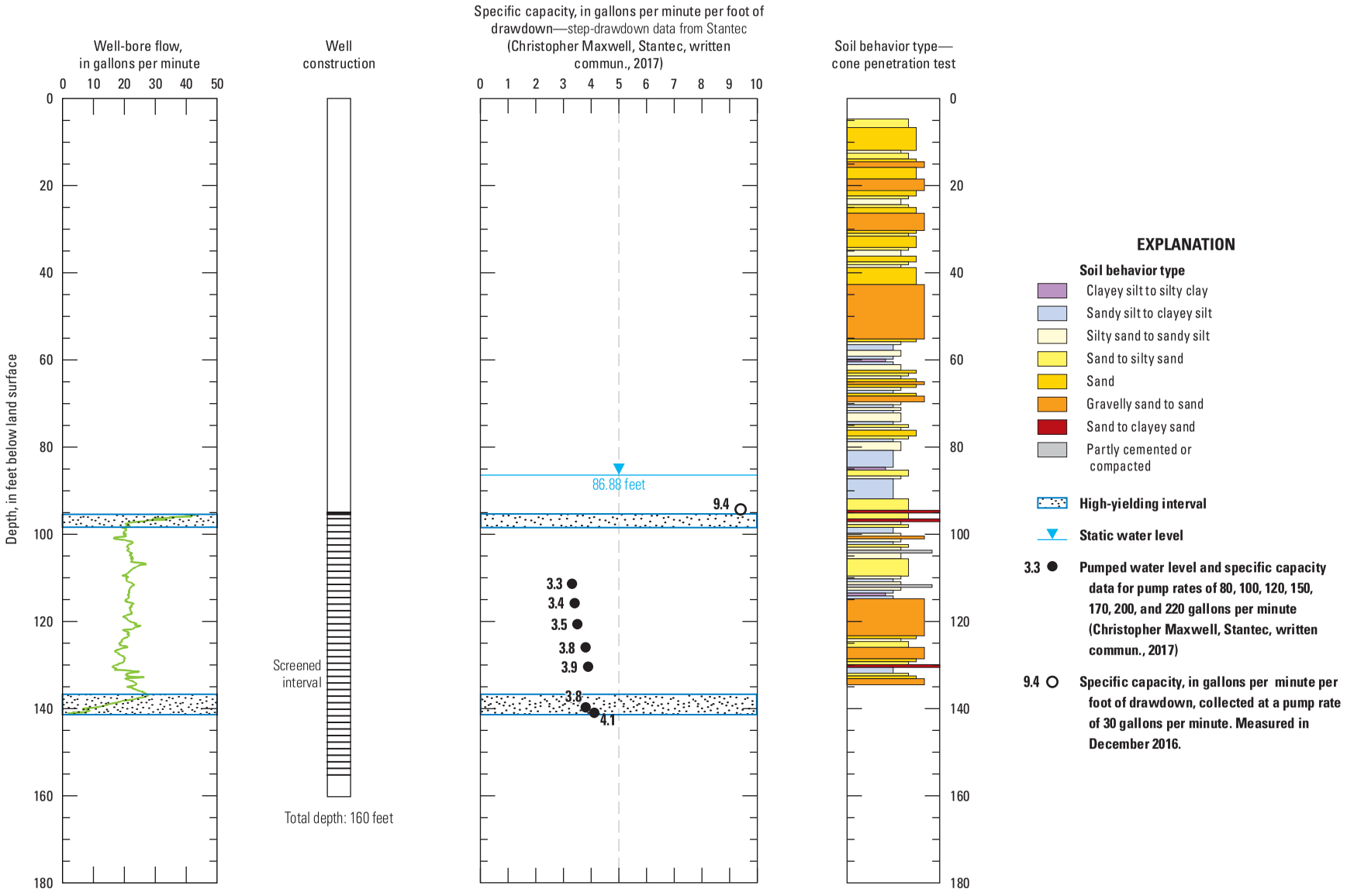

Figure H.17. Well-bore flow and step-drawdown data for Pacific Gas and Electric Company (PG&E) well IW-03, State well number 10N/3W-26L34S, Hinkley Valley, western Mojave Desert, California. Geophysical log data available and well construction information from video log data are available in U.S. Geological Survey (2019); geologic provenance data are available in Miller and others (2020); and specific capacity values are calculated from step-drawdown data (Christopher Maxwell, Stantec, written commun., 2017).

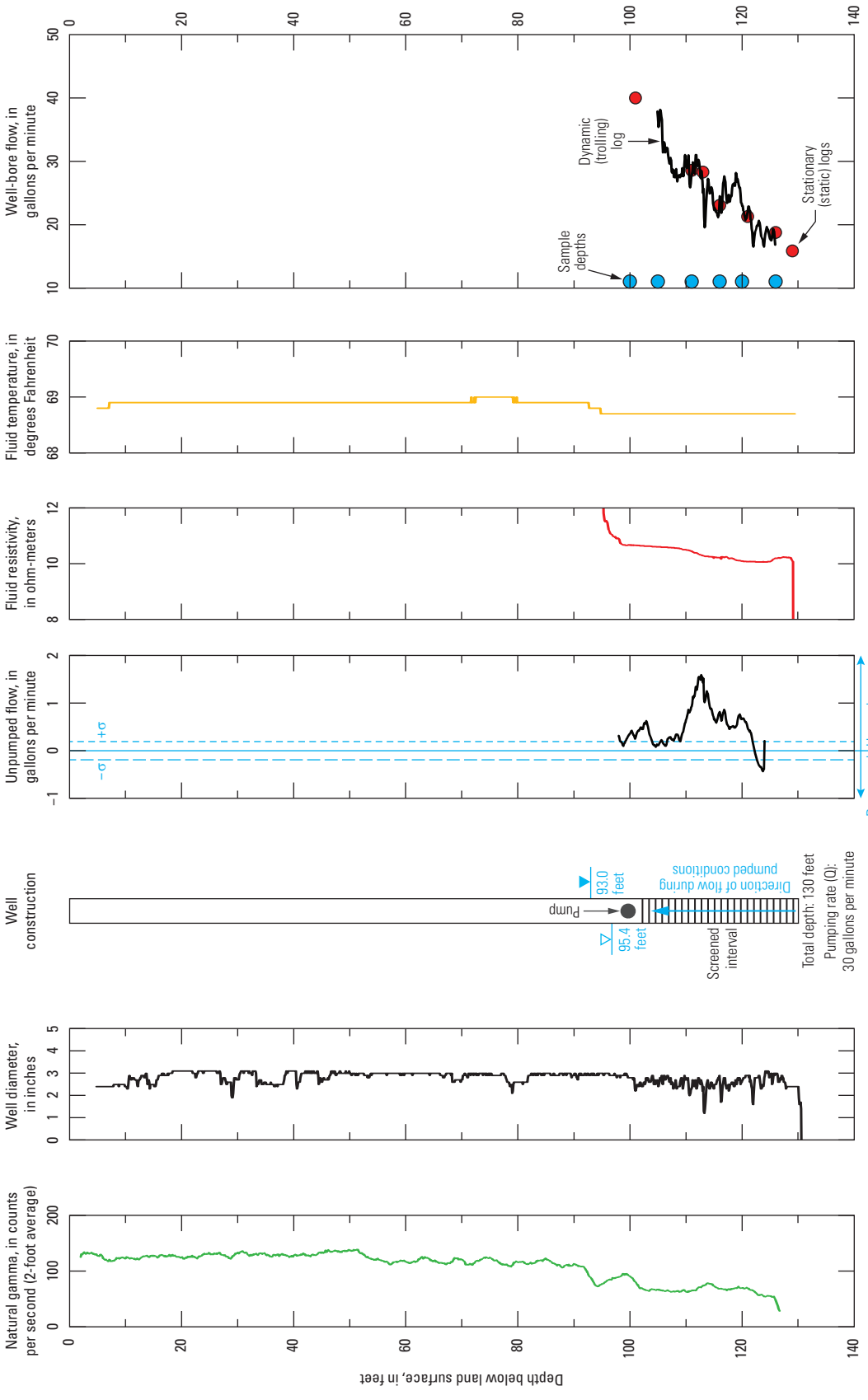

Figure H.18. Selected well-bore flow and other geophysical data collected during unpumped and pumped conditions from well 27-03, State well number 10N/3W-27M3S, Hinkley Valley, western Mojave Desert, California, June 1–5, 2015. Geophysical log data and well construction information from video log data are available in U.S. Geological Survey (2019); geologic provenance data are available in Miller and others (2020); and water chemistry data are available in U.S. Geological Survey (2021).

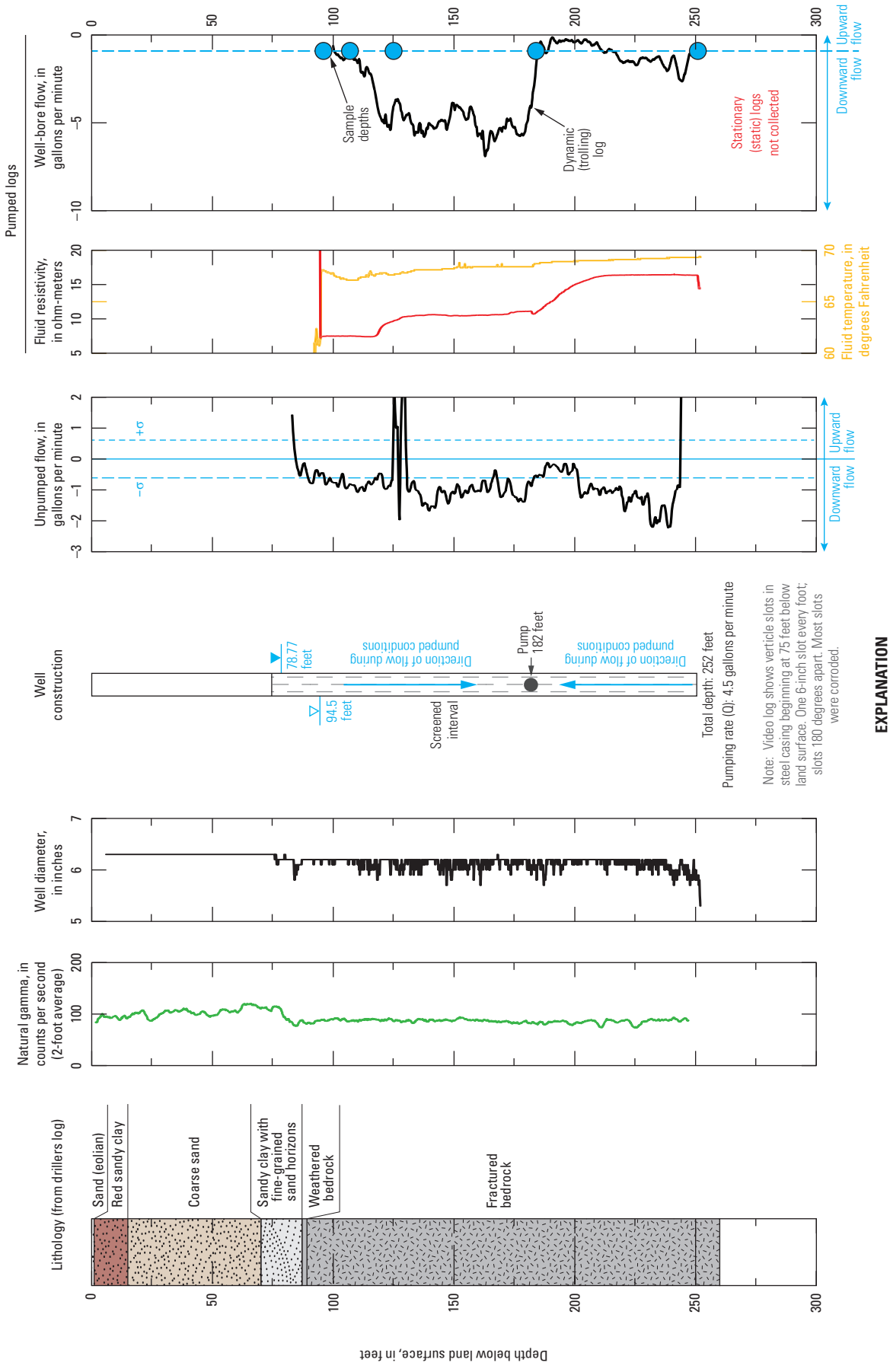

Figure H.19. Selected well-bore flow and other geophysical data collected during unpumped and pumped conditions from well 27-38, State well number 10N-3W-27D7S, Hinkley Valley, western Mojave Desert, California, November 9–13, 2015. Geophysical log data and well construction information from video log data are available in U.S. Geological Survey (2019); geologic data are from driller's log; and water chemistry data are from U.S. Geological Survey (2021).

Unpumped flow data for well 27-38 show downward flow throughout the well. Unpumped flow within unconsolidated deposits and weathered bedrock penetrated by the upper part of the well screen, at depths less than 96 ft bls, was generally within the measurement uncertainty. Higher downward flow rates ranging from 1 to 2 gal/min were measured at depths below 200 ft within the well (fig. H.19).

When pumped at a rate of 4.5 gal/min, well 27-38 had a specific capacity of 0.3 gal/min/ft, with an approximate transmissivity of 60 ft^2/d (Driscoll, 1986). In anticipation of low well yields, the test pump was set at 182 ft bls. Unconsolidated deposits and weathered bedrock penetrated by the upper portion of well 27-38 were largely dewatered as a result of pumping and water level declines to 94.5 ft bls. Almost all water from well 27-38 was yielded from fractured bedrock penetrated by the well above 120 ft bls, with less than 0.5 gal/min yielded from deeper bedrock units below the pump intake (fig. H.19).

Water quality differed with depth in well 27-38. Specific conductance decreased from 1,590 above the pump intake to 730 µS/cm at depths below the pump intake, and the major-ion composition of water within the well changed from calcium-sulfate/chloride above the pump to sodium-chloride below the pump (appendix H.1, table H.1.5). These major-ion compositions are consistent with irrigation return water above the pump intake and water from bedrock aquifers below the pump intake (chapter E, fig. E.9). Above the pump, dissolved-oxygen concentrations within the well ranged from 3.3 to 6.6 mg/L, and Cr(VI) concentrations were comparatively uniform, about 1.2 µg/L. Below the pump, the dissolved-oxygen concentration within the well was 0.4 mg/L, and the Cr(VI) concentration was 0.13 µg/L (appendix H.1, table H.1.5). Water from the well did not have detectable concentrations of tritium at the laboratory reporting level of 0.02 TU (appendix H.1, table H.1.5). Carbon-14 activity ranged from 63 to 76 pmc, with higher activities above the pump intake and lower activities at depths below the pump intake; unadjusted carbon-14 ages ranged from 2,250 ybp above the pump to 3,800 ybp below the pump. Tritium and carbon-14 data indicate that water from well 27-38 was recharged before 1952 and predate Cr(VI) releases from the Hinkley compressor station.

Although saturated during predevelopment, alluvium penetrated by domestic wells in residential areas to the north of well 27-38 was unsaturated at the time of this study (fig. H.8*B*). Domestic wells 22-63 and 22-09 (fig. H.1), sampled as part of this study that were completed in bedrock near well 27-38, had low yields, and well 22-63 went dry during sample collection at pump rates less than 1 gal/min. Domestic wells in this area had sodium/chloride water similar to fractured bedrock penetrated by deeper intervals within well 27-38 (chapter E, figs. E.8, E.9).

H.3.5.4. Well 28N-04

Well 28N-04 (State well number 11N/3W-28R2S) in Water Valley is an agricultural well screened in lake-margin deposits to a depth of about 105 ft and in locally derived alluvium to a depth of 265 ft bls (fig. H.20). Agricultural pumping from the well ceased shortly before data collection in 2015 as a result of declining well yields. The USGS has monitored water levels in this well since 1953 (Dick and Kjos, 2017). In 1953, water levels in well 28N-04 were 26 ft bls, and predevelopment water levels in this part of Water Valley were commonly above land surface (Thompson, 1929; Seymour and Izbicki, 2018).

Unpumped flow logs in well 28N-04 showed upward flow at rates as high as 4 gal/min in lake-margin deposits above 105 ft. Measurable flow was not detected within underlying locally derived alluvial deposits during unpumped conditions.

When pumped at a rate of 27 gal/min, well 28N-04 had a specific capacity of 8.7 gal/min/ft, with an approximate transmissivity of 1,740 ft^2/d. Well-bore flow data showed that almost all the yield from well 28N-04 originated from lake-margin deposits above 105 ft, with deeper locally derived alluvium contributing almost no water to the well (fig. H.20), and the hydraulic conductivity of the lake-margin deposits penetrated by well 28N-04 would be approximately 80 ft/d (Driscoll, 1986). Well 28N-04 is 265 ft deep but could not sustain production rates of 100 gal/min once the overlying lake-margin deposits were desaturated. Water levels in the well gradually declined during the growing season until the upper, more permeable deposits could no longer sustain pumping; after which, the pump failed because water levels in the well declined rapidly to depths below the production pump intake set at 200 ft bls. On the basis of these data, hydraulic conductivity values for locally derived alluvium are less than 2 ft/d at depths below 110 ft.

Water quality did not differ greatly with depth throughout well 28N-04, to a depth of at least 160 ft bls (appendix H.1, table H.1.5). Specific conductance ranged from 516 to 527 µS/cm, and Cr(VI) concentrations ranged from 4.1 to 4.4 µg/L. Stable isotope data were consistent with Mojave River recharge. Tritium was not detected and carbon-14 activities ranging from 63 to 67 pmc, with unadjusted ages ranging from 3,300 to 3,800 ybp, indicated that water from well 28N-04 was recharged prior to the modern (post-1952) era and predates Cr(VI) releases from the Hinkley compressor station. Fluid resistivity logs showed water near the bottom of well 28N-04 (below 250 ft) had a resistivity of about 3.25 ohm-meters, consistent with a specific conductivity of about 2,700 µS/cm (fig. H.20). This water was not present when depth-dependent samples were collected at 255 ft bls.

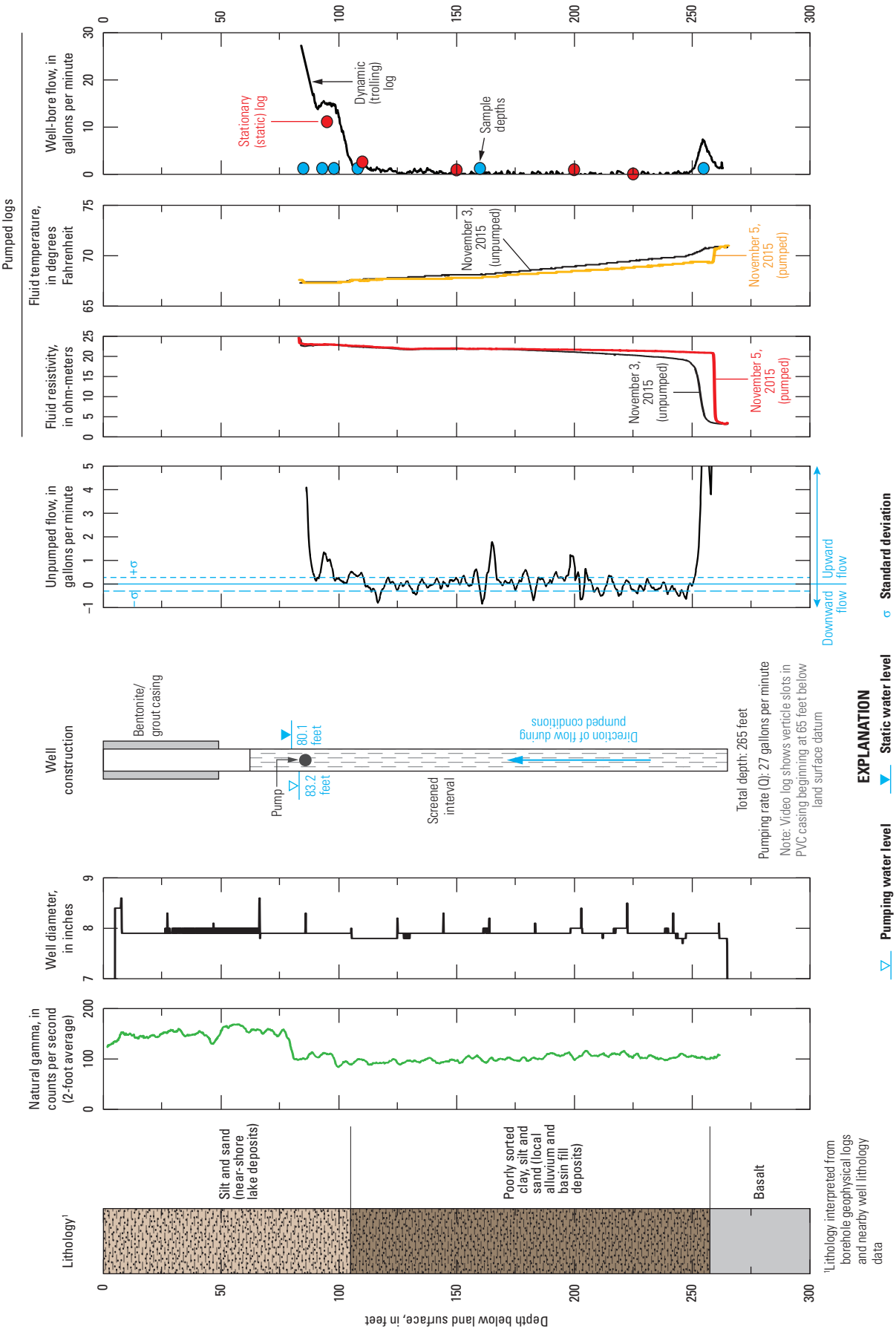

Figure H.20. Selected well-bore flow and other geophysical data collected during unpumped and pumped conditions from well 28N-04, State well number 11N/3W028R11S, Water Valley, western Mojave Desert California, November 2–6, 2015. Geophysical log data and well construction information from video log data are available in U.S. Geological Survey (2019); geologic data are from nearby driller's log information; and water chemistry data are available in U.S. Geological Survey (2021).

H.4. Conclusions

Hydrologic and geophysical data were collected to support updates, provided by Pacific Gas and Electric Company (PG&E) consultants, to an existing groundwater-flow model of Hinkley Valley, California, in the Mojave Desert about 80 miles northeast of Los Angeles, California. These data provide information on predevelopment water levels, groundwater recharge, and selected hydrologic properties of aquifer materials. The U.S. Geological Survey was requested by the Lahontan Regional Water Quality Control Board to provide these data as part of the updated hexavalent chromium, Cr(VI), background study of Cr(VI) concentrations in Hinkley and Water Valleys.

During predevelopment (pre-1930) conditions, water-level altitudes in Hinkley and Water Valleys ranged from about 2,280 feet (ft) above sea level (referenced to the North American Vertical Datum of 1988, NAVD 88) along the Mojave River south of Iron Mountain to about 2,000 ft above sea level (NAVD 88) near Harper (dry) Lake. A predevelopment groundwater-level map, drawn using water-level measurements from 48 wells collected as early as 1918, showed groundwater flow through Hinkley Valley was from recharge areas along the Mojave River northward through Hinkley Gap to discharge areas near the margin of Harper (dry) Lake. Water levels were less than 20 ft below land surface (bls) throughout much of Hinkley Valley prior to pumping for agriculture; and predevelopment depths to water near the Hinkley compressor station were about 27 ft bls. Predevelopment water levels in Water Valley were above land surface, consistent with flowing wells in that area at that time. Water-level declines in Hinkley Valley beginning in the early 1950s were as much as 60 ft near the Hinkley compressor station by 2017, and these declines left formerly saturated, coarse-textured “Mojave-type” deposits above the water table at the time of this study in 2017. Prior to agricultural development, these materials transmitted water from the Mojave River north through Hinkley Valley and into Water Valley.

Areal recharge to groundwater from infiltration of precipitation on the valley floor was negligible. During recent geologic time, chloride associated with infiltrating precipitation has accumulated to high concentrations in the unsaturated zone above the predevelopment water table, but accumulation of high chromium concentrations was not observed in unsaturated materials. As a consequence, mobilization of chromium from the predevelopment unsaturated zone during initial application of irrigation water or initial infiltration of septic discharge, was not considered to be an important source of Cr(VI) to the water table.

The climate of Hinkley and Water Valleys is hyper-arid. Basin Characteristic Model calculations for 1930 to 2015 show that runoff from upland drainages in the local mountains surrounding Hinkley and Water Valleys (excluding drainages south of the Mojave River) averages 64.7 acre-feet per year (acre-ft/yr), with 14.0 acre-ft/yr contributed directly to Hinkley Valley. Runoff and groundwater recharge as infiltration of streamflow from upland areas draining the local mountains does not occur in most years; in the years when it does occur, local runoff to Hinkley Valley was estimated to average 296 acre-feet (acre-ft). In contrast, between 1931 and 2015 average recharge as infiltration of streamflow from the Mojave River was between 13,400 and 17,100 acre-ft/yr; in some years, recharge from the Mojave River exceeded 100,000 acre-ft. Local recharge from infiltration of runoff from upland areas is less than 1 percent of the recharge to Hinkley Valley from infiltration of Mojave River streamflow.

Groundwater movement through Hinkley Gap and groundwater discharge to Harper (dry) Lake are important components of the water budget for the study area. Estimates of predevelopment groundwater movement through Hinkley Gap and groundwater discharge to Harper (dry) Lake, calculated as part of this study, ranged from 570 to 1,900 and 820 to 2,460 acre-ft/yr, respectively, and were slightly lower than previous estimates. At the time of this study (2017) groundwater movement through Hinkley Gap was estimated to be about 83 acre-ft/yr.

Hydraulic-conductivity values estimated from slug-test data from 95 monitoring wells ranged from less than 0.1 to 680 feet per day (ft/d); values were higher in Mojave-type deposits and lower in mudflat/playa deposits. Slug-test data showed generally higher hydraulic conductivities at shallower depths and lower hydraulic conductivities at deeper depths. Median Nuclear Magnetic Resonance (NMR) derived hydraulic-conductivity values for Mojave-type deposits including Mojave River alluvium and lake-margin deposits were 73 and 11 ft/d, respectively; median values for locally derived alluvium and weathered bedrock were 6 and 2 ft/d, respectively; values were highly correlated (coefficient of determination, R^2=0.93) with hydraulic conductivity estimated from slug-test data for those wells. Hydraulic conductivity estimated from NMR data for formerly saturated deposits overlying the water table at the time of this study were as high as 300 ft/d near the Hinkley compressor station. Downgradient from the Hinkley compressor station, NMR-derived hydraulic-conductivity values for formerly saturated material, typically about 150 ft/d, were higher than median hydraulic-conductivity values of 73 ft/d for saturated material. Consistent with NMR data, cone penetration test data showed coarse-textured material in formerly saturated deposits above the 2017 water table near Hinkley Gap, throughout the northern subarea, and near the Hinkley compressor station.

Collectively, hydraulic conductivity and cone penetration data indicate that formerly saturated deposits above the 2017 water table are generally coarse textured with high permeability. These formerly saturated deposits may have allowed groundwater, possibly containing Cr(VI) released from the Hinkley compressor station between 1952 and 1964, to move rapidly downgradient; however, the extent to which deposits above the 2017 water table were saturated at the time of the Cr(VI) releases is not precisely known. The timing of water-level declines in Hinkley Valley is addressed by an updated groundwater-flow model of the area prepared by Pacific Gas and Electric Company (PG&E) consultants as part of the U.S. Geological Survey (USGS) Cr(VI) background study.

The Lockhart fault is an impediment to groundwater flow within Hinkley Valley. Deformation and disruption of unconsolidated aquifer materials, with tilted beds and changes in the depth of key lithologic units penetrated by boreholes, occur across a 1-mile-wide fault zone near the Hinkley compressor station. Ground ruptures associated with the fault extend to the surface, consistent with movement of the fault after deposition of aquifer deposits and with effects on groundwater flow that would extend throughout the deposits. The Mojave River has incised and backfilled faulted deposits, and the Lockhart fault is not an impediment to groundwater flow within those younger deposits along the river. Groundwater-flow directions measured using horizontal point-velocity probes ranged from northeasterly along the eastern part of the fault to northwesterly along the western part of the fault. Groundwater-flow directions generally aligned with the nominal direction of groundwater flow estimated from water-level data near the Mojave River and Hinkley compressor station. To the northwest of the Hinkley compressor station, groundwater-flow directions were deflected to the west along the upgradient side of the fault and within fault splays compared to the nominal direction of groundwater flow. Younger groundwater was present on the upgradient and downgradient sides of the fault, and older groundwater with unadjusted carbon-14 ages of 3,520 and 5,650 years before present was in water from wells within splays of the Lockhart fault to the northwest of the Hinkley compressor station. Consistent with limited groundwater movement across the fault in this area, groundwater and Cr(VI) released from the Hinkley compressor station move to the northwest along the downgradient side of the Lockhart fault. Impediment of groundwater flow within splays of the Lockhart fault may be responsible for high concentrations of Cr(VI) present only short distances downgradient from the Hinkley compressor station more than 65 years after the Cr(VI) releases occurred.

Coupled well-bore flow and depth-dependent water-quality data were collected at five wells within Hinkley and Water Valleys to assess vertical layering of aquifer hydraulic properties and vertical differences in the chemical and isotopic composition of groundwater within the aquifer. Coupled well-bore flow and depth-dependent data are direct measurements of aquifer yields to wells that are more representative of aquifer properties than indirect data inferred from lithologic or geophysical data. The sites were selected to represent a range of hydrologic conditions in Hinkley and Water Valleys.

Data from wells IW-03 and C-01 within the October–December 2015 (Q4 2015) regulatory Cr(VI) plume showed most yield to these wells was through thin, permeable layers within the aquifer. The well-sorted lake-margin (beach) sands that compose these thin units have high permeability with hydraulic conductivities as high as 250 ft/d. These well-sorted sands likely represent lake-margin deposits from lakes that transgressed and regressed across the valley as water levels in the lakes rose and fell in the geologic past. These deposits, present in wells IW-03 and C-01 (0.7 miles farther downgradient), may be areally extensive and have high lateral and longitudinal connectivity within the aquifer that may facilitate downgradient movement of groundwater and Cr(VI) released from the Hinkley compressor station. Depth-dependent water-quality data show a higher fraction of younger (post-1952) water present in the upper zone than in the deeper zone of the upper aquifer at wells IW-03 and C-01.

Well-bore flow data from well 27-03 near the western margin of the Q4 2015 regulatory Cr(VI) plume show a relatively uniform yield from the aquifer to the well with depth, consistent with relatively uniform hydraulic properties in deposits penetrated by the well. Well-bore flow data from well 27-38 (the former Hinkley School well) show almost all water was yielded from fractured bedrock; unconsolidated deposits at the site were rapidly desaturated at a pumping rate of 6 gallons per minute, consistent with low-yielding domestic wells in this area. Well-bore flow data from 27N-04 in Water Valley showed almost all the yield to the well was from permeable Mojave-type deposits near the water table, with almost no water yielded from deeper locally derived alluvium. Data from well 27N-04 indicate that even where coarse-textured deposits are described in well logs, groundwater movement through deeper aquifers in Water Valley is scant. Water from wells 27-38 and 28N-04 was older (post-1952) and likely predated Cr(VI) releases from the Hinkley compressor station. In contrast, water from well 27-03 may represent groundwater recharged from the Mojave River just prior to the modern (post-1952) era.

Pacific Gas and Electric Company and their consultants have monitored groundwater levels and collected aquifer property data within and near the Cr(VI) regulatory plume since Cr(VI) associated with releases from the Hinkley compressor station was first identified within Hinkley Valley. Data collected as part of this study provide additional information on aquifer properties and the aquifer system outside the area monitored by PG&E for regulatory purposes and provide information on formerly saturated deposits above the 2017 water table at the time of this study. Collectively, aquifer property and hydraulic-conductivity data are consistent with groundwater-age data collected as part of this study that showed more rapid movement of groundwater through shallower depths within the aquifer and slower movement of groundwater at depth.

Data from the USGS Cr(VI) background study presented within this chapter were used to support updates by PG&E consultants to an existing PG&E groundwater-flow model of Hinkley Valley. The suitability of the updated model for use by the USGS Cr(VI) background study is evaluated in appendix H.2.

H.5. References Cited

Allison, G.B., and Hughes, M.W., 1978, The use of environmental chloride and tritium to estimate total recharge to an unconfined aquifer: Australian Journal of Soil Research, v. 16, no. 2, p. 181–195. [Available at https://doi.org/10.1071/SR9780181.]

Allison, G.B., Gee, G.W., and Tyler, S.W., 1994, Vadose-zone techniques for estimating groundwater recharge in arid and semiarid regions: Soil Science Society of America Journal, v. 58, no. 1, p. 6–14. [Available at https://doi.org/10.2136/sssaj1994.03615995005800010002x.]

American Public Health Association, 1992, Standard methods for the examination of water and wastewater: Washington, D.C., American Public Health Association, American Water Works Association, and Water Pollution Control Federation, 18th ed., [variously paged].

Aquifer Science and Technology, 2007, Report on the geophysical investigation for the Harper-Hinkley Gap area near Hinkley, California: Waukesha, Wisconsin, Aquifer Science and Technology, p. 35. [Available at https://www.mojavewater.org/wp-content/uploads/2022/10/repgpinvharper-hinkleygapfinal_10981.pdf.]

ARCADIS, 2014, Response to Investigative Order R6V-2013-0087—Implementation of the action plan for the area west of the northwest freshwater injection system for Pacific Gas and Electric Company Hinkley Compressor Station, Hinkley, California Board Order No. R6V-2008-0014 (WDID No. 6B369107001).

ARCADIS, 2016, Annual cleanup status and effectiveness report (January to December 2015) Pacific Gas and Electric Company, Hinkley Compressor Station, Hinkley, California: San Francisco, Calif., Pacific Gas and Electric Company, prepared by ARCADIS, Oakland, Calif., RC000699, [variously paged], accessed February 2016, at https://documents.geotracker.waterboards.ca.gov/esi/uploads/geo_report/5010230779/SL0607111288.PDF.

ARCADIS, 2017, Second quarter 2017 monitoring report for the in situ reactive zone and northwest freshwater injection projects: PG&E Hinkley Compressor Station, Hinkley, California, [variously paged], accessed June 10, 2021, at https://documents.geotracker.waterboards.ca.gov/esi/uploads/geo_report/6561273396/SL0607111288.PDF.

ARCADIS, 2018, Annual cleanup status and effectiveness report (January to December 2017) Pacific Gas and Electric Company, Hinkley Compressor Station, Hinkley, California, [variously paged], accessed February 2018, at https://documents.geotracker.waterboards.ca.gov/esi/uploads/geo_report/4949047982/SL0607111288.PDF.

ARCADIS and CH2M Hill, 2011, Development of a groundwater flow and solute transport model—Addendum #3 to the feasibility study, Pacific Gas and Electric Company, Hinkley Compressor Station, Hinkley, California: Haley & Aldrich, Inc., prepared for Pacific Gas and Electric Company [variously paged], accessed December 6, 2018, at https://geotracker.waterboards.ca.gov/esi/uploads/geo_report/2112934887/SL0607111288.PDF.

ASTM International, 2012, Standard test method for electronic friction cone and piezocone penetration testing of soils D5778-12: ASTM International, v. 4, 20 p.

Bayer-Raich, M., Credoz, A., Guimerà, J., Jordana, S., Sampietro, D., Font-Capó, J., Nief, N., and Grossemy, M., 2019, Estimates of horizontal groundwater flow velocities in boreholes: Groundwater, v. 57, no. 4, p. 525533. [Available at https://doi.org/10.1111/gwat.12820.]

Bayless, E.R., Mandell, W.A., and Ursic, J.R., 2011, Accuracy of flowmeters measuring groundwater flow in an unconsolidated aquifer simulator: Ground Water Monitoring and Remediation, v. 31, no. 2, p. 48–62. [Available at https://doi.org/10.1111/j.1745-6592.2010.01324.x.]

Behroozmand, A.A., Keating, K., and Auken, E., 2015, A review of the principles and applications of the NMR technique for near-surface characterization: Surveys in Geophysics, v. 36, no. 1, p. 27–85. [Available at https://doi.org/10.1007/s10712-014-9304-0.]

Blodgett, D.L., Booth, N.L., Kunicki, T.C., Walker, J.I., and Viger, R.J., 2011, Description and testing of the Geo Data Portal—Data integration framework and web processing services for environmental science collaboration: U.S. Geological Survey Open-File Report 2011–1157, 9 p. [Available at https://doi.org/10.3133/ofr20111157.]

Butler, J.J., Jr., and Garnett, E.J., 2000, Simple procedures for analysis of slug tests in formations of hydraulic conductivity using spreadsheets and scientific graphics software: Kansas Geological Survey Open-File Report 2000–40, accessed March 1, 2019, at https://www.kgs.ku.edu/Hydro/Publications/OFR00_40/.

Butler, J.J., Jr., and Healey, J.M., 1998, Relationship between pumping-test and slug-test parameters—Scale effect or artifact: Ground Water, v. 36, no. 2, p. 305–312. [Available at https://doi.org/10.1111/j.1745-6584.1998.tb01096.x.]

Butler, J.J., Jr., Garnett, E.J., and Healey, J.M., 2003, Analysis of slug tests in formations of high hydraulic conductivity: Groundwater, v. 41, no. 5, p. 620–631. [Available at https://doi.org/10.1111/j.1745-6584.2003.tb02400.x.]

California Department of Water Resources, 1967, Mojave River Ground Water Basins Investigation: California Department of Water Resources Bulletin No. 84, 151 p., accessed January 18, 2022, at https://archive.org/details/mojaverivergroun84cali/page/n5/mode/2up.

Century Geophysical Corporation, 2008, User guide, Slim Hole Induction Tool model numbers 9510, 9511, and 9512: Tulsa, Oklahoma, [variously paged].

CH2M Hill, 2007, CH2M Hill Groundwater background study report—Hinkley compressor station, Hinkley, California: Oakland, Calif., CH2M Hill, [variously paged], accessed January 12, 2018, at http://www.swrcb.ca.gov/lahontan/water_issues/projects/pge/docs/2007_background_study_report.pdf.

CH2M Hill, 2009, Final Report 2009 Well completion report for Northwest Interim Remediation Project—Pacific Gas and Electric Company, Hinkley Compressor Station, Hinkley, California: Oakland, Calif., CH2M Hill, [variously paged], accessed August 22, 2018, at https://geotracker.waterboards.ca.gov/esi/uploads/geo_report/1239488005/SL0607111288.PDF.

CH2M Hill, 2013, Conceptual site model for groundwater flow and the occurrence of chromium in groundwater of the western area—Pacific Gas and Electric Company Hinkley Compressor Station, Hinkley, California Oakland, Calif., CH2M Hill, [variously paged], accessed December 10, 2019, at https://geotracker.waterboards.ca.gov/esi/uploads/geo_report/7274906218/SL0607111288.PDF.

Conkling, H., 1934, Mojave River investigation: California Department of Water Resources Bulletin No. 34, 249 p., accessed January 18, 2022, at https://openlibrary.org/works/OL7645771W/Mojave_River_investigation.

Cunningham, W.L., and Schalk, C.W., 2011, Groundwater technical procedures of the U.S. Geological Survey: U.S. Geological Survey Techniques and Methods, book 1, chap. A1, 151 p. [Available at https://doi.org/10.3133/tm1A1.]

Daly, C., Halbleib, M., Smith, J.I., Gibson, W.P., Doggett, M.K., Taylor, G.H., Curtis, J., and Pasteris, P.P., 2008, Physiographically sensitive mapping of climatological temperature and precipitation across the conterminous United States: International Journal of Climatology, v. 28, no. 15, p. 2031–2064. [Available at https://doi.org/10.1002/joc.1688.]

Dibblee, T.W., Jr., 1967, Areal geology of the western Mojave Desert, California: U.S. Geological Survey Professional Paper 522, 153 p. [Available at https://doi.org/10.3133/pp522.]

Dick, M.C., and Kjos, A.R., 2017, Regional water table (2016) in the Mojave River and Morongo groundwater basins, southwestern Mojave Desert, California: U.S. Geological Survey Scientific Investigations Map 3391, scale 1:170,000. [Available at https://doi.org/10.3133/sim3391.]

Dlubac, K., Knight, R., Song, Y.-Q., Bachman, N., Grau, B., Cannia, J., and Williams, J., 2013, Use of NMR logging to obtain estimates of hydraulic conductivity in the High Plains aquifer, Nebraska, USA: Water Resources Research, v. 49, no. 4, p. 1871–1886. [Available at https://doi.org/10.1002/wrcr.20151.]

Driscoll, F.G., 1986, Groundwater and wells (2d. ed.): St. Paul, Minn., Johnson Filtration Systems, Inc., 1089 p.

Drost, W., Klotz, D., Koch, A., Moser, H., Neumaier, F., and Rauert, W., 1968, Point dilution methods of investigating groundwater flow by means of radioisotopes: Water Resources Research, v. 4, no. 1, p. 125–146. [Available at https://doi.org/10.1029/WR004i001p00125.]

Flint, L.E., and Flint, A.L., 2014, California basin characterization model—A dataset of historical and future hydrologic response to climate change, (ver. 1.1, May 2017): U.S. Geological Survey data release, accessed December 19, 2010, at https://doi.org/10.5066/F76T0JPB.

Flint, L.E., Flint, A.L., Thorne, J.H., and Boynton, R., 2013, Fine-scale hydrologic modeling for regional landscape applications—The California basin characterization model development and performance: Ecological Processes, v. 2, article no. 25, 21 p., accessed December 13, 2019, at https://doi.org/10.1186/2192-1709-2-25.

Flint, L.E., Flint, A.L., and Stern, M.A., 2021, The basin characterization model—A regional water balance software package: U.S. Geological Survey Techniques and Methods book 6, chap. H1, 85 p., accessed June 2, 2021, at https://doi.org/10.3133/tm6H1.

Freeze, R.A., and Cherry, J.A., 1979, Groundwater: Englewood Cliffs, N.J., Prentice-Hall, Inc., 604 p.

Geonics Limited, 2005, EM39 conductivity: Geonics Limited, [variously paged], accessed May 1, 2008, at http://www.geonics.com/html/em39.html.

Greene, E.A., and Shapiro, A.M., 1995, Methods of conducting air-pressurized slug tests and computation of type curves for estimating transmissivity and storativity: U.S. Geological Survey Open-File Report95–424, 43 p. [Available at https://doi.org/10.3133/ofr95424.]

Groover, K.D., Izbicki, J., Pappas, K.L., and Johnson, C.D., 2017, Estimation of hydraulic conductivity in formerly saturated alluvium using nuclear magnetic resonance: Geological Society of America Abstracts with Programs, v. 49, no. 6, accessed December 13, 2019, at https://doi.org/10.1130/abs/2017AM-300564.

Groover, K.D., Izbicki, J.A., Larsen, J.D., Dick, M.C., Nawikas, J., and Kohel, C.A., 2021, Hydrologic data in Hinkley and Water Valleys, San Bernardino County, California, 2015–2018: U.S. Geological Survey data release, available at https://doi.org/10.5066/P9BUXAX1.

Haddon, E.K., Miller, D.M., Langenheim, V.E., Liu, T., Walkup, L.C., and Wan, E., 2018, Initiation and rate of slip on the Lockhart and Mt. General faults in southern Hinkley Valley, California, *in* Miller, D.M., ed., The Mojave River from sink to source—The 2018 Desert Symposium Field Guide and Proceedings, April 2018, accessed August 16, 2019, at http://www.desertsymposium.org/2018%20DS%20Against%20the%20Current.pdf.

Haley and Aldrich, Inc., 2010, Feasibility study, Pacific Gas and Electric Company Hinkley compressor station, Hinkley, California—Prepared for Pacific Gas and Electric Company, San Francisco, California, San Diego, California: Burlington, Mass., Haley and Aldrich, Inc., [variously paged], with 3 addendums, accessed November 27, 2018, at https://www.waterboards.ca.gov/lahontan/water_issues/projects/pge/fsr083010.html.

Halford, K.J., and Kuniansky, E.L., 2002, Documentation of spreadsheets for the analysis of aquifer-test and slug-test data: U.S. Geological Survey Open-File Report 2002–197, ver. 1.2, 51 p. [Available at https://doi.org/10.3133/ofr02197.]

Hardt, W.F., 1971, Hydrologic analysis of Mojave River Basin, California, using electric analog model: U.S. Geological Survey Open-File Report 72–157, 84 p. [Available at https://doi.org/10.3133/ofr72157.]

Helsel, D.R., Hirsch, R.M., Ryberg, K.R., Archfield, S.A., and Gilroy, E.J., 2020, Statistical methods in water resources: U.S. Geological Survey Techniques and Methods, book 4, chap. A3, 458 p. [Available at https://doi.org/10.3133/tm4A3.] (Supersedes USGS Techniques of Water-Resources Investigations, book 4, chap. A3, version 1.1.)

Hillel, D., 1982, Introduction to soil physics: Orlando, Florida, Academic Press, 364 p.

Izbicki, J.A., 2004, A small-diameter sample pump for collection of depth-dependent samples from production wells under pumping conditions: U.S. Geological Survey Fact Sheet 2004–3096, 2 p. [Available at https://doi.org/10.3133/fs20043096.]

Izbicki, J.A., Christensen, A.H., Hanson, R.T., Martin, P.M., Crawford, S.M., and Smith, G.A., 1999, U.S. Geological Survey combined well-bore flow and depth-dependent water sampler: U.S. Geological Survey Fact Sheet 196–99, 2 p. [Available at https://doi.org/10.3133/fs19699.]

Izbicki, J.A., Clark, D.A., Pimental, M.I., Land, M., Radyk, J.C., and Michel, R.L., 2000a, Data from a thick unsaturated zone underlying Oro Grande and Sheep Creek washes in the western part of the Mojave Desert, near Victorville, San Bernardino County, California: U.S. Geological Survey Open-File Report 2000–262, 133 p., accessed December 19, 2019, at https://doi.org/10.3133/ofr00262.

Izbicki, J.A., Radyk, J.C., and Michel, R.L., 2000b, Water movement through a thick unsaturated zone underlying an intermittent stream in the western Mojave Desert, southern California, USA: Journal of Hydrology, v. 238, no. 3–4, p. 194–217, accessed December 13, 2019, at https://doi.org/10.1016/S0022-1694(00)00331-0.

Izbicki, J.A., Radyk, J.C., and Michel, R.L., 2002, Movement of water through the thick unsaturated zone underlying Oro Grande and Sheep Creek Washes in the western Mojave Desert, USA: Hydrogeology Journal, v. 10, no. 3, p. 409–427, accessed December 13, 2019, at https://doi.org/10.1007/s10040-002-0194-8.

Izbicki, J.A., Johnson, R.U., Kulongoski, J., and Predmore, S., 2007, Ground-water recharge from small intermittent streams in the western Mojave Desert, California, *in* Stonestrom, D.A., Constants, J., Ferre, T.P.A., and Leake, S.T., eds., Ground-recharge in the arid and semiarid southwestern United States: U.S. Geological Survey Professional Paper 1703–G, p. 157–184. [Available at https://doi.org/10.3133/pp1703G.]

Izbicki, J.A., Teague, N.F., Hatzinger, P.B., Böhlke, J.K., and Sturchio, N.C., 2015, Groundwater movement, recharge, and perchlorate occurrence in a faulted alluvial aquifer in California (USA): Hydrogeology Journal, v. 23, p. 467–491. [Available at https://doi.org/10.1007/s10040-014-1217-y.]

Jacobs Engineering Group, Inc., 2019, Ground water flow modeling to support the Hinkley chromium background study, San Bernardino County, California, Project no. 706888CH, for Pacific Gas and Electric Company: Redding, Calif., Jacobs Engineering Group, Inc., [variously paged], with Appendixes A through H.

James, S.C., Jepsen, R.A., Beauheim, R.L., Pedler, W.H., and Mandell, W.A., 2006, Simulations to verify horizontal flow measurements from a borehole flowmeter: Groundwater, v. 44, no. 3, p. 394–405. [Available at https://doi.org/10.1111/j.1745-6584.2005.00140.x.]

Jennings, C.W., 1977, Geologic map of California: California Division of Mines and Geology, Geologic Data Map No. 2, scale 1:750,000.

Jennings, C.W., with modifications by Gutierrez, C., Bryant, W., Saucedo, G., and Wills, C., 2010, Geologic map of California: California Geological Survey, Geologic Data Map No. 2, scale 1:750,000.

Johnson, C.D., and Williams, J.H., 2003, Hydraulic logging methods—A summary and field demonstration in Conyers, Rockdale County, Georgia, *in* Williams, L.J., ed., Methods used to assess the occurrence and availability of ground water in fractured crystalline bedrock—An excursion into areas of Lithonia Gneiss in eastern metropolitan Atlanta, Georgia: Georgia Geologic Survey, Guidebook 23, p. 40–47, accessed January 18, 2022 at https://pubs.er.usgs.gov/publication/70206234.

Jury, W.A., Gardner, W.R., and Gardner, W.H., 1991, Soil Physics (5th ed.): New York, N.Y., John Wiley and Sons, 328 p.

Kearl, P.M., and Roemer, K., 1998, Evaluation of groundwater flow directions in a heterogeneous aquifer using the colloidal borescope: Advances in Environmental Research, v. 2, no. 1, p. 12–23.

Kerfoot, W.B., 1988, Monitoring well construction and recommended procedures using a heat-pulsing flowmeter, *in* Collins, A.G., and Johnson, A.I., eds., Ground-water contamination—Field methods (Special Technical Publication 963): Philadelphia, Pa., American Society for Testing and Materials, p. 146–161.

Kerfoot, W.B., 1995, Independent verification of heat pulse groundwater flowmeter results through long term observation and tracer tests on Superfund sites, *in* Hydrocarbon Contaminated Soils: Amherst, Mass., Amherst Scientific Publishers, p. 37–49.

Keys, W.S., 1990, Borehole geophysics applied to ground-water investigations. U.S Geological Survey Techniques of Water-Resources Investigations, book 2, chap. E2, 150 p., accessed December 12, 2019, at https://pubs.usgs.gov/twri/twri2-e2/.

Knight, R., Walsh, D.O., Butler, J.J., Jr., Grunewald, E., Liu, G., Parsekian, A.D., Reboulet, E.C., Knobbe, S., and Barrows, M., 2015, NMR logging to estimate hydraulic conductivity in unconsolidated aquifers: Groundwater, v. 54, no. 1, p. 104–114. [Available at https://doi.org/10.1111/gwat.12324.]

Kunkel, F., 1962, Preliminary map showing valley-fill areas and source, occurrence and movement of ground water in the western part of the Mojave Desert region,California: U.S. Geological Survey Hydrologic Atlas 31. [Available at https://doi.org/10.3133/ha31.]

Lahontan Regional Water Quality Control Board, 2012, Staff report summary and discussion—Peer review of Pacific Gas & Electric Company's 2007 groundwater chromium background study report: South Lake Tahoe, Calif. Regional Water Quality Control Board, Lahontan Region, 59 p., accessed November 20, 2018, at https://www.waterboards.ca.gov/lahontan/water_issues/projects/pge/docs/encl_1.pdf.

Lahontan Regional Water Quality Control Board, 2013, Final environmental impact report—Comprehensive groundwater cleanup strategy for historical chromium discharges from PG&E's Hinkley Compressor Station, San Bernardino County: South Lake Tahoe, Calif., California Regional Water Quality Control Board, Lahontan Region, [variously paged], accessed November 20, 2018, at https://www.waterboards.ca.gov/rwqcb6/water_issues/projects/pge/docs/feir/vol1_intro.pdf.

Langenheim, V.E., Morita, A.Y., Martin, A.J., Jordan, J., and Haddon, E.K., 2019, Gravity data of the Hinkley area, southern California: U.S. Geological Survey data release, available at https://doi.org/10.5066/P9FV5LG5.

Laton, R.W., Foster, J., Ebbs, V., Blazevic, M., Napoli, N., and Perez, R., 2007, Harper Lake basin, San Bernardino County, California hydrogeologic report: California State University Fullerton, Department of Geological Sciences, 127 p.

Legchenko, A., and Valla, P., 2002, A review of the basic principles for proton magnetic resonance sounding measurements: Journal of Applied Geophysics, v. 50, no. 1–2, p. 3–19. [Available at https://doi.org/10.1016/S0926-9851(02)00127-1.]

Legchenko, A., Baltassat, J.-M., Beauce, A., and Bernard, J., 2002, Nuclear magnetic resonance as a geophysical tool for hydrogeologists: Journal of Applied Geophysics, v. 50, no. 1–2, p. 21–46. [Available at https://doi.org/10.1016/S0926-9851(02)00128-3.]

Lines, G.C., 1996, Ground-water and surface-water relations along the Mojave River, southern California: U.S. Geological Survey Water-Resources Investigations Report 95–4189, 43 p., accessed December 6, 2018, at https://pubs.er.usgs.gov/publication/wri954189.

Lunne, T., Robertson, P.K., and Powell, J.J.M., 1997, Cone penetration testing in geotechnical practice: London, U.K., Spon Press.

Miller, D.M., Haddon, E.K., Langenheim, V.E., Cyr, A.J., Wan, E., Walkup, L.C., and Starratt, S.W., 2018a, Middle Pleistocene infill of Hinkley Valley by Mojave River sediment and associated lake sediment—Depositional architecture and deformation by strike-slip faults, *in* Miller, D.M., ed., The Mojave River from sink to source: The 2018 Desert Symposium Field Guide and Proceedings, April 2018, p. 58–65, accessed November 27, 2018, at http://www.desertsymposium.org/2018%20DS%20Against%20the%20Current.pdf.

Miller, D.M., Reynolds, R.M., Groover, K.D., Buesch, D.C., Brown, H.J., Cromwell, G.A., Densmore, J., Garcia, A.L., Hughson, D., Knott, J.R., and Lovich, J., 2018b, Against the current—The Mojave River from sink to source: The 2018 Desert Symposium field trip road log: The 2018 Desert Symposium Field Guide and Proceedings, April 1, 2018, accessed November 27, 2018, at http://www.desertsymposium.org/2018%20DS%20Against%20the%20Current.pdf.

Miller, D.M., Langenheim, V.E., and Haddon, E.K., 2020, Geologic map and borehole stratigraphy of Hinkley Valley and vicinity, San Bernardino County, California: U.S. Geological Survey Scientific Investigations Map 3458, 2 sheets, scale 1:24,000, pamphlet 23 p. [Available at https://doi.org/10.3133/sim3458.]

Mojave Water Agency, 2014, Geospatial library: Mojave Water Agency, accessed May 22, 2014, at https://www.mojavewater.org/data-maps/geospatial-library/.

Natural Resources Conservation Service, 2006, U.S. general soil map (SSURGO/STATSGO2): accessed December 13, 2019, at https://www.nrcs.usda.gov/wps/portal/nrcs/detail/soils/survey/geo/?cid=nrcs142p2_053631.

Neter, J., and Wasserman, W., 1974, Applied linear statistical models: Homewood, Ill., Richard D. Irwin Inc., 842 p.

Newhouse, M.W., Izbicki, J.A., and Smith, G.A., 2005, Comparison of velocity-log data collected using impeller and electromagnetic flowmeters: Groundwater, v. 43, no. 3, p. 434–438. [Available at https://doi.org/10.1111/j.1745-6584.2005.0030.x.]

Noce, T.E., Holzer, T.L., and Havach, G.A., 2003, Subsurface exploration with the cone penetration testing truck: U.S. Geological Survey Fact Sheet 028–03, 2 p. [Available at https://doi.org/10.3133/fs02803.]

Pacific Gas and Electric Company, 2011, Addendum #2 to the feasibility study: San Francisco, Calif., Pacific Gas and Electric Company, [variously paged], accessed May 7, 2020, at https://www.waterboards.ca.gov/lahontan/water_issues/projects/pge/docs/addndm2.pdf.

Paillet, F.L., 2000, Flow logging in difficult boreholes—Making the best of a bad deal, *in* Proceedings of the 7th International Symposium on Borehole Geophysics for Minerals, Geotechnical, and Groundwater Applications, Denver, Colo., 2000: The Minerals and Geotechnical Logging Society, A Chapter at Large of the Society of Professional Well Log Analysts, Houston, Tex., p. 125–135.

Paillet, F.L., Hite, L., and Carlson, M., 1999, Integrating surface and borehole geophysics in ground water studies—An example using electromagnetic soundings in South Florida: Journal of Environmental & Engineering Geophysics, v. 4, no. 1, p. 45–55. [Available at https://doi.org/10.4133/JEEG4.1.45.]

Prudic, D.E., 1994, Estimates of percolation rates and ages of water in unsaturated sediments at two Mojave Desert sites, California–Nevada: U.S. Geological Survey Water-Resources Investigations Report 94–4160, 19 p. , accessed December 13, 2019, at https://doi.org/10.3133/wri944160.

Robertson, P.K., 1990, Soil classification using the cone penetration test: Canadian Geotechnical Journal, v. 27, no. 1, p. 151–158. [Available at https://doi.org/10.1139/t90-014.]

Seymour, W.A., 2016, Hydrologic and geologic controls on groundwater recharge along the Mojave River floodplain aquifer: San Diego State University, Department of Geography, Master's Thesis, 73 p., accessed November 20, 2018, at https://digitallibrary.sdsu.edu/islandora/object/sdsu%3A1599.

Seymour, W.A., and Izbicki, J.A., 2018, Predevelopment water-levels in the Centro area of the Mojave River groundwater basin, *in* Miller, D.M., ed., The Mojave River from sink to source: The 2018 Desert Symposium Field Guide and Proceedings, April 2018, accessed November 27, 2018, at http://www.desertsymposium.org/2018%20DS%20Against%20the%20Current.pdf.

Stamos, C.L., and Predmore, S.K., 1995, Data and water-table map of the Mojave River ground-water basin, San Bernardino County, California, November 1992: U.S. Geological Survey Water-Resources Investigations Report 95–4148, scale 1:125,000, 1 sheet. [Available at https://doi.org/10.3133/wri954148.]

Stamos, C.L., Martin, P., Nishikawa, T., and Cox, B.F., 2001, Simulation of ground-water flow in the Mojave River Basin, California: U.S. Geological Survey Water-Resources Investigations Report 2001–4002, 129 p. [Available at https://doi.org/10.3133/wri014002.]

Stantec, 2013, Compliance with provision 1.C. of Cleanup and Abatement Order R6V-2008-0002-A4 and requirements of Investigation Order R6V-2013-0029: Prepared for Pacific Gas and Electric Company's Hinkley Compressor Station, Project No. 185702675, [variously paged]. [Available at https://geotracker.waterboards.ca.gov/esi/uploads/geo_report/8126426041/SL0607111288.PDF.]

Stone, R.S., 1957, Groundwater resonance in the western part of the Mojave Desert, California—with particular respect to the boron content of well water: U.S. Geological Survey Open-File Report 57–107, 102 p., accessed December 6, 2018, at https://doi.org/10.3133/ofr57107.

Thompson, D.G., 1929, The Mohave Desert region, California, a geographic, geologic, and hydrologic reconnaissance: U.S. Geological Survey Water Supply Paper578, 759 p. [Available at https://doi.org/10.3133/wsp578.]

U.S. Environmental Protection Agency, 2007, Method 7010—Graphite furnace atomic absorption spectrophotometry: U.S. Environmental Protection Agency, accessed April 19, 2018, at https://www.epa.gov/sites/production/files/2015-12/documents/7010.pdf.

U.S. Geological Survey, 2019, USGS GeoLog Locator: accessed December 16, 2019, at https://doi.org/10.5066/F7X63KT0.

U.S. Geological Survey, 2021, USGS water data for the Nation: U.S. Geological Survey National Water Information System database, accessed January 6, 2021, at https://doi.org/10.5066/F7P55KJN.

Young, S.C., and Pearson, H.S., 1995, The electromagnetic borehole flowmeter—Description and application: Groundwater Monitoring and Remediation, v. 15, no. 4, p. 138–147. [Available at https://doi.org/10.1111/j.1745-6592.1995.tb00561.x.]

Appendix H.1. Selected Site Information, Geophysical Log, Hydrologic, Core-Extraction, and Depth-Dependent Water-Quality Data for Hinkley and Water Valleys, California

This appendix contains tables of (1) well-construction data, geophysical log availability, and hydraulic-conductivity values from slug-test data for selected wells (table H.1.1 available for download at https://doi.org/10.313/pp1885); (2) predevelopment water-level data for selected wells (table H.1.2 available for download at https://doi.org/10.313/pp1885); (3) monthly runoff from upland drainages (table H.1.3 available for download at https://doi.org/10.313/pp1885); (4) water extraction data for core material from selected sites (table H.1.4 available for download at https://doi.org/10.313/pp1885); and (5) depth-dependent well-bore flow, water chemistry, and isotope data for selected sites (table H.1.5 available for download at https://doi.org/10.313/pp1885). Geophysical-log data available from selected wells (table H.1.1) include cone penetration (CPT), electromagnetic (EM) induction, nuclear magnetic resonance (NMR), and point velocity probe (PVP) logs. Geophysical-log data and methods of analyses are available in the U.S. Geological Survey (USGS) GeoLog Locator (U.S. Geological Survey, 2019; https://webapps.usgs.gov/GeoLogLocator/#!/). Slug-test data and methods of analyses are available in Groover and others (2021). Well location, measurement data, and predevelopment water-level data from 48 wells collected as early as 1918 in Hinkley and Water Valleys (table H.1.2) are from Thompson (1929), Conkling (1934), or California Department of Water Resources (1967). Data for these wells and predevelopment water-level data for additional wells in surrounding areas are available online (U.S. Geological Survey, 2021). Monthly runoff data from 1930 to 2015 for 22 upland drainages contributing streamflow and groundwater recharge to Hinkley and Water Valleys were calculated using the Basin Characteristic Model (BCM; Flint and others, 2013, 2021; Flint and Flint, 2014). Water-extraction data from core material collected at four selected well sites (including replicate and blank analyses) and analyzed for selected soluble anions (including bromide, chloride, sulfate, and nitrate) and chromium (table H.1.4) were prepared and analyzed using methods provided by Izbicki and others (2000). Depth-dependent water chemistry and isotope data were collected at five sites in Hinkley and Water Valleys. Data collected at each well included (1) a set of geophysical logs collected according to manufacturer calibration and operation specifications under unpumped and pumped conditions (table H.1.1; U.S. Geological Survey, 2019; https://webapps.usgs.gov/GeoLogLocator/#!/), (2) water-quality samples collected from the surface discharge of pumps within the well (table H.1.5), and (3) water-quality samples collected during pumped conditions from selected depths within the well (table H.1.5) using methods described by Izbicki and others (1999, 2015) and Izbicki (2004). Water-extraction data from core material and depth-dependent water chemistry and isotope data, including replicate and blank data, also are available online (U.S. Geological Survey, 2021).

References Cited

California Department of Water Resources, 1967, Mojave River ground water basins investigation: California Department of Water Resources Bulletin No. 84, 151 p., accessed January 18, 2022, at https://archive.org/details/mojaverivergroun84cali/page/n5/mode/2up.

Conkling, H., 1934, Mojave River investigation: Sacramento, Calif., State of California Department of Water Resources Bulletin No. 47, 249 p., accessed January 18, 2022, at https://openlibrary.org/works/OL7645771W/Mojave_River_investigation.

Flint, L.E., and Flint, A.L., 2014, California basin characterization model—A dataset of historical and future hydrologic response to climate change, (ver. 1.1, May 2017): U.S. Geological Survey data release, accessed December 19, 2019 at https://doi.org/10.5066/F76T0JPB.

Flint, L.E., Flint, A.L., Thorne, J.H., and Boynton, R., 2013, Fine-scale hydrologic modeling for regional landscape applications—The California basin characterization model development and performance: Ecological Processes, v. 2, article no. 25, 21 p., accessed December 13, 2019, at https://doi.org/10.1186/2192-1709-2-25.

Flint, L.E., Flint, A.L., and Stern, M.A., 2021, The basin characterization model—A regional water balance software package: U.S. Geological Survey Techniques and Methods, book 6, chap. H1, 85 p., accessed June 2, 2021, at https://doi.org/10.3133/tm6H1.

Groover, K.D., Izbicki, J.A., Larsen, J.D., Dick, M.C., Nawikas, J., and Kohel, C.A., 2021, Hydrologic data in Hinkley and Water Valleys, San Bernardino County, California, 2015–2018: U.S. Geological Survey data release, available at https://doi.org/10.5066/P9BUXAX1.

Izbicki, J.A., 2004, A small-diameter sample pump for collection of depth-dependent samples from production wells under pumping conditions: U.S. Geological Survey Fact Sheet 2004–3096, 2 p. [Available at https://doi.org/10.3133/fs20043096.]

Izbicki, J.A., Christensen, A.H., Hanson, R.T., Martin, P.M., Crawford, S.M., and Smith, G.A., 1999, U.S. Geological Survey combined well-bore flow and depth-dependent water sampler: U.S. Geological Survey Factsheet 196–99, 2 p. [Available at https://doi.org/10.3133/fs19699.]

Izbicki, J.A., Clark, D.A., Pimental, M.I., Land, M., Radyk, J.C., and Michel, R.L., 2000, Data from a thick unsaturated zone underlying Oro Grande and Sheep Creek washes in the western part of the Mojave Desert, near Victorville, San Bernardino County, California: U.S. Geological Survey Open-File Report 2000–262, 133 p., accessed December 19, 2019, at https://doi.org/10.3133/ofr00262.

Izbicki, J.A., Teague, N.F., Hatzinger, P.B., Böhlke, J.K., and Sturchio, N.C., 2015, Groundwater movement, recharge, and perchlorate occurrence in a faulted alluvial aquifer in California (USA): Hydrogeology Journal, v. 23, p. 467–491. [Available at https://doi.org/10.1007/s10040-014-1217-y.]

Thompson, D.G., 1929, The Mohave Desert region, California, a geographic, geologic, and hydrologic reconnaissance: U.S. Geological Survey Water Supply Paper578, 759 p. [Available at https://doi.org/10.3133/wsp578.]

U.S. Geological Survey, 2019, USGS GeoLog Locator: accessed December 16, 2019, at https://doi.org/10.5066/F7X63KT0.

U.S. Geological Survey, 2021, USGS water data for the Nation: U.S. Geological Survey National Water Information System database, accessed January 6, 2021, at https://doi.org/10.5066/F7P55KJN.

Appendix H.2. Comparison of Groundwater-Age and Chemical Data with Groundwater-Flow Model Particle-Track Results, Hinkley and Water Valleys, California

Hinkley Valley Groundwater-Flow Models

Prior to this study, two groundwater-flow models had been developed for the Hinkley Valley area, about 80 miles (mi) northeast of Los Angeles, California (fig. H.2.1). The Pacific Gas and Electric Company (PG&E) model (ARCADIS and CH2M Hill, 2011) simulates groundwater flow in that part of Hinkley Valley near and downgradient from the Hinkley compressor station between 1990 and 2010 and the PG&E model has been used to evaluate various hexavalent chromium, Cr(VI), plume-management alternatives. The U.S. Geological Survey (USGS) regional model (Stamos and others, 2001) simulates groundwater flow in the larger Mojave River groundwater basin between 1931 and 1999, and the USGS model has been used to evaluate regional water-management alternatives. Although not calibrated to groundwater-age (time since recharge) data, the performance of this model was evaluated with respect to regional groundwater isotope and age data (Izbicki and others, 2004). The USGS regional model has less hydrogeologic detail in the Hinkley area than the PG&E model but simulates groundwater flow from predevelopment (pre-1930) to 1999 and includes the period of Cr(VI) releases from the PG&E Hinkley compressor station (1952–64). Although each model is suitable for its intended use, neither model was suitable, without modification, for the purposes of the USGS Cr(VI) background study.

In support of the USGS Cr(VI) background study, the PG&E groundwater-flow model (ARCADIS and CH2M Hill, 2011) was updated by PG&E consultants (Jacobs Engineering Group, Inc., 2019). The updated model, known as the Hinkley Chromium Background Study Model (HCBSM; Jacobs Engineering Group, Inc., 2019), includes a larger areal extent and longer period for simulation of groundwater flow in Hinkley Valley and part of Water Valley than the PG&E groundwater-flow model (ARCADIS and CH2M Hill, 2011), and it has more detailed aquifer property data than the USGS regional model (Stamos and others, 2001).

The HCBSM was developed using the computer program MODHMS/MODFLOW-SURFACT (HydroGeoLogic, Inc., 2011) by Jacobs Engineering Group, Inc. (2019), to include temporal data from Stamos and others (2001), aquifer property data from ARCADIS and CH2M Hill (2011), and data provided in this chapter. The computer program MODHMS/MODFLOW-SURFACT (HydroGeoLogic, Inc., 2011) is proprietary, and the model was converted into MODFLOW-NWT (Niswonger and others, 2011), which is in the public domain. Details of model construction, including model grid and layering, boundary conditions, and simulation of aquifer properties, are provided in Jacobs Engineering Group, Inc. (2019).

The areal extent of the HCBSM includes (1) Hinkley Valley and portions of Water Valley, (2) the October–December 2015 (Q4 2015) regulatory Cr(VI) plume extent (ARCADIS, 2016), and (3) the maximum mapped extent of groundwater having Cr(VI) concentrations greater than the 3.1 micrograms per liter (µg/L) interim regulatory background Cr(VI) concentration (fig. H.2.1; ARCADIS, 2016). Hydrologic features within Hinkley and Water Valleys that are important to groundwater flow and Cr(VI) movement downgradient from the Hinkley compressor station and simulated within the HCBSM include the Mojave River, the Lockhart fault, the Mount General fault, Hinkley Gap, and groundwater-discharge areas near Harper (dry) Lake (fig. H.2.1).

The simulation period for the HCBSM is from 1930 to 2015. The updated groundwater-flow model was calibrated to predevelopment water-level data and to steady-state water-budget data that could be measured or estimated. The HCBSM also was calibrated to transient water-level data and water-budget data (including intermittent/episodic recharge from the Mojave River) for the simulation period 1931–2015. The HCBSM simulation includes the period of Cr(VI) releases from the PG&E Hinkley compressor station, between 1952 and 1964, and groundwater recharge and movement during several large magnitude streamflows within the intermittent Mojave River that occurred during the simulation period.

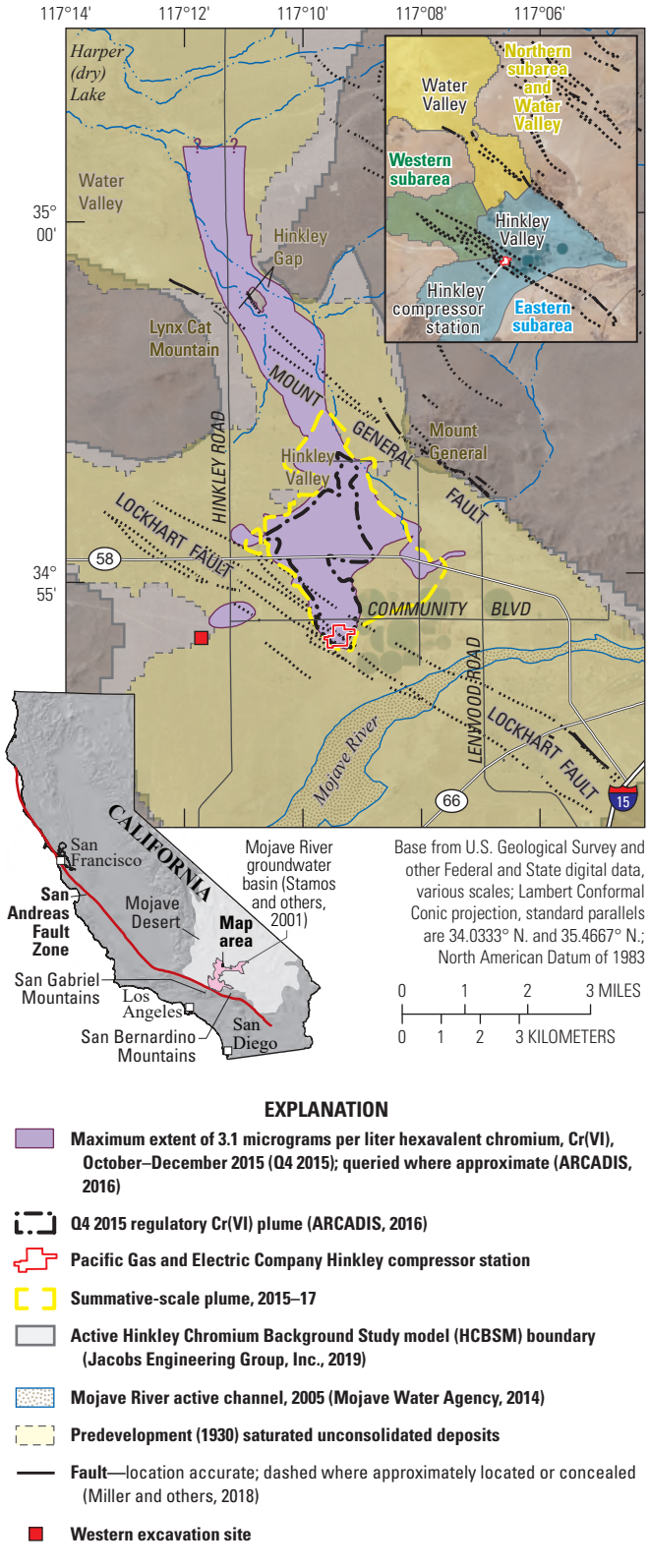

Figure H.2.1. Location of Hinkley and Water Valleys, western Mojave Desert, California.

Simulations within the HCBSM provided reasonable matches to measured water levels from wells distributed throughout Hinkley and Water Valleys that averaged 3 percent of measured values (Jacobs Engineering Group, Inc., 2019). Although simulated values for recharge as infiltration of streamflow from the Mojave River within the HCBSM differed slightly from values within the USGS regional model, between October 1930 and September 2000, cumulative simulated infiltration extracted from the USGS regional model and the HCBSM were 1.002 and 1.004 million acre-feet, respectively (Jacobs Engineering Group, Inc., 2019). Other elements of the water budget within the HCBSM including groundwater discharge near Harper (dry) Lake, groundwater flow through Hinkley Gap, local recharge, pumping, and irrigation and septic return were simulated within published ranges or within ranges estimated in this chapter (Jacobs Engineering Group, Inc., 2019). Details of model calibration including steady-state and transient calibration and water-budget analyses are provided in Jacobs Engineering Group, Inc. (2019).

The movement of hexavalent chromium released from the Hinkley compressor station between 1952 and 1964 and the end of the HCBSM simulation period (2015), integrates the combined effects of recharge, pumping, and the distribution of aquifer hydraulic properties, including the interconnectedness of high-permeability aquifer materials, in a manner that cannot be assessed from point data. Solute transport was not simulated by the HCBSM; instead, groundwater movement and Cr(VI) movement were inferred from the movement of simulated particles within the HCBSM.

Particle simulations were run forward through time to represent recharge from the Mojave River and releases from the Hinkley compressor station, Forward-particle simulations done by Jacobs Engineering Group, Inc. (2019), calculated particle location at selected model timesteps using the computer program MODPATH (Pollock, 1994, 2016). Details of forward-particle simulations including particle-releases representing recharge from the Mojave River and representing historical Cr(VI) release locations at the Hinkley compressor station are provided by Jacobs Engineering Group, Inc. (2019).

In addition to forward-particle simulations, reverse-particle simulations were calculated from selected wells backward through time from 2015 to the beginning of the simulation period. Reverse-particle tracks were used to determine where water at those wells originated. Reverse-particle tracks were not calculated for all wells sampled as part of the USGS Cr(VI) background study, although some reverse-particle tracks were calculated for selected production wells, which were not sampled. Details of reverse-particle track calculations and results are provided by Jacobs Engineering Group, Inc. (2019).

Purpose and Scope

Groundwater-age data and Cr(VI) concentrations downgradient from the Hinkley compressor station were compared to simulated particle-track data calculated using the HCBSM (Jacobs Engineering Group, Inc., 2019). The purpose of these comparisons was to determine if HCBSM results could be used to refine estimates of anthropogenic Cr(VI) extent and the summative-scale Cr(VI) plume extent using an iterative process described by Izbicki and Groover (2016, 2018). Repeating published model documentation was beyond the scope of this work and readers are referred to Jacobs Engineering Group, Inc. (2019), for details of model construction, calibration, and particle-track calculations. Additional particle-track analyses not discussed in this appendix are available in Jacobs Engineering Group, Inc. (2019).

Comparison Between Groundwater-Age Data and Hinkley Chromium Background Study Model Particle-Simulation Results

Three comparisons between groundwater-age data and HCBSM particle-simulation results are presented. These comparisons address (1) groundwater movement in shallow and deep zones within the upper aquifer, (2) groundwater movement in the western subarea, and (3) groundwater and anthropogenic Cr(VI) movement downgradient from the Hinkley compressor station. Groundwater age was evaluated on the basis of tritium data and tritium/helium-3 ages calculated for post-1952 groundwater and carbon-14 data for older groundwater (chapter F).

Groundwater Movement in Shallow and Deep Zones Within the Upper Aquifer

Groundwater-age data collected as part of the USGS Cr(VI) background study show younger groundwater ages in the shallow zone of the upper aquifer than in the deep zone (chapter F, figs. F.13*A*, F.13*B*). Detectable tritium within the shallow zone of the upper aquifer extended throughout Hinkley Valley as far downgradient as well MW-174S1 in Water Valley (fig. H.2.2*A*), about 7.4 mi downgradient from the Mojave River. The farthest downgradient well in the deep zone containing detectable tritium was well MW-128S3 (fig. H.2.2*B*), near the leading edge of the Q4 2015 regulatory Cr(VI) plume and about 3.8 mi downgradient from the Mojave River. These data indicate more rapid movement of water through the shallow zone compared to the deep zone within the upper aquifer.

The distribution of groundwater ages with depth in the aquifer is consistent with hydraulic property data (appendix H.1, table H.1.1) that show higher hydraulic conductivities within the shallow zone than within the deep zone of the upper aquifer. Nuclear magnetic resonance data show higher hydraulic conductivities within formerly saturated alluvium beneath the Hinkley compressor station (fig. H.12), and in formerly saturated alluvium farther downgradient in Hinkley and Water Valleys (fig. H.13), than in saturated alluvium at the time of this study. The groundwater-age data also are consistent with coupled well-bore flow data from wells IW-03 and C-01 within the Q4 2015 regulatory Cr(VI) plume (figs. H.15, H.16) that show most well yield is from thin, highly permeable, and laterally continuous beach sands within the shallow zone of the upper aquifer.

The HCBSM forward-particle simulations of recharge from infiltration of 1958 streamflow within the Mojave River (Jacobs Engineering Group, Inc., 2019) show particle locations at model timesteps between 1958 and the end of the simulation in September 2015 (fig. H.2.2). Particles were released into the simulation from active river and stream model cells along the Mojave River (Jacobs Engineering Group, Inc., 2019). The leading edge of the particle front represents particle locations at the end of the HCBSM simulation in 2015. Particles were not timestamped (Jacobs Engineering Group, Inc., 2019); consequently, particle locations at different times within the simulation cannot be evaluated. Consistent with interpretations presented in this professional paper, HCBSM particle simulations show that not all water recharged from the Mojave River during the period of Cr(VI) releases would have passed near the Hinkley compressor station and would contain anthropogenic Cr(VI). However, all water containing anthropogenic Cr(VI) would have been recharged from the Mojave River and would have passed near the Hinkley compressor station.

In contrast to groundwater-age data, HCBSM forward-particle simulations representing recharge from the Mojave River in 1958 show less movement of particles within the shallow zone (fig. H.2.2*A*). The forward-particle simulations also show greater movement of particles within the deep zone of the upper aquifer between 1958 and 2015 (fig. H.2.2*B*).

Parts of the shallow zone were dry as a result of agricultural pumping and water-level declines beginning in the early 1950s (Stone, 1957; California Department of Water Resources, 1967). Unsaturated conditions within the shallow zone may have limited groundwater and simulated-particle movement (and Cr(VI) movement) through that part of the aquifer in the early 1950s. The HCBSM simulations do not show particles within the shallow zone reaching downgradient wells within the northern subarea or Water Valley (fig. H.2.2*A*).

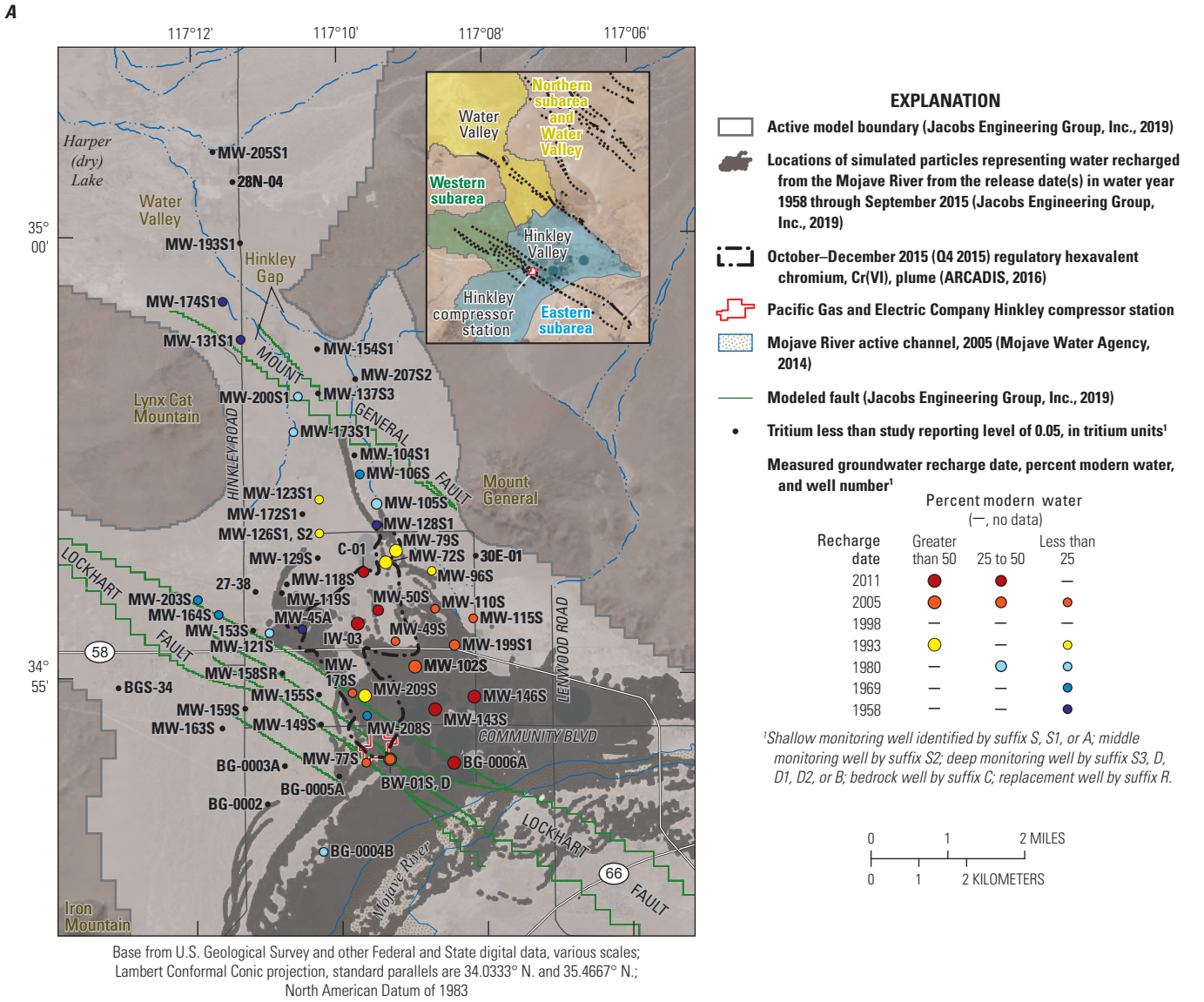

Figure H.2.2. Groundwater-recharge date and locations of simulated particles representing water recharged from the Mojave River from the time of recharge in 1958 through September 2015 within *A*, the shallow zone and *B*, the deep zone of the upper aquifer, Hinkley and Water Valleys, western Mojave Desert, California. Groundwater recharge data were calculated from tritium and helium data in U.S. Geological Survey (2021); calculated groundwater recharge data and percent modern water are available in chapter G (table G.1.1); and particle location data are available in Jacobs Engineering Group, Inc. (2019).

Simulated particles within the deep zone of the upper aquifer extend downgradient into parts of the northern subarea where tritium was not detected in water from wells (fig. H.2.2*B*) and older groundwater was present. Carbon-14 activities in water from well MW-104D, near the leading edge of the simulated particle front in the deep zone of the upper aquifer, were 8.9 percent modern carbon (pmc; chapter E, appendix E.1, table E.1.1) with an unadjusted age greater than 20,000 years before present (ybp). Water from wells MW-105D and MW-79D, upgradient from well MW-104D and within the simulated-particle distribution (fig. H.2.2*B*), have carbon-14 activities of 44 and 67 pmc (chapter E, appendix E.1, table E.1.1) with unadjusted ages of 6,800 and 3,300 ybp, respectively, that predate simulated 1958 recharge from the Mojave River.

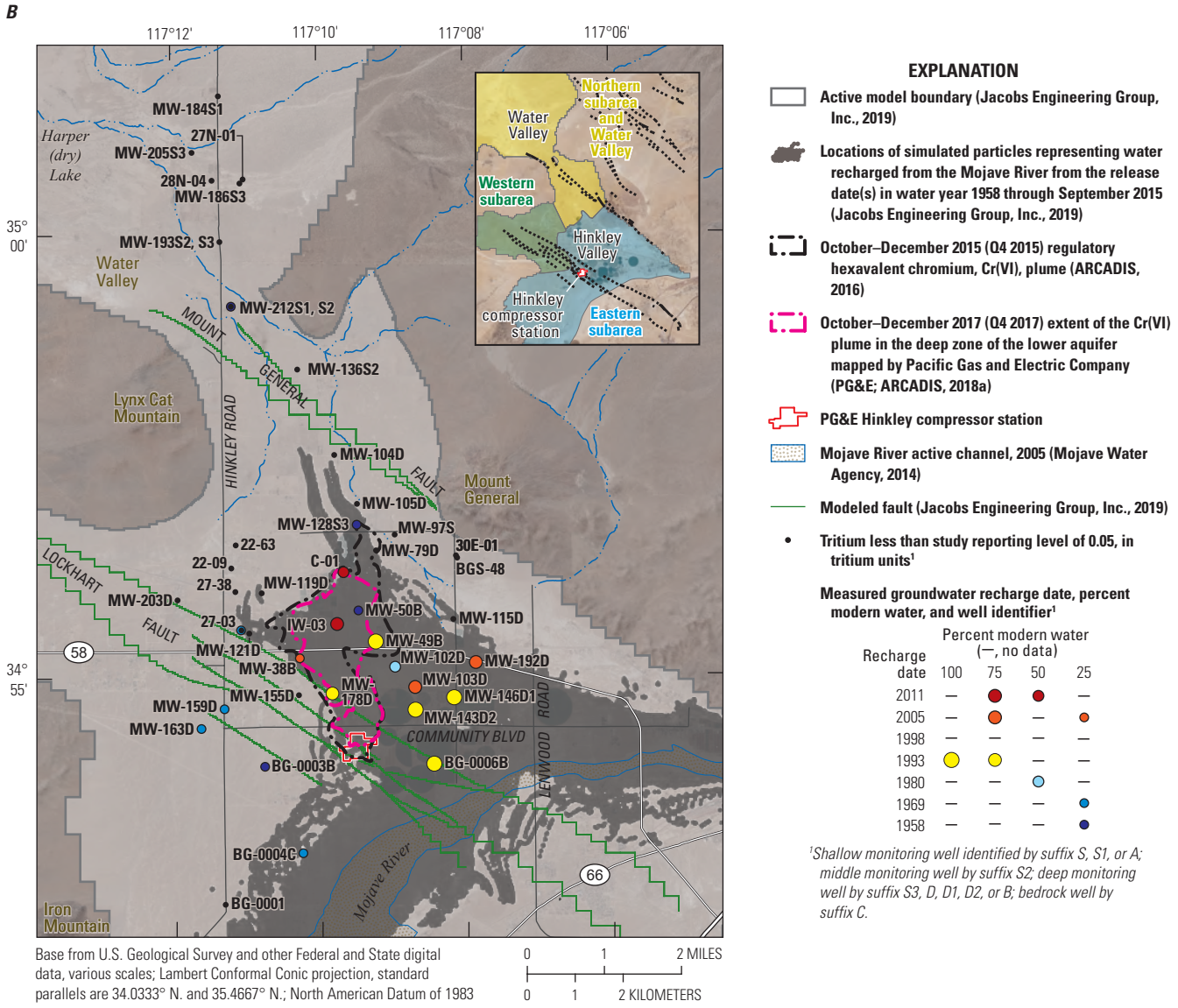

Figure H.2.2.—Continued

Forward-particle simulations also were calculated for water recharged from the Mojave River in 1969, 1993, 2005, and 2011 to the end of the simulation in September 2015 (fig. H.2.3). Calculations and particle releases within the HCBSM were similar to simulations of particles representing 1958 recharge from the Mojave River (Jacobs Engineering Group, Inc., 2019). Results for forward-particle simulations of 1969, 1993, and 2005 recharge were aggregated (fig. H.2.3) with only particles representing 2011 recharge shown separately. Similar to the results for 1958 recharge (fig. H.2.2*A*), HCBSM simulated particles within the shallow zone of the upper aquifer do not reach downgradient wells within the northern subarea and Water Valley that have low tritium concentrations and small percentages of post-1952 groundwater (fig. H.2.3*A*). However, simulated particles are more abundant in the shallow zone within the upper aquifer than simulated particles from 1958 recharge (fig. H.2.2*A*); possibly as a result of decreased agricultural pumping in the mid to late 1980s (Stamos and others, 2001; Jacobs Engineering Group, Inc., 2019). Similar to 1958 simulations, particles within the deep zone also reached wells that do not contain measurable tritium and have older groundwater ages that predate simulated 1969, 1993, 2005, and 2011 recharge from the Mojave River (fig. H.2.3*B*).

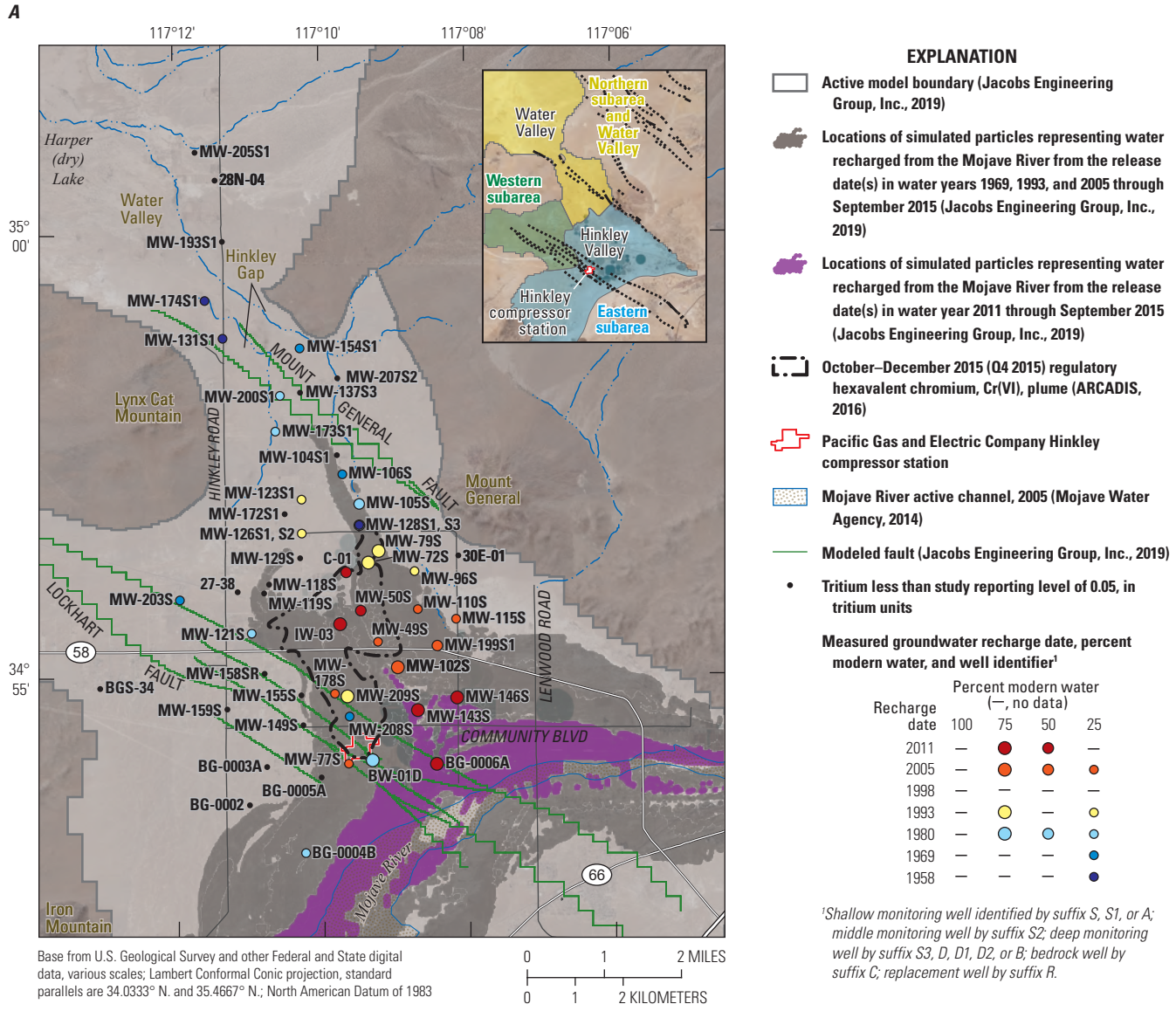

Figure H.2.3. Groundwater-recharge date and locations of simulated particles representing water recharged from the Mojave River in 1969, 1980, 1993, 2005, and 2011, from the time of recharge through September 2015 within *A*, the shallow zone and *B*, the deep zone of the upper aquifer, Hinkley and Water Valleys, western Mojave Desert, California. Groundwater recharge date and percent modern water were calculated from tritium and helium data in U.S. Geological Survey (2021); calculated groundwater recharge data are available in chapter G (table G.1.1); particle location data are available from Jacobs Engineering Group, Inc. (2019).

Measured groundwater-recharge dates for wells C-01, MW-50S, and IW-03 in the shallow zone of the upper aquifer in the eastern subarea are younger than groundwater-recharge dates in nearby and upgradient wells closer to the Mojave River (fig. H.2.3*A*). Water from these wells contains a high fraction of irrigation return water. Loss of helium-3, when the water was pumped to the surface for irrigation, may have reset the tritium/helium-3 ratio resulting in younger groundwater ages in water from these wells (chapter F) and may be responsible for differences in groundwater age and forward-particle simulation results at these wells.

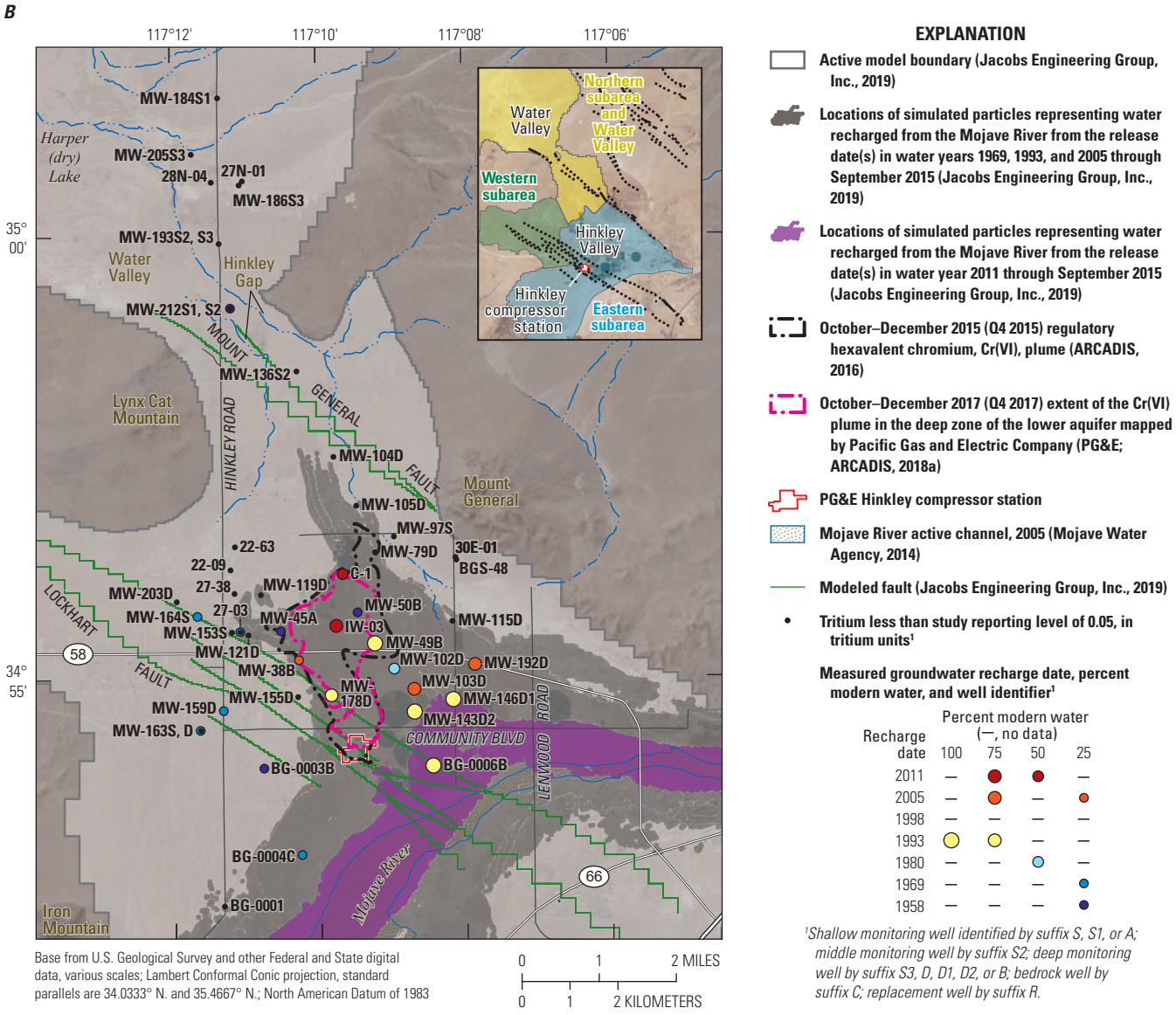

Figure H.2.3.—Continued

Given the uncertainty associated with interpreting low concentrations of tritium (chapter F), it may be reasonable that HCBSM particle simulations would not exactly duplicate the extent of post-1952 water measured as part of the USGS Cr(VI) background study in water from downgradient wells in the shallow zone of the upper aquifer. However, HCBSM simulations show greater movement of groundwater within the deep zone of the upper aquifer than within the shallow zone. Simulated particles within the deep zone extend into areas where groundwater does not contain measurable tritium, is old, and was recharged more than 20,000 ypb. The HCBSM particle-simulation results were not consistent with the measured distribution of groundwater-age data within shallow and deep zones of the upper aquifer (chapter F), and results were not consistent with the vertical distribution of aquifer hydraulic property data or with measured well-bore flow data collected as part of this study.

Groundwater Movement in the Western Subarea

Groundwater-age data collected as part of the USGS Cr(VI) background study show low-level tritium concentrations in water from some shallow wells in the western subarea on the downgradient side of the Lockhart fault (fig. H.2.2*A*). However, only water from well MW-121S had detectable tritium and carbon-14 activities consistent with post-1952 groundwater (chapter F). Tritium was not detected in monitoring wells MW-119S, MW-119D, or MW-118S in the western subarea to the north of the Lockhart fault (fig. H.2.2; chapter E, appendix E.1, table E.1.1); consistent with older (pre-1952) groundwater in that area.

The distribution of forward particles representing recharge from infiltration of 1958 streamflow within the Mojave River, calculated using the HCBSM, shows particle locations within the shallow zone of the upper aquifer that moved through wells MW-119S, MW-119D, and MW-118S in the western subarea and reached the northern subarea near well MW-129S (fig. H.2.2*A*). The HCBSM particle simulations (fig. H.2.3*A*) indicate particle movement continued through the western subarea into the northern subarea until at least 1969 (Jacobs Engineering Group, Inc., 2019). The HCBSM particle simulations do not show movement of younger (post 1952) water through the western subarea into the northern subarea within the deep zone of the upper aquifer (figs. H.2.2*B*, H.2.3*B*). Although saturated during predevelopment conditions, a bedrock high separates the western subarea from the northern subarea. Water-level data in 2017 (figs. H.8*C*, H.8*D*) and low well yields at the time of this study (2015–18) indicate that the shallow and deep zones of the upper aquifer in this area were largely dry and the bedrock high limited groundwater flow between the subareas.

The HCBSM results that show particle movement from the Mojave River through the shallow zone within the upper aquifer, underlying the western subarea into the northern subarea, are not consistent with the distribution of measured groundwater-age data (chapter F). The HCBSM shows water moving through wells MW-119S, MW-119D, and MW-118S as late as 1969 (Jacobs Engineering Group, Inc, 2019); however, tritium was not detected in water from these wells (chapter E, appendix E.1, table E.1.1). The decay-corrected tritium concentration of 1969 recharge water in 2016 (at the time of this study) was 3.5 tritium units (TU; chapter F); if present, given the study reporting level of 0.05 TU, 1969 water would have been detected at mixing fractions less than 2 percent. In contrast to HCBSM simulations, tritium was detected farther downgradient in water from wells MW-123S, MW-126S1, and MW-126S2 in the northern subarea at concentrations as high as 0.32 TU in water from well MW-126S2 (chapter E. appendix E.1, table E.1.1). The HCBSM simulated-particle distribution through this area is not consistent with the measured distribution of groundwater-age data and is implausible with younger groundwater downgradient from older groundwater. Younger (post-1952) groundwater in this part of the northern subarea likely moved directly downgradient from the eastern subarea within the shallow zone of the upper aquifer (fig. H.2.2*A*). As previously discussed, HCBSM particle-simulation results do not show groundwater within the shallow zone of the upper aquifer moving downgradient from the eastern subarea and were not consistent with the measured distribution of groundwater-age data (fig. H.2.2*A*).

Measured groundwater-ages in the shallow and deep zones within the upper aquifer are consistent with a bedrock high separating the western and northern subareas. Measured groundwater-age data do not indicate that groundwater flowed from the western subarea into the northern subarea after groundwater levels declined below bedrock altitudes. Simulation of groundwater movement within the HCBSM through the shallow zone between the western and northern subareas after groundwater levels declined may act to pull particles released from the Mojave River in the eastern subarea toward the west along the downgradient side of the Lockhart fault into areas where groundwater-age data show post-1952 groundwater is not present.

Groundwater and Anthropogenic Hexavalent Chromium Movement Downgradient from the Hinkley Compressor Station

Groundwater and anthropogenic Cr(VI) movement downgradient from the Hinkley compressor station was evaluated on the basis of HCBSM forward-particle simulations from the historical Cr(VI) release locations within the Hinkley compressor station (fig. H.2.4). Groundwater and anthropogenic Cr(VI) movement also were evaluated on the basis of reverse-particle tracks from selected wells calculated using the HCBSM (Jacobs Engineering Group, Inc., 2019).

The summative-scale Cr(VI) plume developed as part of this study (fig. H.2.1) shows that part of the aquifer where water from wells may contain some fraction of anthropogenic Cr(VI) released from the Hinkley compressor station. Not all wells within the summative-scale Cr(VI) plume have Cr(VI) concentrations greater than the 95-percent upper tolerance limit (UTL_{95}) values calculated in chapter G within this professional paper (chapter G, table G.5), and wells having concentrations less than UTL_{95} values may not be of regulatory concern. The Q4 2015 regulatory Cr(VI) plume lies within the summative-scale Cr(VI) plume extent and includes wells having Cr(VI) concentrations of regulatory concern greater than the interim regulatory background value of 3.1 µg/L. The summative-scale Cr(VI) plume and the Q4 2015 regulatory Cr(VI) plume include wells used by PG&E for hydraulic control of Cr(VI) and extraction wells used by PG&E for Cr(VI) remediation by land treatment (chapter A, fig. A.6). Hexavalent chromium concentrations in water from some wells outside the summative-scale Cr(VI) plume may exceed 3.1 µg/L but were interpreted as natural on the basis of the summative-scale analyses (chapter G, table G.1).

Forward-Particle Simulations

The HCBSM forward-particle simulations of releases from the Hinkley compressor station were calculated for the period 1952–65 to the end of the simulation in September 2015 (fig. H.2.4); this includes the period of Cr(VI) releases from the Hinkley compressor station. The years 1952–65 also include the period of increasing agricultural pumping and subsequent water-level declines and was a comparatively dry period with some recharge from the Mojave River in 1958 (Stamos and others, 2001; Jacobs Engineering Group, Inc., 2019). Particle positions for each model timestep after the release to September 2015 were calculated, and the particle extent shows the simulated position of the particles in September 2015. Particles were not timestamped (Jacobs Engineering Group, Inc., 2019); consequently, particle locations at different times within the simulation period cannot be evaluated.

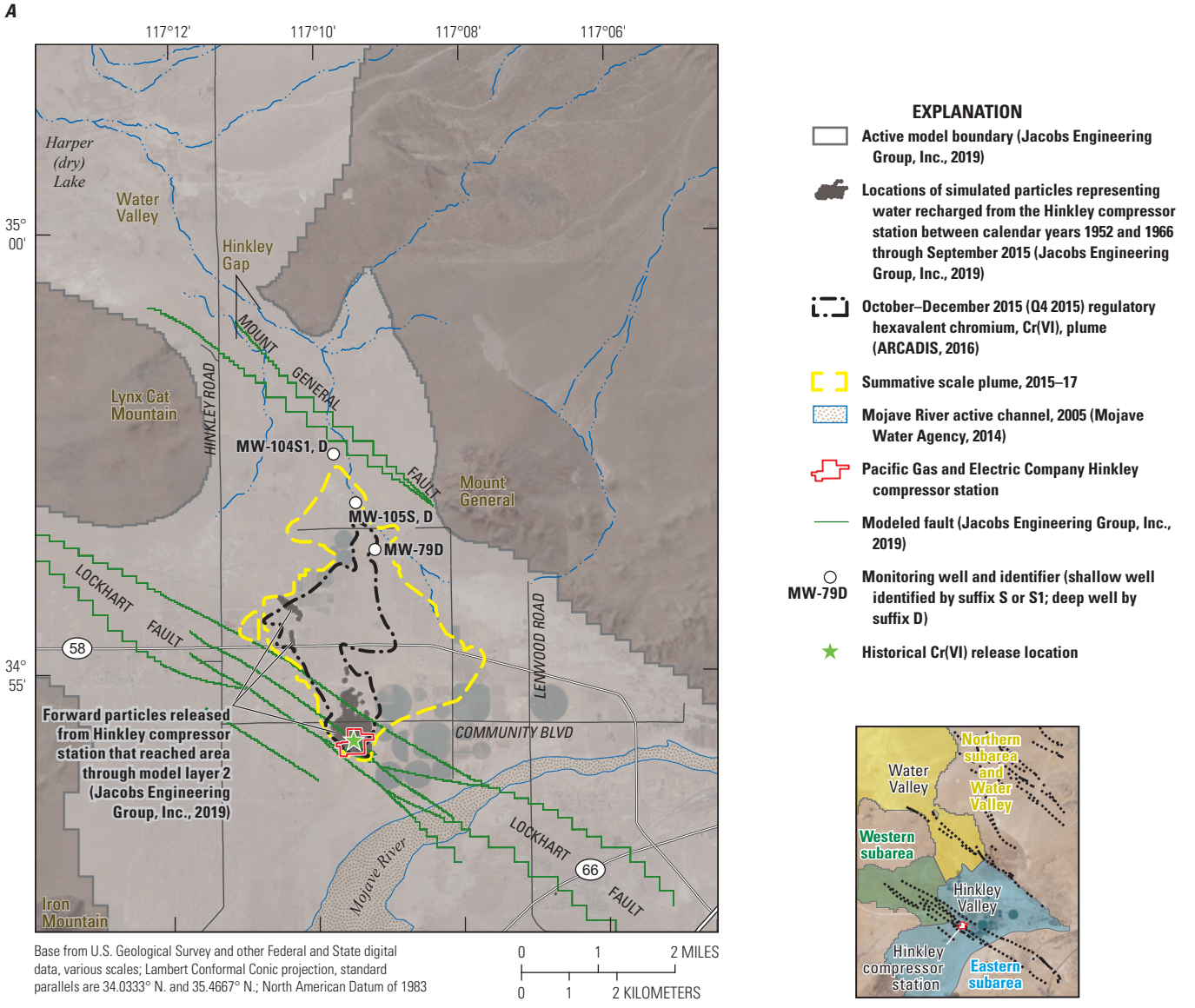

Figure H.2.4. Locations of simulated particles released from the Hinkley compressor station between 1952 and 1965 from the time of release through September 2015 within *A*, the shallow zone and *B*, the deep zone of the upper aquifer, Hinkley and Water Valleys, western Mojave Desert, California. Particle location data are available from Jacobs Engineering Group, Inc. (2019).

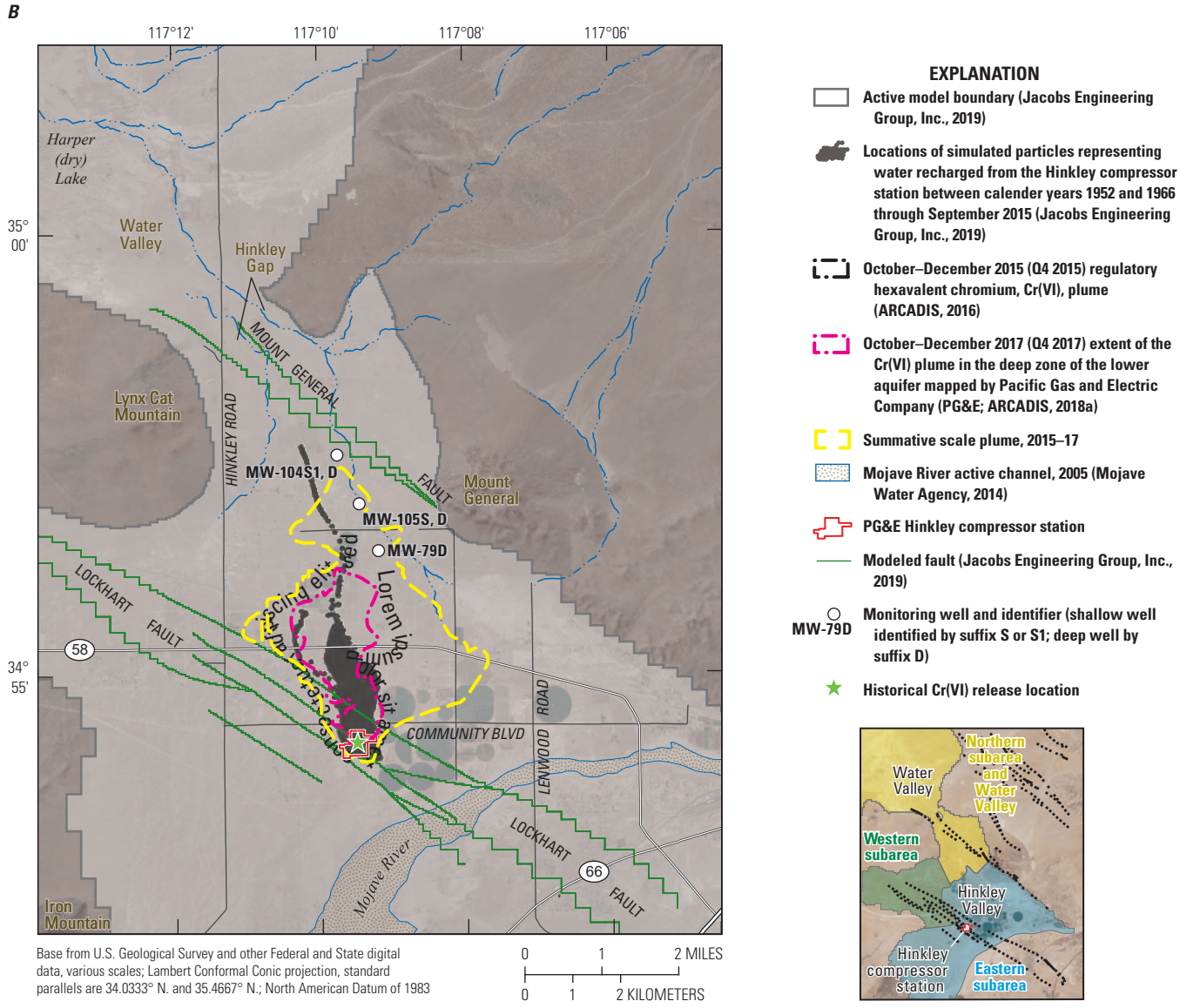

Figure H.2.4.—Continued

Within the shallow zone of the upper aquifer, HCBSM simulated particles representing Cr(VI) releases between 1952 and 1965 extend less than 0.5 mi downgradient from the Hinkley compressor station (fig. H.2.4*A*). Although the downgradient movement of particles may have been restricted by the simulation of aquifer properties and the Lockhart fault within this area, much of the shallow zone within the upper aquifer was desaturated by agricultural pumping during this period (Stone, 1957; California Department of Water Resources, 1967). Some simulated particles, and presumably Cr(VI) released from the Hinkley compressor station, were removed by pumping during this period; although the magnitude of the Cr(VI) release is uncertain, this is consistent with differences between the potential magnitude of the Cr(VI) released into groundwater (chapter A) and the estimated mass of Cr(VI) remaining within the regulatory Cr(VI) plume downgradient from the Hinkley compressor station in 2010 (Lahontan Regional Water Quality Control Board, 2013).

The HCBSM simulations show some particles extend beyond the northernmost extent of the Q4 2015 regulatory Cr(VI) plume and beyond the October–December 2017 (Q4 2017) PG&E mapped extent of Cr(VI) greater than 3.1 µg/L within the deep zone of the upper aquifer (fig. H.2.4*B*; ARCADIS, 2018a). Similar to forward particles representing recharge from the Mojave River, simulated particles released from the Hinkley compressor station between 1952 and 1965 extend into areas within the deep zone of the upper aquifer where water from wells have unadjusted carbon-14 ages ranging from 3,550 to greater than 20,000 ybp that predate releases from the Hinkley compressor station.

The HCBSM forward-particle tracks extend more than 2,000 feet (ft) to the southeast of the release location within the Hinkley compressor station within splays of the Lockhart fault, crossgradient to the nominal regional groundwater gradient in the shallow and deep zones of the upper aquifer (fig. H.2.4). With the exception of the 1958 streamflow, 1952–65 was a dry period with little or no flow in the Mojave River, and groundwater movement at that time would have been controlled largely by local pumping. Simulated 1952 through 1965 HCBSM particle-track results are similar to increases in Cr(VI) concentrations measured southeast of the Hinkley compressor station and east of the regulatory Cr(VI) plume during an 8-year dry period from 2011 to 2019 with no flow in the Mojave River (ARCADIS, 2018b; Lahontan Regional Water Quality Control Board, 2018).

Forward-particle simulations from the Hinkley compressor station were done for three additional periods: 1966–72, 1973–92, and 1993–2015, with particle locations calculated from the time of release to the end of the simulation in September 2015. These periods represent different conditions within Hinkley Valley, especially with respect to activities at the Hinkley compressor station after the Cr(VI) releases ended and agricultural pumping declined (Jacobs Engineering Group, Inc., 2019). Although 1969 was not the largest streamflow during the simulation, the Mojave River was largely uncontrolled by levees at that time, and 1969 represents the largest flooded area simulated within the HCBSM (Jacobs Engineering Group, Inc., 2019). The 1993–2015 period includes remediation activities at the site and declining agricultural pumping as a result of adjudication of the Mojave River groundwater basin (Jacobs Engineering Group, Inc., 2019). Although Cr(VI) was no longer used at the Hinkley compressor station during these later periods, Cr(VI) within the aquifer would have moved downgradient with water recharged from the Mojave River. The later periods have been consolidated into figure H.2.5.

During the 1966–72, 1973–92, and 1993–2015 periods, HCBSM simulated particles within the shallow zone of the upper aquifer extended from the Hinkley compressor station along the downgradient side of the Lockhart fault into the western subarea. Simulated particles extended into the western subarea beyond the northwest injection barrier (installed to limit the westward movement of the Cr(VI) plume; chapter A, fig. A.6) and past the Q4 2015 regulatory Cr(VI) plume extent. Particles simulated within the HCBSM reached areas where Cr(VI) concentrations in monitoring wells averaged less than 2.0 µg/L during this study, and regulatory Cr(VI) concentrations have not exceeded the interim Cr(VI) background value of 3.1 µg/L. Simulated HCBSM particles extend toward the northern subarea and pass near wells MW-118S, MW-119S, and 27-38 (the former Hinkley school well) and near former residential areas within the western part of the community of Hinkley Valley, where groundwater ages predate releases from the Hinkley compressor station.

As previously discussed, the western and northern subareas are separated by a bedrock high, and formerly saturated alluvium in this area was above the water level at the time of this study in 2017 (figs. H.8*C*, H.8*D*). Simulated movement of water through this area within the HCBSM after water levels declined may have acted to pull particles from the Hinkley compressor station to the northwest into parts of the aquifer within the western subarea where Cr(VI) concentrations are low, outside the summative scale Cr(VI) plume extent, and appear to be natural (chapter G, fig. G.2).

Additionally, the specific yield simulated within the HCBSM is 0.25 (unitless) for fine-textured mudflat/playa deposits in the eastern subarea near Mount General (Jacobs Engineering Group, Inc., 2019). Fine-textured materials contain considerable water in storage, but they do not yield this water freely from storage as water levels decline, and literature-accepted values of specific yield from clay and sandy clay textured materials range from 0.02 to 0.07 (Johnson, 1967). The HCBSM-simulated releases of water from storage within these materials as water levels declined may have acted to push particles from the Hinkley compressor station to the northwest into parts of the aquifer within the western subarea where Cr(VI) concentrations are low and appear natural. Model-simulated specific yield values for fine-textured materials in the northern subarea may have similarly affected particle distributions by providing a source of water from storage within modeled aquifer materials that is not actually present.

The HCBSM forward-particle results differ from the extent of anthropogenic Cr(VI) identified by the regulatory Cr(VI) plume extent. Hexavalent chromium concentrations within the Q4 2015 regulatory Cr(VI) plume, in parts of the eastern subarea where forward particles from the Hinkley compressor station did not reach (figs. H.2.4*A*, H.2.5*A*), were as high as 16 µg/L in water from well MW-50S (sampled as part of this study), and regulatory Cr(VI) concentrations in water from well MW-128S1, near the leading edge of the Q4 2015 regulatory Cr(VI) plume, have been as high as 20 µg/L. These concentrations are greater than Cr(VI) concentrations in the western subarea where HCBSM simulated-forward particles from the Hinkley compressor station were present. Natural Cr(VI) concentrations extracted from pore water within mudflat/playa deposits in the eastern subarea were as high as 3.3 µg/L (chapter E, table E.6), and natural Cr(VI) concentrations in older groundwater isolated from surface sources of recharge by mudflat/playa deposits in this area were as high as 3.6 µg/L. On the basis of these data, neither mudflat/playa deposits nor older groundwater are plausible sources of Cr(VI) concentrations as high as 20 µg/L measured within the regulatory Cr(VI) plume where HCBSM forward particles from the Hinkley compressor station did not reach.

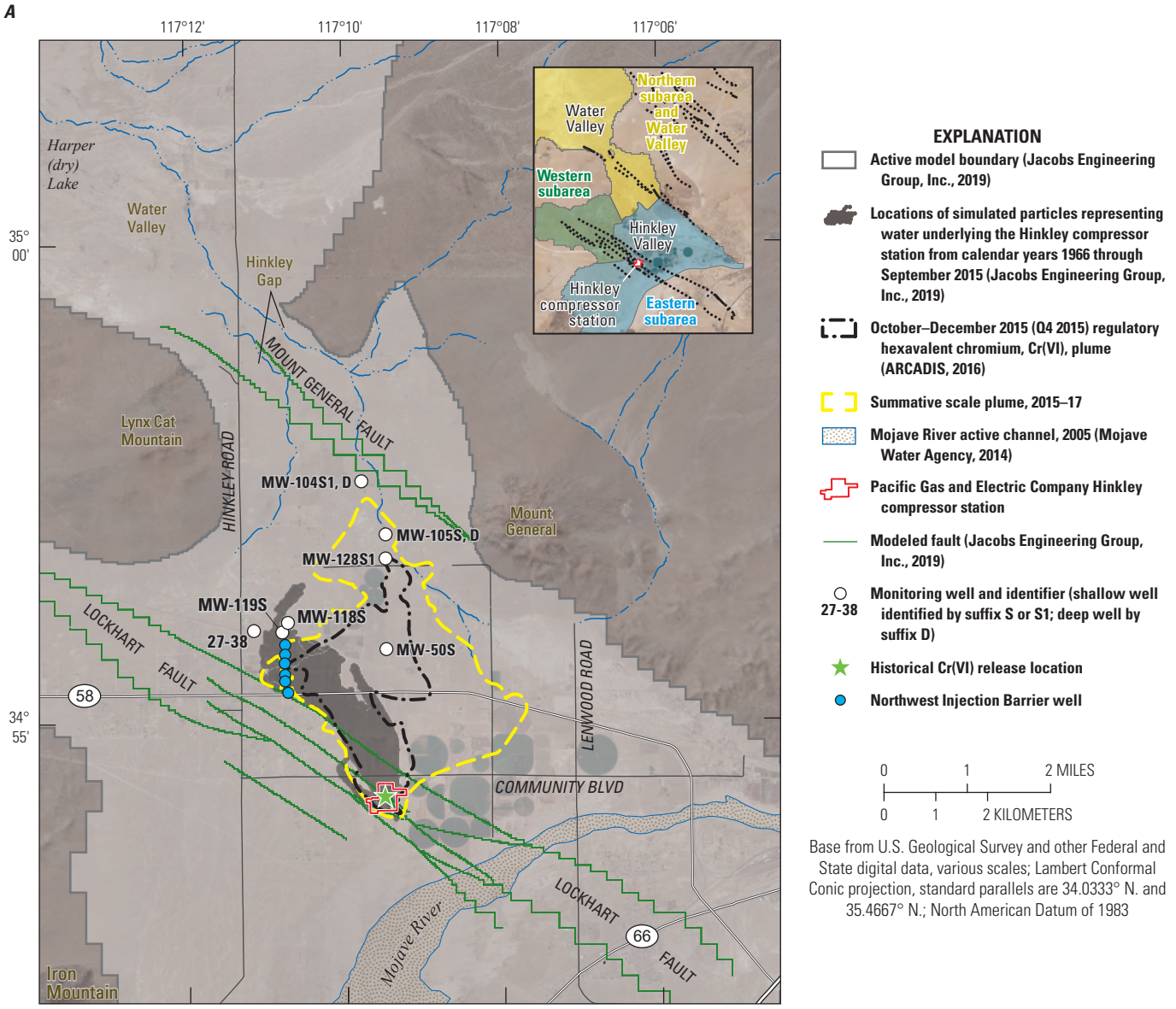

Figure H.2.5. Locations of simulated particles released from the Hinkley compressor station between 1966–72, 1973–92, and 1993–2015 from the time of release through September 2015 for *A*, the shallow zone and *B*, the deep zone of the upper aquifer, Hinkley and Water Valleys, western Mojave Desert, California. Particle location data are from Jacobs Engineering Group, Inc. (2019).

B

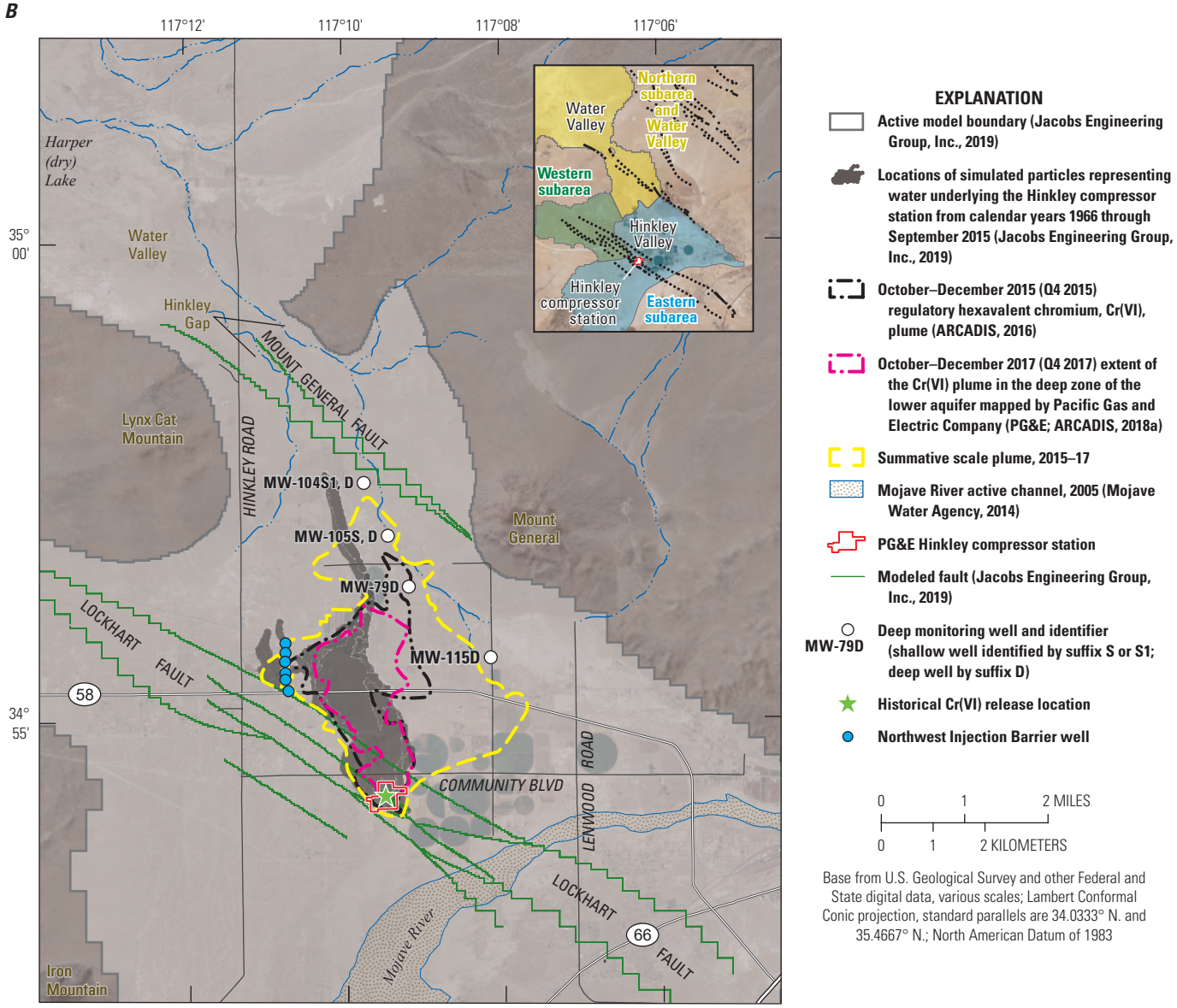

Figure H.2.5.—Continued

Reverse-Particle Simulations

In addition to forward-particle simulations representing releases from the Hinkley compressor station, reverse-particle tracks were calculated for a number of wells in Hinkley and Water Valleys. The purpose of these calculations was to determine if water yielded by selected wells (simulated as particles) may have passed near the Hinkley compressor station and could contain anthropogenic Cr(VI) (Jacobs Engineering Group, Inc., 2019).

Production wells 10N/3W-23R02, GS-23-15, 10N/3W-23H06, and 23-08 are used by PG&E for hydraulic control of the leading edge of the regulatory Cr(VI) plume. The HCBSM results show reverse particles from these wells do not extend back to the Hinkley compressor station as would be expected for wells used to control downgradient movement of the Cr(VI) plume (Jacobs Engineering Group, Inc., 2019).

Reverse-particle tracks within the shallow and deep zone of the upper aquifer for well C-01 used to extract Cr(VI) containing groundwater for land application and reduction of Cr(VI) to trivalent chromium, Cr(III), within the soil zone (chapter A), also do not extend back to the Hinkley compressor station (Jacobs Engineering Group, Inc., 2019). Regulatory concentrations in water from well C-01 have been as high as 7.1 µg/L. Reverse particle tracks were calculated for well IW-03, within the regulatory Cr(VI) plume 0.7 mi upgradient from well C-01; well IW-03 also is used for land application and reduction of Cr(VI) to Cr(III). Although reverse-particle tracks within the shallow zone of the upper aquifer penetrated by well IW-03 do not extend back to the Hinkley compressor station, reverse-particle tracks within the deep zone of the upper aquifer extend back to the Hinkley compressor station (Jacobs Engineering Group, Inc., 2019). Regulatory Cr(VI) concentrations in well IW-03 have been as high as 6.0 µg/L. Coupled well-bore flow and depth-dependent data collected from wells C-01 and IW-03 (figs. H.15, H.16) show that these wells derive a large percentage of their yield from well-sorted near-shore lake deposits (beach sands) within the shallow zone that have high lateral and longitudinal hydraulic connectivity within the upper aquifer that was not simulated by the HCBSM.

Hexavalent chromium concentrations in water from wells MW-178S and MW-178D, within the Q4 2015 regulatory Cr(VI) plume about 0.5 mi to the northwest of the Hinkley compressor station, were 150 and 190 µg/L, respectively. Purge water from the wells was visibly discolored by chromium at the time of sample collection in March 2017. Regulatory Cr(VI) concentrations in water from wells MW-178S and MW-178D have been as high as 270 and 290 µg/L, respectively. The HCBSM-simulated reverse-particle tracks from wells MW-178S and MW-178D do not extend back to the Hinkley compressor station. Instead, reverse-particle tracks cross the Lockhart fault and pass through portions of the aquifer having Cr(VI) concentrations less than 1 µg/L (fig. H.2.6, particle tracks for well MW-178D shown in Jacobs Engineering Group, Inc., 2019). Water from wells MW-178S and MW-178D had tritium concentrations of 0.5 and 0.76 TU, respectively, with carbon-14 activities of 112 and 119 pmc, respectively (chapter E, appendix E.1, table E.1.1), consistent with younger (post-1952) groundwater recharged from the Mojave River. Simulated reverse-particle tracks for well MW-178S do not originate from the Mojave River during the period of model simulation from 1931 through 2015 and the simulated particles indicate older (post-1952) groundwater that predates releases from the Hinkley compressor station should be present in water from these wells (Jacobs Engineering Group, Inc., 2019).

Wells used for hydraulic control of the Cr(VI) regulatory plume and wells used to mitigate high Cr(VI) concentrations within the regulatory Cr(VI) plume (including wells used for extraction for land treatment of Cr(VI) containing groundwater) should have a hydrologic history traceable to the Hinkley compressor station. Similarly, wells within 0.5 mi of the Hinkley compressor station, having Cr(VI) concentrations sufficiently high to visibly discolor purge water from the well, also should have a hydrologic history traceable to the Hinkley compressor station. Reverse-particle tracks calculated by the HCBSM do not simulate an anthropogenic Cr(VI) source associated with releases from the Hinkley compressor station for water from these wells.

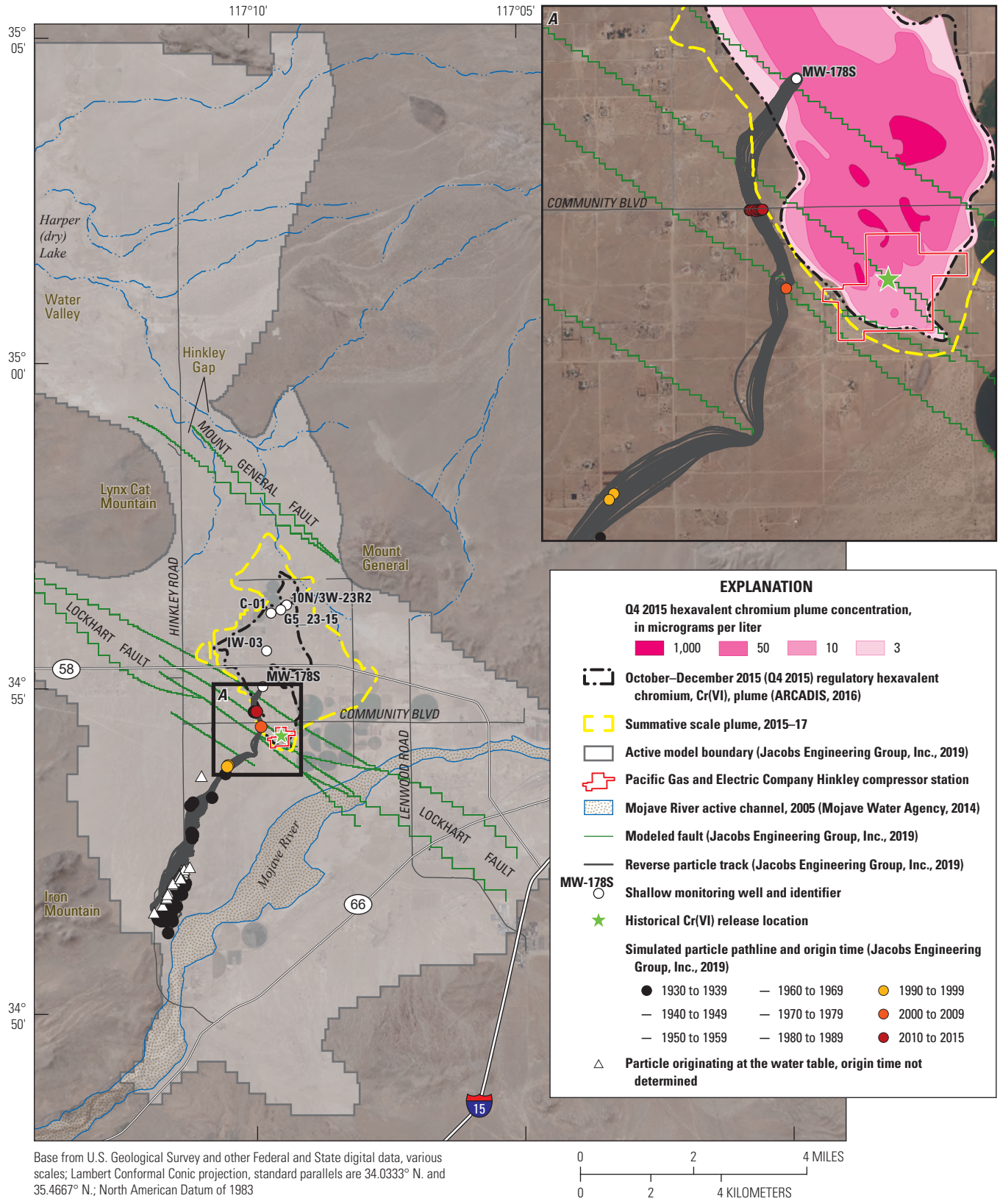

Figure H.2.6. Reverse-particle tracks in the shallow zone of the upper aquifer from well MW-178S, within the October–December 2015 (Q4 2015) regulatory hexavalent chromium, Cr(VI), plume, Hinkley Valley, western Mojave Desert, California, 1930–2015. Particle location data are from Jacobs Engineering Group, Inc. (2019).

Conclusions

Hexavalent chromium, Cr(VI), released from the Hinkley compressor station between 1952 and 1964, has moved downgradient with groundwater within unconsolidated aquifer deposits in Hinkley Valley over a period of more than 60 years. The movement of Cr(VI) over this time integrates the combined effects of recharge, pumping, and the distribution of aquifer hydraulic properties, including the interconnectedness of high-permeability aquifer materials, in a manner that cannot be assessed solely from water level and hydraulic data. Comparisons of forward-particle simulations with measured age data show that the Hinkley Chromium Background Study Model (HCBSM) particle-simulation results differ from the vertical and spatial distribution of measured groundwater age within Hinkley and Water Valleys. Additionally, forward-particle simulations calculated from historical release locations within the Hinkley compressor station using the HCBSM did not duplicate the October–December 2015 (Q4 2015) regulatory Cr(VI) plume extent or the summative scale Cr(VI) plume extent estimated as part of this study. Similarly, reverse-particle tracks from (1) wells used for hydraulic control of the Cr(VI) regulatory plume, (2) wells used for extraction for land treatment of Cr(VI) containing groundwater, and (3) monitoring wells having high Cr(VI) concentrations less than 0.5 mile downgradient from the Hinkley compressor station do not extend back to the Hinkley compressor station.

The HCBSM represents the Pacific Gas and Electric Company's (PG&E) and their consultants' understanding of the groundwater-flow system in Hinkley and Water Valleys based on interpretation of water-level and hydraulic data. Differences between measured groundwater-age and Cr(VI) concentration data and the HCBSM simulated particle results may be attributed to (1) conceptual differences in aquifer properties within the shallow and deep zones of the upper aquifer, (2) conceptual differences in groundwater movement between the western and northern subareas as groundwater levels declined as a result of agricultural pumping beginning in the early 1950s, (3) simulation of specific yield within the HCBSM outside of literature published ranges, and (4) conceptualization of groundwater flow near the Lockhart fault.

Differences between measured groundwater-age data, Cr(VI) regulatory data, and HCBSM particle simulations were not reconciled within the timeframe of this study; consequently, the HCBSM was not used to iteratively evaluate and refine the summative-scale Cr(VI) plume extent as proposed in the study design. The HCBSM is not a U.S. Geological Survey (USGS) product and does not represent the understanding of the groundwater-flow system supported by chemical, groundwater-age, and aquifer property data developed as part of this study.

References Cited

ARCADIS, 2016, Annual cleanup status and effectiveness report (January to December 2015) Pacific Gas and Electric Company, Hinkley Compressor Station, Hinkley, California: San Francisco, Calif., Pacific Gas and Electric Company, prepared by ARCADIS, Oakland, Calif., RC000699, [variously paged], accessed February 2016, at https://documents.geotracker.waterboards.ca.gov/esi/uploads/geo_report/5010230779/SL0607111288.PDF.

ARCADIS, 2018a, Annual cleanup status and effectiveness report (January to December 2017), Pacific Gas and Electric Company, Hinkley Compressor Station, Hinkley, California: ARCADIS, [variously paged], accessed August 14, 2019, at https://documents.geotracker.waterboards.ca.gov/esi/uploads/geo_report/4949047982/SL0607111288.PDF.

ARCADIS, 2018b, Workplan for investigation of increasing southeastern area chromium concentrations and associated remedial actions, Pacific Gas and Electric Company, Hinkley Compressor Station, Hinkley, California: ARCADIS, 40 p., accessed August 14, 2019, at https://geotracker.waterboards.ca.gov/esi/uploads/geo_report/2149594247/SL0607111288.PDF.

ARCADIS and CH2M Hill, 2011, Development of a groundwater flow and solute transport model—Addendum 3 to the feasibility study: ARCADIS and CH2M Hill, app. G, [variously paged], accessed September 4, 2019, at https://geotracker.waterboards.ca.gov/esi/uploads/geo_report/2112934887/SL0607111288.PDF.

California Department of Water Resources, 1967, Mojave River ground-water basins investigation: California Department of Water Resources Bulletin 84, 151 p., accessed December 6, 2018, at https://archive.org/details/mojaverivergroun84cali/page/n5/mode/2up.

HydroGeoLogic, Inc., 2011, MODHMS/MODFLOW-SURFACT, a comprehensive MODFLOW-based hydrologic modeling system software program: Reston, Va., HydroGeoLogic, Inc.

Izbicki, J.A., and Groover, K., 2016, A plan for study of natural and man-made hexavalent chromium, Cr(VI), in groundwater near a mapped plume, Hinkley, California: U.S. Geological Survey Open-File Report 2016–1004, 12 p., accessed April 19, 2018, at https://doi.org/10.3133/ofr20161004.

Izbicki, J.A., and Groover, K., 2018, Natural and man-made hexavalent chromium, Cr(VI), in groundwater near a mapped plume, Hinkley, California—Study progress as of May 2017, and a summative-scale approach to estimate background Cr(VI) concentrations: U.S. Geological Survey Open-File Report 2018–1045, 28 p., accessed April 19, 2018, at https://doi.org/10.3133/ofr20181045.

Izbicki, J.A., Stamos, C.L., Nishikawa, T., and Martin, P., 2004, Comparison of ground-water flow model particle-tracking results and isotopic data in the Mojave River ground-water basin, southern California, USA: Amsterdam, The Netherlands, Journal of Hydrology , v. 292, no. 1–4, p. 30–47. [Available at https://doi.org/10.1016/j.jhydrol.2003.12.034.]

Jacobs Engineering Group, Inc., 2019, Ground water flow modeling to support the Hinkley chromium background study, San Bernardino County, California. Project no. 706888CH, for Pacific Gas and Electric Company: Redding, Calif., Jacobs Engineering Group, Inc., [variously paged], accessed March 24, 2020, at https://geotracker.waterboards.ca.gov/view_documents?global_id=T10000010367&enforcement_id=6411598, with Appendixes A through H at https://geotracker.waterboards.ca.gov/view_documents?global_id=T10000010367&enforcement_id=6411607.

Johnson, A.I., 1967, Specific yield—Compilation of specific yields for various materials: U.S. Geological Survey Water Supply Paper 1662-D, 74 p. [Available at https://pubs.usgs.gov/wsp/1662d/report.pdf.]

Lahontan Regional Water Quality Control Board, 2013, Draft environmental impact report—Comprehensive groundwater cleanup strategy for historical chromium discharges from PG&E's Hinkley Compressor Station, San Bernardino County: South Lake Tahoe, Calif., California Regional Water Quality Control Board, Lahontan Region, [variously paged], accessed November 20, 2018, at https://www.waterboards.ca.gov/rwqcb6/water_issu es/projects/pge/feir.html.

Lahontan Regional Water Quality Control Board, 2018, Acceptance of workplan for investigation of increasing chromium concentrations, PG&E, Hinkley compressor station, San Bernardino County: Lahontan Regional Water Quality Control Board, 3 p., accessed August 4, 2019, at https://geotracker.waterboards.ca.gov/regulators/deliverable_documents/9753584921/PG&E%20Retraction%20and%20New%20Accept%20Letter%2011-1-18.pdf.

Miller, D.M., Haddon, E.K., Langenheim, V.E., Cyr, A.J., Wan, E., Walkup, L.C., and Starratt, S.W., 2018, Middle Pleistocene infill of Hinkley Valley by Mojave River sediment and associated lake sediment—Depositional architecture and deformation by strike-slip faults, *in* Miller, D.M., ed., The Mojave River from sink to source: The 2018 Desert Symposium Field Guide and Proceedings, April 2018, p. 58–65, accessed November 27, 2018, at http://www.desertsymposium.org/2018%20DS%20Against%20the%20Current.pdf.

Mojave Water Agency, 2014, Geospatial library: Mojave Water Agency, accessed May 22, 2014, at https://www.mojavewater.org/data-maps/geospatial-library/.

Niswonger, R.G., Panday, S., and Ibaraki, M., 2011, MODFLOW-NWT, A Newton formulation for MODFLOW-2005: U.S. Geological Survey Techniques and Methods, book6, chap. A37, 44 p. [Available at https://www.usgs.gov/software/modflow-nwt-a-newton-formulation-modflow-2005.]

Pollock, D.W., 1994, User's guide for MODPATH/MODPATH-PLOT, version 3—A particle-tracking post-processing package for MODFLOW, the U.S. Geological Survey finite-difference ground-water flow model: U.S. Geological Survey Open-File Report 94–464, 249 p. [Available at https://pubs.er.usgs.gov/publication/ofr94464.]

Pollock, D.W., 2016, User guide for MODPATH version 7—A particle-tracking model for MODFLOW: U.S. Geological Survey Open-File Report 2016–1086, 35 p. [Available at https://doi.org/10.3133/ofr20161086.]

Stamos, C.L., Martin, P., Nishikawa, T., and Cox, B., 2001, Simulation of groundwater flow in the Mojave River basin, California: U.S. Geological Survey Water-Resources Investigations Report 01–4002, 129 p. [Available at https://pubs.usgs.gov/wri/wri014002/pdf/wrir014002.pdf.]

Stone, R.S., 1957, Groundwater resonance in the western part of the Mojave Desert, California, with particular respect to the boron content of well water: U.S. Geological Survey Open-File Report 57–107, 102 p., accessed December 6, 2018, at https://doi.org/10.3133/ofr57107.

U.S. Geological Survey, 2021, USGS water data for the Nation: U.S. Geological Survey National Water Information System database, accessed January 6, 2021, at https://doi.org/10.5066/F7P55KJN.

For more information concerning the research in this report, contact the

Director, California Water Science Center
U.S. Geological Survey
6000 J Street, Placer Hall
Sacramento, California 95819
https://www.usgs.gov/centers/ca-water/

Publishing support provided by the U.S. Geological Survey
Science Publishing Network, Sacramento Publishing Service Center

Groover and others—**Chapter H: Predevelopment Water Levels, Groundwater Recharge, and Selected Hydrologic Properties of Aquifer Materials**—PP 1885-H

ISSN 2330-7102 (online)
https://doi.org/10.3133/pp1885H